The CaM kinase, CMK-1, mediates a negative feedback mechanism coupling the *C. elegans* AMPA receptor, GLR-1, with its own transcription

A thesis

submitted by

Benjamin Joseph Moss

In partial fulfillment of the requirements for the degree of

Doctor of Philosophy

in

Neuroscience

TUFTS UNIVERSITY

Sackler School of Graduate Biomedical Sciences

May, 2017

Advisor:

Peter Juo

Abstract

Chronic changes in synaptic activity result in compensatory alterations in AMPA-type glutamate receptors (AMPARs), but the mechanisms underlying this process have not been fully elucidated. In this thesis, I investigate a feedback mechanism that bidirectionally regulates transcription of the *C. elegans* AMPAR, GLR-1, in response to chronic changes in synaptic activity.

It was previously shown that GLR-1 trafficking mutants with decreased synaptic GLR-1, such as animals with mutations in the kinesin *klp-4* or the deubiquitinating enzyme *usp-46*, exhibit increased levels of *glr-1* transcript. In Chapter 2, I show that this increase in *glr-1* mRNA is due in part to increased *glr-1* promoter activity assayed with a *glr-1* transcriptional reporter (*Pglr-1::NLS-GFP::LACZ*). *glr-1* null mutants exhibit similar increases in *glr-1* transcription, suggesting that decreased synaptic GLR-1 is sufficient to trigger the feedback mechanism. Increased *glr-1* transcriptional activity could be due to decreased synaptic GLR-1 protein levels or decreased glutamatergic transmission. To assay whether synaptic activity regulates *glr-1* transcription, I measured the *glr-1* transcriptional reporter in animals with mutations in the presynaptic vesicular glutamate transporter *eat-4*/VGLUT. In *eat-4* mutants, which have reduced presynaptic glutamate release, I found similar increases in the *glr-1* transcriptional reporter. These data suggest that chronic reduction of synaptic activity is sufficient to trigger the feedback pathway. To test whether acute reductions in synaptic activity trigger the feedback pathway, I utilized exogenous expression of a histamine-gated chloride channel to reduce activity specifically and acutely in *glr*-1-expressing cells. I found increased *glr-1* transcriptional

reporter fluorescence after one and four hours of activity suppression, suggesting that decreased GLR-1 activity can repress *glr-1* transcription. The feedback mechanism is bidirectional, as *unc-11*/AP180 clathrin adaptin endocytic mutants, which accumulate synaptic GLR-1, exhibit decreased *glr-1* transcription and animals with increased GLR-1 signaling, such as animals expressing a dominant-active version of the receptor (GLR-1(A/T), also exhibit decreased *glr-1* transcription. These findings suggest that the feedback mechanism responds to both decreases and increases in activity.

In Chapter 3, investigation of signaling pathways mediating the synapse-to-nucleus feedback pathway revealed that the CMK-1/CaM kinase pathway normally functions to repress *glr-1* transcription. Analysis of *cmk-1 loss-of function;glr-1* and *cmk-1 gain-of-function*;*glr-1* double mutants suggests that CMK-1/CaMK functions in the same pathway as decreased synaptic activity to regulate *glr-1* transcription. In support of this, the subcellular distribution of GFP-tagged CMK-1/CaMK shifts from the nucleus to the cytoplasm in *glr-1* mutants and from the cytoplasm to the nucleus in *unc-11* mutants.

In Chapter 4, the establishment of a yeast-one-hybrid (Y1H) system to screen for transcription factors necessary for the feedback mechanism is presented. Initial screening demonstrates the discovery of a candidate regulator of the *glr-1* promoter. Together, these results reveal a bidirectional homeostatic feedback mechanism where changes in synaptic activity trigger CMK-1/CaMK translocation between the nucleus and cytoplasm to regulate *glr-1* transcription. The establishment of a Y1H to probe for transcription factors

required for *glr-1* expression, both basally and in the feedback mechanism, provides the basis for identification of novel AMPAR regulatory factors.

Acknowledgements

I would first like to thank my advisor, Peter Juo, for guiding me through this project and creating a wonderful, enriching environment in which to develop as a scientist. From the first day, Peter has been supportive of my goals and has always made himself available when the inevitable roadblock arises. It has been a privilege to work in Peter's lab. All the members of the Juo lab, former and current have been incredibly helpful, from patiently teaching me to pick worms to thoughtfully critiquing my data. I have tried, and surely failed, to give as much help as I have taken. These members include: Lina Dahlberg, Steve Garafalo, Molly Hodul, Eric Luth, Annette McGehee, Kaitlyn Markoja, Mike Monteiro, Lidia Park, and Sam Williams.

I would also like to thank my thesis committee: Larry Feig and Michele Jacob, for always offering thoughtful critiques of my project and for their consideration of my pursuit of the MD/PhD degree, and Mike Francis for taking the time to serve on my defense committee. I also thank the Neuroscience program for engaging classes and creating a collegiate research environment, and the MD/PhD program for the opportunity to be here as well as the occasional nourishment along the way.

Finally I am grateful to my family for their endless and seemingly bottomless support throughout my life and prolonged education. And to Liz, for being present and always carrying more than her share of the load.

Table of Contents

List of Figures

Chapter 2

Chapter 3

Chapter 4

List of Abbreviations

AD	Alzheimer's disease
AMPAR	α-Amino-3-hydroxy-5-methyl-4-isoxazolepropionic acid receptor
APV	(2*R*)-amino-5-phosphonovaleric acid
Arc/Arg3.1	Activity-regulated cytoskeleton-associated protein
BDNF	Brain-derived neurotrophic factor
BIC	Bicuculline
CaM	Calmodulin
CaMKI-IV	Calmodulin kinase I-IV
CaMKK	Calmodulin kinase kinase
cAMP	Cyclic adenosine monophosphate
CBP	CREB-binding protein
CDK-5	Cyclin-dependent kinase 5
CNQX	6-Cyano-7-nitroquinoxaline-2,3-dione
CNS	Central nervous system
CP-AMPAR	Calcium-permeable AMPAR
CRE	cAMP response element
CREB	cAMP response element-binding protein
crh-1	CREB homolog (*C. elegans*)
DUB	Deubiquitining enzyme
EAT-4/VGLUT	Vesicular glutamate transporter (*C. elegans*)
EPSC	Excitatory postsynaptic current
ER	Endoplasmic reticulum
GABA	γ-Aminobutyric acid
GLR-1	AMPAR homolog (*C. elegans*)
GluA1-4	AMPAR subunit
GluR	Glutamate receptor
GRIP1	Glutamate receptor-interacting protein 1
HDAC	Histone deacetylase
HisCl	Histamine-chloride channel
iGluRs	Ionotropic glutamate receptor
IP3	Inositol triphosphate
KLP-4/Kif13A	Kinesin-like protein (*C. elegans*)
LTD	Long-term depression
LTP	Long-term potentiation
MAPK	Mitogen-activated protein kinases
MeCP2	Methyl CpG binding protein 2
mEPSC	Mini excitatory postsynaptic current
miR	Micro RNA
NLS	Nuclear localization signal
NMDAR	*N*-Methyl-D-aspartic acid
NMR-1	NMDAR homolog (*C. elegans*)
NRSE	Neuron-restrictive silencer element
NSF	N-ethylmaleimide-sensitive factor
Pglr-1	*glr-1* promoter

PICK1	PRKCA-binding protein
Plk-2	Polio-like kinase 2
PS1	Presenilin-1
PSD	Postsynaptic density
RA	Retinoic acid
REST	RE1-silencing transcription factor
RT-qPCR	Real-time quantitative PCR
TNFα	Tumor necrosis factor α
TSS	Transcription start site
TTX	Tetrodotoxin
UNC-11/AP180	Clathrin adaptin homolog (*C. elegans*)
UNC-13	MUNC-13 homolog (*C. elegans)*
UNC-2/VGCC	Voltage-gated calcium channel homolog (*C. elegans*)
USP-46	Ubiquitin-specific protease homolog (*C. elegans*)
UTR	Untranslated region
VGCC	Voltage-gated calcium channel
VNC	Ventral nerve cord
Y1H	Yeast-one-hybrid

Chapter 1

Introduction

Synaptic plasticity

The human brain is a highly specialized organ that captures, stores, and processes vast quantities of information. Information is largely encoded in the pattern and strength of synaptic connections made between neurons. These synapses are plastic in that they can grow, shrink, strengthen, and weaken in response to changes in the environment. Synaptic plasticity, thus, allows our nervous system to respond to changes in the environment by learning and remembering. The past several decades of research have shed light on the mechanisms that underlie synaptic plasticity, allowing us to learn about the biological and chemical substrates of learning itself.

The first evidence that alterations in synaptic strength underlie plasticity and learning came in 1973 when Bliss and Lomo showed that brief, repetitive activation of hippocampal excitatory synapses causes long-lasting enhancement of synaptic strength (Bliss and Lomo 1973). This phenomenon of long-term potentiation (LTP) has now been studied in depth and is well-accepted as a neural correlate of learning and memory. LTP is a form of Hebbian plasticity, which refers to an associative learning paradigm where connections between neurons that fire at the same time are strengthened. For example high frequency stimulation of presynaptic neurons causes coincident activation of postsynaptic neurons, which creates long-lasting connections between the pre- and postsynaptic neurons. In contrast, low frequency stimuli leads to weakening of synaptic connections, known as long-term depression (LTD). Together, LTP and LTD have provided a cellular model allowing researchers to elucidate the basic mechanisms underlying learning and memory. One of the fundamental discoveries has been the

importance of AMPA receptors (AMPARs), a class of glutamate receptors (GluRs), in mediating changes in synaptic strength.

Glutamate receptors: overview

Glutamate receptors mediate the majority of excitatory neurotransmission in the brain and can be divided into two broad classes. Metabotropic GluRs are G-protein coupled receptors that activate downstream signaling pathways and can indirectly activate ion channels. Ionotropic glutamate receptors (iGluRs) are tetrameric, voltage-gated ion channels that lead directly to depolarization of the postsynaptic membrane. iGluRs themselves can be divided into three classes, originally named by their selective responsiveness to different molecules. Kainate receptors, perhaps the least studied of the three classes, are present throughout the central nervous system (CNS), though not at all excitatory synapses, and are thought to function as modulators of synaptic transmission and neuronal excitability (Traynelis et al. 2010). NMDA receptors (NMDARs) are located synaptically and extrasynaptically and play critical roles in synaptic plasticity. Their activation by glutamate triggers a postsynaptic current with a slow rise and long decay time. At resting, NMDARs are blocked by a magnesium ion, which, upon postsynaptic depolarization, is removed, allowing an inward flow of calcium and sodium ions. Given these features, NMDARs act as coincidence detectors, sensing the co-occurrence of postsynaptic depolarization (by removal of the magnesium block) and presynaptic glutamate release. The inward flow of calcium ions through NMDARs triggers downstream signaling pathways critical for LTP and LTD (Rebola et al. 2010,

Hunt and Castillo 2012). Many of these signaling pathways converge on regulation of the third class of iGluRs, AMPARs.

AMPA receptors: trafficking and posttranslational modifications

AMPARs are tetrameric cation channels assembled from four subunits (GluA1-GluA4) to form homo- or heteromeric channels. Structurally, all AMPARs share an extracellular N-terminal domain followed by an S1 and S2 domain, which form the glutamate binding site. Three hydrophobic segments span the membrane (M1, M3, and M4) and one hydrophobic segment (M2) forms a hairpin domain that dips into the membrane and contributes to the channel pore. The C-terminal cytoplasmic tail (C-tail) contains binding sites for many regulatory proteins and plays critical roles in receptor trafficking and function (Bredt and Nicoll 2003, Lu and Roche 2012). Unlike NMDARs, which mediate the slow component of postsynaptic depolarization, AMPAR currents have a fast rise and short decay time and mediate the majority of charge transfer during synaptic transmission. As such, AMPAR currents are the primary driving force of excitatory neurotransmission. The specific kinetics of the receptor are determined by its subunit composition. Most AMPARs in the mammalian forebrain are composed of GluA1/GluA2 subunits, with lesser expression of GluA2/GluA3 receptors. GluA4 is highly enriched in cerebellar tissue, where it pairs with GluA2. Tetrameric AMPARs are permeable to calcium unless they contain GluA2, which undergoes mRNA editing making it impermeable to calcium. Thus, GluA2-lacking receptors are referred to as calcium-permeable AMPARs (CP-AMPARs). CP-AMPARs not only differ in their permeability to calcium, but are also inwardly rectifying and sensitive to specific pharmacologic

blockade (Anggono and Huganir 2012, Lee 2012). The ability of synapses to contain either calcium-permeable or calcium-impermeable AMPARs contributes to synaptic plasticity and plays critical roles in development and plasticity.

Editing of the GluA2 subunit is just one of many ways that neurons modify AMPARs. The well-studied AMPAR trafficking pathway from the soma to the synapse, offers many additional key points of AMPAR regulation. After transcription in the nucleus, AMPAR mRNA can undergo translation and packaging into vesicles in the ER/Golgi or the mRNA itself can be trafficked out to dendrites where its translation can be regulated directly by changes in synaptic activity (Grooms et al. 2006). AMPAR proteins are trafficked to synapses by kinesin or dynamin-dependent vesicle trafficking followed by SNARE-mediated vesicle fusion into the postsynaptic membrane. The exact location of vesicle fusion is still under investigation but is likely either directly at synaptic spines or at dendrites where AMPARs can then enter the synapse by lateral diffusion (Anggono and Huganir 2012). AMPARs interact with the actin network and numerous proteins at the post-synaptic density (PSD), and many of these interactions are determined by C-tail binding sites. Endocytosis of AMPARs occurs adjacent to the PSD at the endocytic zone or in the somatodendritic compartment and is mediated by clathrin and dynamin. After endocytosis, AMPARs can be recycled back to the synapse or undergo degradation via the lysosome or proteasome (Anggono and Huganir 2012, Lu and Roche 2012). Neurons take advantage of nearly all of these trafficking steps to regulate the abundance of AMPARs at synapses.

Posttranslational modifications afford yet another opportunity for regulation of AMPAR localization and channel properties. AMPAR subunits are phosphorylated by several different kinases and these phosphorylation sites control trafficking and conductance properties. Many phosphorylation events are mediated by changes in activity, such as in LTP and LTD. AMPARs can also be palmitoylated, which can alter protein trafficking, localization and function. Finally AMPAR ubiquitination regulates endocytosis and leads to receptor degradation. The abundance of regulatory points in the AMPAR trafficking pathway and in posttranslational modifications make these receptors critical players in synaptic plasticity (Lu and Roche 2012).

AMPARs in LTP and LTD

Although pre- versus postsynaptic mechanisms for LTP and LTD have been hotly debated for many years (Lisman 2009), there is abundant evidence that postsynaptic regulation of AMPARs is one of the primary driving forces of the changes in synaptic strength that occur during synaptic plasticity. Most LTP protocols result in a selective increase in the amplitude of AMPA excitatory postsynaptic currents (EPSCs), but not NMDAR EPSCs (although there are less well-studied mechanisms that do alter NMDAR EPSCs (Kauer et al. 1988, Muller et al. 1988, Nicoll 2003)), suggesting that LTP leads to increases in the number of postsynaptic AMPARs. More definitive evidence came from a study showing that uncaging glutamate directly onto synaptic spines leads to increases in AMPAR EPSCs specifically at potentiated spines (Matsuzaki et al. 2004). Additionally, LTP stimulation leads directly to an influx of AMPARs at synapses (Segal 2005, Molnar 2011), and this parallels synaptic strengthening (Huganir and Nicoll 2013). Various

mechanisms underlie changes in AMPAR abundance at synapses, including decreased AMPAR endocytosis in LTP and enhanced AMPAR endocytosis in LTD (Anggono and Huganir 2012), regulation by synaptic scaffolding proteins that interact with AMPARs, regulation of the phosphorylation state of AMPARs, increased or decreased ubiquitin-mediated degradation, and changes in AMPAR transcription and translation (Bredt and Nicoll 2003, Grooms et al. 2006, Yi and Ehlers 2007, Bassani et al. 2013).

Synaptic scaling: overview

Soon after LTP and LTD became accepted as neural correlates of learning and memory, it was recognized that if there were not mechanisms to keep LTP and LTD in check, synapses could undergo runaway potentiation or depression, leading to excessively high or low firing rates. For example, if excitatory input to a postsynaptic neuron causes potentiation resulting in a stronger connection, that synapse will be more likely to excite the neuron, leading to further synaptic strengthening. This sort of runaway potentiation or depression would place the firing rate of the neuron outside of its ideal functional range (Bear 1995, Miller 1996).

Several mechanisms have been proposed to maintain neuronal activity within a homeostatic range, including balancing conductance properties, regulating synapse number, or manipulating the threshold for the induction of LTP or LTD (Turrigiano 2008). One theoretical solution used in computational models of neural networks is to globally scale each synapse based on prior activity of the neuron (Abbott and Nelson 2000). Thus, if a given synapse experiences high levels of activity and is potentiated

while a neighboring synapse receives no activity, global scaling will reduce the strength of each synapse by a common factor determined by prior neuronal activity. This would prevent excessive neuronal firing caused by the highly activated synapse. This theory was first experimentally verified by several landmark studies published in 1998.

The first published evidence of a scaling mechanism that would prevent runaway LTP and LTD, stabilize synaptic weights, and keep neuronal firing within a target range, came from the Nelson lab. Turrigiano et. al. tested whether a synapse's prior history of activity could alter postsynaptic properties by subjecting neurons to chronic increases or decreases in neuronal activity and recording AMPAR mini EPSCs (mEPSCs) (Turrigiano et al. 1998). mEPSCs are postsynaptic currents that correspond to the release of a single presynaptic vesicle. Typically, changes in mEPSC frequency correspond to changes in either vesicle release or synapse number, while changes in mEPSC amplitude correspond to changes in the number of postsynaptic receptors. Using whole-cell voltage-clamp recordings in primary culture of rat visual cortical pyramidal neurons, they showed that chronically decreasing overall activity with tetrodotoxin (TTX) (a sodium channel blocker that prevents action potentials) or CNQX (an AMPAR antagonist) leads to increased mEPSC amplitude, while increasing overall activity with bicuculline (BIC) (a $GABA_A$ receptor antagonist) leads to decreased mEPSC amplitude. Thus, prior history of chronic excitation scales down the postsynaptic response, while chronic inhibition scales it up (Turrigiano et al. 1998).

When amplitudes of mEPSCs from untreated cells were plotted against TTX- or BIC-treated amplitudes, the treated cells scaled by the same multiplicative factor. This type of scaling implies that a synapse's initial weight is multiplied by, as opposed to adding or subtracting, a common factor, thus allowing neurons to scale according to their prior history of activity. Furthermore, chronic changes in activity lead to compensatory changes specifically in neuronal firing rate, consistent with a scaling mechanism that functions to restrain neuronal firing within a target set-point. This paper also provided the first evidence that these compensatory changes involve alterations in the number of postsynaptic receptors. Pulses of glutamate onto the postsynaptic membrane lead to higher mEPSC amplitude in TTX-treated cells compared to control cells. There was no effect on mEPSC frequency, indicating that chronic changes in activity do not effect synapse number or presynaptic release mechanisms. Together these findings suggest that the mechanism for increased mEPSC is postsynaptic. This paper laid the ground work for research into what is now referred to as homeostatic synaptic scaling, and highlights several key features of this phenomenon: scaling occurs bidirectionally in response to chronic changes in activity; scaling is multiplicative; and scaling correlates with changes in postsynaptic glutamate receptors (Turrigiano et al. 1998).

Two other papers published in the same year supported these findings. In a similar effort to understand the way in which a neuron's prior history of postsynaptic activity affects its electrochemical properties, O'Brien et. al. investigated mEPSCs of cultured spinal neurons after chronic increases in activity (by application of $GABA_AR$ and glycine antagonists) or decreases in activity (by application of GluR antagonists) (O'Brien et al.

1998). Like Turrigiano et al., they found that chronic inhibition leads to increased mEPSC amplitude while chronic increases in activity lead to decreased mEPSC amplitude with no changes in mEPSC frequency. O'Brien et. al. went on to more specifically investigate whether or not changes in mEPSC amplitude were due to changes in surface AMPARs by measuring labeled GluA1 and GluA2. They found that increased activity leads to decreased surface AMPARs, and decreased activity leads to increased surface AMPARs. This evidence was corroborated by Lissin, et al. who showed that increased activity in hippocampal culture induced by application of picrotoxin (a $GABA_AR$ antagonist) leads to decreased labeled GluA1 and AMPAR mEPSCs (Lissin et al. 1998). Together these papers, in three different cellular models (cortical, spinal, and hippocampal neuron cultures), established a mechanism whereby neurons can modulate postsynaptic AMPARs in response to prior postsynaptic activity. Importantly, this mechanism provides a way for neurons to avoid runaway LTP and LTD and maintain firing within a target range.

Moreover, synaptic scaling is not just an *in vitro* phenomenon. Similar experimental paradigms in mouse models also lead to synaptic scaling. Several days of intraocular TTX, monocular deprivation, and binocular enucleation all scale up AMPAR mEPSCs in layer V1 2/3 pyramidal neurons (Pozo and Goda 2010). This *in vivo* mechanism likely also depends on regulation of synaptic AMPARs, since monocular deprivation or two days of dark-rearing are associated with increased AMPAR abundance and mEPSC amplitude in the visual cortex (Desai et al. 2002, Goel et al. 2006, Pozo and Goda 2010). From these studies, it has been hypothesized that synaptic scaling could play a prominent

role in the nervous system during development. Neurodevelopment is a time of rapid change in synaptic strengths across the brain and synaptic scaling may help maintain network homeostasis. Likewise, synaptic scaling may also have a role in regeneration after injury (Lee 2012).

Synaptic scaling: a global or local phenomenon?

Initial work on synaptic scaling exposed the entire neuronal culture to the same pharmacological agents, raising the questions of whether synaptic scaling can be induced cell-autonomously and if local (e.g. dendritic or synaptic) activity blockade or enhancement can induce local scaling. Several lines of evidence suggest that synaptic scaling is cell-autonomous. Overexpression of an inwardly rectifying potassium channel (Kir2.1) that inhibits neuronal activity in single cells results in upregulation of mEPSCs in neurons expressing this channel (Burrone et al. 2002). Perfusion of TTX directly onto the soma of a neuron in culture also induces increased mEPSCs and AMPAR expression (Ibata et al. 2008), suggesting that blockade of activity within a neuron is sufficient to trigger scaling in that neuron. Scaling down is also cell-autonomous: in a model of increased activity, optogenetic stimulation of neurons for 24 hours leads to cell-autonomous decreases in AMPAR-mediated mEPSCs (Goold and Nicoll 2010).

Whether or not synaptic scaling can be induced locally at individual dendrites, or even at individual synapses is a matter of ongoing debate. While local application of TTX to a small region of dendrites fails to alter synaptic AMPARs in that region (Ibata et al. 2008), addition of the NMDAR antagonist, APV, to local dendritic perfusion of TTX does

increase synaptic AMPAR expression (Sutton et al. 2006). This differential response may be due to APV-induced blockade of NMDAR mEPSCs, which have been hypothesized to stabilize synaptic function (Sutton et al. 2006). Furthermore, inhibition of a subset of neurons in culture by transgenic expression of Kir2.1 channels leads to a homeostatic increase specifically at the corresponding synapse (Hou et al. 2008, Hou et al. 2011). This suggests that if a neuron senses long-term deprivation of activity at a specific synapse, it will attempt to raise that synapse's gain by increasing the amount of AMPARs. The discrepancy between results highlights the variation in scaling protocols, and demonstrates that subtle differences in protocols can have meaningful effects on neuronal function. Importantly, different scaling protocols may trigger different, independent scaling mechanisms. Theoretically, one scaling mechanism may function locally in response to activity and AMPAR blockade, and another may respond to activity blockade alone by globally scaling all synapses in the neuron (Turrigiano et al. 1998, Lee 2012). Further research is needed to explore these different mechanisms.

While most of the evidence for synaptic scaling points to postsynaptic mechanisms, it is important to note that certain models also indicate presynaptic mechanisms. These studies have shown an effect not only on mEPSC amplitudes, but also on mEPSC frequencies, highlighting increases in presynaptic vesicle pool size, increased turnover rate per vesicle, and enlarged presynaptic active zones (Thiagarajan et al. 2005, Pozo and Goda 2010). It has been hypothesized that presynaptic mechanisms may be more prominent in younger neuronal cultures or specific to certain synapses, though the reasons and

mechanisms behind this difference have not yet been resolved (Turrigiano 2008, Lee 2012).

Synaptic scaling: AMPAR subunit regulation

Complex regulation of AMPARs underlies acute forms of plasticity like LTP and LTD and, accordingly, similar mechanisms have been observed in synaptic scaling. There is conflicting evidence about which AMPAR subunits are regulated in response to chronic changes in activity. While some studies suggest that both GluA1 and GluA2 can be regulated (O'Brien et al. 1998, Wierenga et al. 2005), other studies point to specific regulation of GluA1 (Ju et al. 2004, Thiagarajan et al. 2005, Soares et al. 2013) or GluA2 (Ibata et al. 2008, Gainey et al. 2009). It is likely that the discrepancy is due to differences in the models used in each study, and may underlie the differences between local and global scaling discussed above. For example, simultaneous blockade of network activity with TTX and of NMDARs with APV leads to selective upregulation of GluA1, while blocking with TTX alone leads to upregulation of GluA1 and GluA2 (Lee 2012). Thus, activity blockade with TTX triggers a global response that upregulates AMPARs containing GluA1 and GluA2, while simultaneous activity blockade and NMDAR antagonism triggers a local response that upregulates GluA1. In light of the calcium-impermeability that GluA2 confers to AMPARs, different stimuli are likely to cause differential GluA2 expression. Specifically, blocking NMDARs may provide a signal to the neuron to increase overall calcium permeability of the postsynaptic membrane, increasing GluA1, but not GluA2 expression.

In fact, there is now ample evidence that synaptic scaling leads to the upregulation and insertion of calcium-permeable AMPARs (CP-AMPARs) into the postsynaptic membrane. CP-AMPAR antagonism blocks the mEPSC amplitude increase induced by NMDAR or AMPAR antagonism but not by TTX (Thiagarajan et al. 2005, Sutton et al. 2006). This is consistent with differential regulation of the GluA2 subunit in response to different stimuli. However, there is also evidence that CP-AMPAR antagonism blocks mEPSC amplitude increases in response to TTX alone (Soares et al. 2013, Kim and Ziff 2014), which is inconsistent with data suggesting that TTX leads to upregulation of GluA1 and GluA2. It is likely that these differences are due to the difference in models, as studies showing a lack of CP-AMPAR-dependent response to TTX were done in hippocampal culture, while studies showing a CP-AMPAR-dependent response to TTX were done in cortical neurons or organotypic hippocampal slices. Although further work will be necessary to unravel the precise functional differences in these models, it is clear that selective regulation of the GluA2 subunit is an important feature of synaptic scaling.

Synaptic scaling: signaling molecules

A host of molecules and mechanisms have been proposed to mediate the changes in mEPSCs and AMPARs involved in synaptic scaling. These include the signaling molecules TNFα, BDNF, and retinoic acid, and the cell-adhesion proteins N-cadherin and beta-catenin. TNFα scavengers block increases in mEPSCs and AMPAR expression induced by TTX, and glial expression of TNFα is necessary for scaling up (Stellwagen and Malenka 2006). While short-term BDNF application (several hours) increases surface GluA1, GluA2, and GluA3 (Caldeira et al. 2007), 48 hours of treatment blocks

increased mEPSC amplitudes induced by TTX treatment (Rutherford et al. 1998). Blocking BDNF prevents the decrease in surface GluA1 induced by BIC (Reimers et al. 2014). Additionally, knock-down of downstream effectors of BDNF, like MSK1, prevents TTX-induced increases in mEPSCs and surface GluA1 (Correa et al. 2012), suggesting that BDNF functions in both scaling up and down. Retinoic acid (RA) is another signaling molecule implicated in synaptic scaling. Twenty-four hour treatment of neurons in culture or slices with TTX and APV enhances RA synthesis and application of exogenous RA increases neurotransmission primarily through increased AMPAR surface expression and mEPSCs (Aoto et al. 2008). RA's mechanism of action appears to be through translation, as transcriptional inhibitors do not block its homeostatic effects (Maghsoodi et al. 2008). Cell-adhesion molecules have also been implicated, as a dominant-negative version of N-cadherin compromises TTX-induced scaling up of AMPARs, whereas deletion of β-catenin eliminates global homeostatic regulation (Okuda et al. 2007, Vitureira et al. 2012).

It has also been demonstrated that specific intracellular signaling pathways are important for synaptic scaling. The PI3K-Akt pathway, which induces protein synthesis and promotes AMPAR insertion into the membrane (Schratt et al. 2004) plays an essential role in scaling. Presenilin-1 (PS1), an activator of the PI3K-Akt pathway is necessary for scaling up AMPAR insertion in response to activity blockade (Pratt et al. 2011). Furthermore, several lines of evidence suggest that polo-like kinase 2 (Plk-2) is critical for scaling down synaptic strength. Plk-2 disrupts the interaction of GluA2 and N-ethylmaleimide-sensitive factor (NSF, a necessary component of the SNARE machinery

whose interaction with GluA2 is required for GluA2 plasma membrane insertion), which leads to loss of surface GluA2 and decreased AMPAR current (Evers et al. 2010). Additionally, miR-134 is upregulated by chronic high network activity, leading indirectly to increased Plk-2 and decreased surface GluA2 (Fiore et al. 2014).

Proteins controlling AMPAR trafficking and recruitment to the synapse offer additional targets for regulation in synaptic scaling. The AMPAR binding proteins PICK1 and GRIP1 have both been implicated in scaling. While knockout of PICK1, which typically drives removal of synaptic GluA2-containing AMPARs occludes TTX-induced scaling up (Anggono et al. 2011), GRIP1, which competes with PICK1 for binding the GluA2 C-tail and positively regulates postsynaptic GluA2 abundance, is necessary and is recruited to synapses for scaling up (Gainey et al. 2015). One critical trafficking step, mediated by the immediate early gene Arc/Arg3.1, is regulation of exo- and endocytosis of receptors from the synapse. Arc/Arg3.1 interacts with components of the endocytic machinery, including endophilin and dynamin, to increase the rate of AMPAR endocytosis. Treatment with chronic TTX leads to decreased Arc/Arg3.1 expression while treatment with BIC leads to increased Arc/Arg3.1 expression (Shepherd et al. 2006). Moreover, overexpression of Arc blocks scaling up of synaptic AMPARs induced by activity blockade, consistent with Arc/Arg3.1's role promoting AMPAR endocytosis (Shepherd et al. 2006). AMPAR degradation is also altered in synaptic scaling. Scaling down leads to AMPAR internalization and ubiquitination through the E3 ligase Nedd4 which leads to local degradation of AMPARs (Scudder et al. 2014). Interestingly, Nedd4 also accumulates at synapses after synaptic activation (Hou et al. 2011).

As the list of molecules involved in synaptic scaling continues to grow, it will be important to understand the relationships between the various signaling pathways and to determine discrete mechanisms for scaling up versus scaling down. There is not complete concordance between the molecules implicated in scaling up and scaling down, suggesting that there might be two separate signaling pathways regulating these phenomenon. However, one broad category of intracellular signaling molecules that may underlie many of the diverse scaling mechanisms described above is intracellular calcium signaling.

Calcium signaling and synaptic plasticity

Calcium has been well-established as a critical signaling molecule in various forms of synaptic plasticity, such as LTP and LTD. The flow of calcium ions into the postsynaptic membrane triggers downstream kinases that perform a diverse set of functions for the neuron.

One of the major regulatory proteins involved in calcium signaling is calmodulin (CaM). Binding of calcium to CaM induces a conformational change exposing a hydrophobic residue which promotes interactions of the Ca^{2+}/CaM complex to numerous effectors such as the Ca^{2+}/CaM-dependent kinases (CaMKs). CaMKs are a ubiquitous and highly conserved group of serine/threonine kinases that phosphorylate a wide range of downstream targets (Wayman et al. 2008). They are present in most mammalian tissues and highly abundant in the brain. Currently, there are five well-studied CaMKs (CaMK

kinase (CaMKK), and CaMKI-IV). All of the CaMKs except for CaMKIII share canonical motifs of the Ser/Thr kinase family, indicating that CaMKIII may be part of a different family. CaMKIII phosphorylates a single target protein, eukaryotic elongation factor-2, which suppresses translation elongation, and may have roles in regulating mGluRs in LTD. CaMKK, CaMKI, CaMKII, and CaMKIV have similar structures including a catalytic domain and an autoinhibitory domain. CaMKII also has a C-terminal association domain, which allows it to form complex oligomers critical for its functionality (Wayman et al. 2008).

CaMKK, CaMKI, and CaMKIV are members of the CaMK cascade and their activity is regulated in a similar manner. Binding of Ca^{2+}/CaM relieves intramolecular autoinhibition which leads to basal kinase activity and exposes an activation loop domain (this domain is not present in CaMKII). Phosphorylation of the CaMKI and CaMKIV activation loop (Thr200) by CaMKK leads to increased kinase activity and allows CaMKI and CaMKIV to function even when calcium levels are low (Chow et al. 2005). Once activated, these kinases go on to perform various roles for the cell, many relating to regulatory roles in synaptic plasticity.

One of the key downstream targets of several CaMKs is the transcription factor cAMP-response element (CRE) binding protein (CREB). CREB is a member of a family of cAMP-responsive genes belonging to the basic-domain, leucine zipper class of proteins. While canonically thought to activate transcription by binding CRE elements, alternative splicing can generate repressive isoforms. For example, alternative splicing can create

truncated CREB proteins which lack the DNA binding domain or nuclear localization signal (De Cesare et al. 1999). CREB-mediated transcription is classically activated by calcium influx through L-type calcium channels and NMDARs. Activation then leads to either CaMK or MAPK signaling (Deisseroth et al. 2003). Together, the CaMK-CREB pathway is a canonical mediator of synapse-to-nucleus signaling, allowing information from synapses to regulate gene expression.

Members of the CaMK family have critical roles in LTP and LTD. CaMKII is essential for LTP (Malenka and Bear 2004). CaMKII phosphorylates AMPARs to regulate their synaptic abundance and biochemical properties. CaMKII's role in phosphorylating CREB during LTP gives it a key function in activity-induced gene transcription. CaMKI has also been implicated indirectly in CREB-mediated transcription as well as in regulation of dendritic branching and spine formation. One of its roles in LTP may be in regulating trafficking of CP-AMPARs (Wayman et al. 2008).

CaMKIV is part of a synapse-to-nucleus signaling mechanism that regulates transcription during synaptic plasticity (Wayman et al. 2008). CaMKIV is expressed predominantly in the nucleus (Matthews et al. 1994, Bito et al. 1996, Kang et al. 2001) and can directly phosphorylate CREB, leading to activation of a transcriptional response (Enslen et al. 1994, Matthews et al. 1994, Sun et al. 1994, Bito et al. 1996, Hardingham et al. 2001, Chow et al. 2005). CaMKIV also phosphorylates CREB binding protein (CBP), whose activation is critical for CREB-mediated gene expression (Impey et al. 2002, Chow et al. 2005). As would be expected for a gene that regulates CREB and LTP, CaMKIV

knockout mice have impaired LTP, LTD, and long term memory (Kang et al. 2001). Other downstream targets of CaMKIV, such as the histone deacetylase, HDAC-4 highlights its importance in regulating gene expression.

Calcium signaling and synaptic scaling

Given the importance of calcium signaling in short term forms of synaptic plasticity like LTP and LTD, it is not surprising that some of the same molecular pathways are utilized in synaptic scaling. Calcium signals may be the critical trigger that neurons respond to in synaptic scaling, as L-type calcium channel blockade phenocopies TTX treatment, leads to increased GluA1, and blocks AMPAR depression in the setting of increased activity (Thiagarajan et al. 2005, Ibata et al. 2008, Goold and Nicoll 2010). Additionally, calcium transients are decreased in models of scaling up and blocking these transients phenocopies TTX-induced scaling up (Ibata et al. 2008).

The CaMK family is also important for synaptic scaling. CaMKII has several isoforms with complementary functions in scaling. αCaMKII overexpression decreases AMPAR mEPSC amplitudes, while βCaMKII overexpression increases mEPSCs (Groth et al. 2011). Additionally, transport of AMPARs to the postsynaptic membrane during activity blockade depends on CaMKII phosphorylation of GluA1 (Bassani et al. 2013). However CaMKII may not be required for activity-induced scaling down of AMPARs, as CaMKII inhibitors do not block depression of mEPSCs (Goold and Nicoll 2010).

The CaMKK signaling cascade also plays a role in synaptic scaling. Inhibitors of CaMKK lead to increased AMPAR mEPSC amplitudes and block photostimulation-induced scaling down (Ibata et al. 2008, Goold and Nicoll 2010). Chronic TTX treatment leads to reduced phospho-CaMKIV in the nucleus, suggesting that normally, activated nuclear CaMKIV represses AMPARs. Consistent with this idea, a dominant-negative CaMKIV mimics the effects of TTX on GluA1 and mEPSCs (Ibata et al. 2008). CaMKIV is also involved in scaling down, because a dominant-negative CaMKIV blocks homeostatic downregulation of AMPARs (Goold and Nicoll 2010).

Together, these results suggest that the CaMKK/CaMKIV signaling pathway negatively regulates AMPARs and that in scaling up there is decreased activation of this pathway. If the downstream target of this pathway is CREB, then CREB should also negatively regulate AMPARs and be decreased in scaling up. However, according to one study, scaling up induces calcium release from the ER which maintains CREB activity for up to 48 hours (Kim and Ziff 2014). This correlates CREB activity with AMPAR scaling up and is inconsistent with less activated CaMKIV during scaling up, since decreased activated CaMKIV should lead to less phosphorylated CREB. One important consideration is the timing of measurements during scaling. While less-activated nuclear CaMKIV was reported at four hours after TTX treatment, increased CREB activity was reported after 48 hours. It would be interesting to measure activated CaMKIV at 48 hours and activated CREB at four hours, to determine if the activity of these two proteins is correlated. More research will be needed to address the role of CREB in synaptic scaling.

Regulation of AMPAR expression in synaptic scaling

The CaMKK/CaMKIV/CREB signaling pathway is a well-studied regulator of transcription. Several lines of evidence support the idea that both transcriptional and translational regulation mediate synaptic scaling. Synaptic scaling up increases protein synthesis in dendrites (Sutton et al. 2004) and increases the abundance of both pre-existing and recently synthesized GluA1 (but not GluA2) (Ju et al. 2004). Furthermore, increased GluA1 at synapses is dependent on local protein synthesis (Sutton et al. 2006).

Several studies have also shown direct effects of scaling on AMPAR mRNA levels. BIC-induced scaling down leads to decreased GluA2 mRNA (Qiu et al. 2012), while chronic activity blockade with TTX and APV upregulates GluA1 mRNA (Orlandi et al. 2011). Posttranscriptional regulation has been invoked to explain some of these changes. TTX and APV treatment leads to increased expression of a GFP reporter under control of the GluA1 3'UTR, suggesting that 3'UTR-mediated regulation of mRNA stability is important for scaling up. miR-92a levels decrease after TTX and APV treatment, which relieves repression of a miR-92a target site in the GluA1 mRNA 3'UTR (Letellier et al. 2014), implicating miRNAs as a mechanism regulating AMPAR mRNA levels. RA also regulates GluA1 mRNA in response to activity blockade by removing the RA receptor α translational block from the GluA1 5'UTR. Thus, regulation of AMPAR mRNA and its translation are important mechanisms for both synaptic scaling up and scaling down.

Multiple studies have emphasized the role of transcription in both synaptic scaling up and scaling down. The transcriptional inhibitor actinomycin D blocks TTX-induced increases

in GluA2 even in the earliest phase of synaptic scaling (within 4 hours) (Ibata et al. 2008, Gainey et al. 2015) and blocks photostimulation-induced scaling down (Goold and Nicoll 2010). Recently, several studies have highlighted specific mechanisms that regulate transcription in synaptic scaling. For example, BIC-induced decreases in GluA2 mRNA are mediated by the transcriptional repressor MeCP2 (Qiu et al. 2012). Recent work also suggests a role for DNA methylation, as knockdown of DNA methyltransferase phenocopies chronic TTX-induced AMPAR mEPSC scaling up, and this effect is transcription-dependent (Meadows et al. 2015). Additionally, expression of Tet3, a protein involved in the methylation pathway, is regulated by bidirectional changes in activity and Tet3 knockdown cells have increased surface GluA1 (Yu et al. 2015). Thus, one mechanism regulating gene expression in synaptic scaling may be methylation, though it is unclear precisely how this leads to increased AMPARs. RNA sequencing data comparing cells treated with Tet3 knock-down in the setting of chronic TTX vs. Tet3 knock-down alone implicates GluA3, Arc, and BDNF (Yu 2015). Thus DNA methylation may be altered to either directly or indirectly regulate AMPAR subunit expression through intermediates like Arc and BDNF.

For synaptic scaling to involve a transcriptional response, there must be a signaling pathway that communicates synaptic information to the nucleus. In fact, there are several well-known mechanisms that mediate responses to glutamatergic transmission and transcription. In one pathway, synaptic activation of glutamate receptors leads to depolarization and calcium entry through L-type voltage-gated calcium channels (VGCC). There may also be secondary calcium signaling through release from the ER or

Golgi by activation of ryanodine or IP3 receptors. Calcium influx into the cytoplasm then triggers numerous signaling pathways, most prominently CaMKs, to relay a signal to the nucleus (Bading 2013). It was previously not known how mammalian CaMKs signaled to the nucleus, but a recent study has proposed a novel mechanism where, with the assistance of several CaMKII isoforms, $Ca^{2+/}$CaM translocates from the synapse to the nucleus where it activates the nuclear CaMK cascade (CaMKK phosphorylates CaMKIV) to regulate gene transcription (Ma et al. 2014, Cohen et al. 2015). This pathway was shown to occur in cultured superior cervical ganglion neurons after depolarization with either KCl or a train of spikes (Ma et al. 2014). Thus, it is not known whether the same signaling pathway regulates CaMKIV transcription in synaptic scaling.

Clinical implications of AMPAR regulation and synaptic scaling

Global regulation of AMPARs has been implicated in several clinical diseases including Fragile X syndrome, schizophrenia, Alzheimer's disease (AD), amyotrophic lateral sclerosis, stroke, Parkinson's disease, depression, and epilepsy (Orlandi et al. 2011). A post mortem analysis of patients with major depressive disorder found increased mRNA for many GluR genes (Gray et al. 2015). It is likely that regulation of AMPARs in synaptic scaling contributes to some of these pathologies. For example, defects in synaptic scaling specifically have been postulated to contribute to AD and epilepsy. Mice with a familial AD mutation in presenilin-1 have impaired AMPAR mEPSC scaling up (Pratt et al. 2011). Trasande et al. examined network activity of hippocampal slices after 48 hours of activity-deprivation, and found that slices exhibited a spontaneous bursting firing pattern reminiscent of epilepsy (Trasande and Ramirez 2007). This suggests that,

while synaptic scaling may stabilize synapses and neuronal firing under normal conditions, there is the possibility for it to become pathological and lead to aberrant network activity. A recent theory has also proposed that synaptic scaling is a critical mediator of sleep, suggesting that sleep disorders may be caused by aberrant homeostatic plasticity (Tononi and Cirelli 2006). Currently, however, the role of synaptic scaling in disease is incompletely understood and more research will likely provide novel therapeutic targets in synaptic scaling pathways.

Since its discovery, the function and mechanisms of synaptic scaling have begun to come into focus. It is hypothesized that synaptic scaling operates both *in vitro* and *in vivo* to stabilize synaptic weights, prevent runaway potentiation and depression, and keep neuronal firing within a target range. While the evidence is increasing that scaling performs all of these functions, it has yet to be shown that it operates physiologically *in vivo* to control neuronal firing rates, nor has it been directly demonstrated to prevent runaway potentiation and depression. Future studies will have to devise models within which to test these hypothesis. It is clear, however, that there is a mechanism both *in vitro* and *in vivo* that responds to alterations in postsynaptic activity and glutamatergic transmission by homeostatically and multiplicatively adjusting synaptic strengths. Many signaling molecules and pathways have been implicated in both scaling up and scaling down, but a model unifying these various pathways is still wanting. A simplified model states that neurons utilize calcium signaling pathways, like the CaMKs, to respond directly to changes in calcium transients, leading to changes both in the regulation of

AMPAR trafficking and synthesis, as well as regulation of the multitude of proteins that regulate AMPARs.

C. elegans as a model system

The mammalian brain contains around 100 billion neurons and over 100 trillion synapses. A single hippocampal neuron can have 10,000 synapses. While advances in studying the mammalian brain in slice and *in vivo* have made remarkable progress, the complexity of the brain still remains a considerable obstacle for many areas of research. Since Sydney Brenner began using *C. elegans* in the 1970s to study development and the nervous system, this small nematode has greatly informed our understanding of mammalian biology. Significant achievements in *C. elegans* include the first fully sequenced genome of a metazoan, the discovery of RNA interference (RNAi), the unraveling of genetically programmed cell death pathways, and the first use of GFP as a biological marker (Corsi et al. 2015).

C. elegans is a microscopic nematode that dwells in several environments, most commonly rotting fruit or vegetable matter. *C. elegans* hatches as .25 mm larvae and grows to be up to 1mm long, passing through four larval stages (L1-L4) before reaching adulthood, where animals can live for several weeks. Hermaphrodites have two X chromosomes, while males, with one X chromosome, arise at a frequency of .2% due to chromosomal nondisjunction. Animals grow from egg to egg-laying adult in about three days, and one adult can have up to 300 genetically identical progeny (Corsi et al. 2015).

This allows for *C. elegans* to be grown quickly in the laboratory and makes it easy to generate hundreds of identical progeny for phenotypic and genotypic assessment.

C. elegans shares multiple tissues in common with mammals, such as a nervous system, intestine, reproductive system, glands, and muscle. Each animal has the exact same number of cells, and the lineage of each cell has been mapped. Additionally, although the genome is relatively small (100 MB), *C. elegans* has over twenty-thousand protein coding genes and 38% of these genes have predicted orthologs in the human genome, while 60-80% of human genes have predicted orthologs in the *C. elegans* genome (Corsi et al. 2015). The *C. elegans* genome shares similar features of gene expression with mammals, such as alternative splicing, miRNAs, introns, and 5' and 3' untranslated regions (UTRs). Thus, *C. elegans* offers many advantages as a model organism for studying the nervous system including its fully sequenced genome, the invariant cell number among progeny, short life cycle, ease of maintenance, simple behavioral assays, and the wide availability of genetic mutants. Additionally, *C. elegans* are transparent, allowing for *in vivo* use of fluorescent proteins.

***C. elegans*: nervous system and GluRs**

The nervous system of *C. elegans* has proven especially useful as a field of study. Each hermaphrodite animal has exactly 302 neurons and roughly 7,000 synaptic connections. All of these connections, including gap junctions, have been mapped by serial electron microscopy (EM) (White et al. 1986). Like mammals, the nervous system contains sensory neurons, interneurons, and motor neurons. Neurons in *C. elegans* share many of

the same neurotransmitter and receptor systems as mammals. In particular, the glutamate signaling system has a high degree of homology. There are ten ionotropic GluRs in *C. elegans*, 8 non-NMDA type (*glr-1* to *glr-8*) and two NMDA type (*nmr-1* and *nmr-2*) receptors. The GluRs have many conserved regions with mammalian GluRs (Brockie and Maricq 2006). Of the non-NMDA type receptors, GLR-1 is most homologous to AMPA receptor subunits, sharing 56% homology (Hart et al. 1995, Maricq et al. 1995, Brockie et al. 2001).

GLR-1 is expressed predominantly in a group of neurons in the head as well as a pair of neurons in the tail. Processes from these neurons extend along the ventral side of the animal where they make synapses with sensory neurons, other interneurons, and motor neurons. *glr-1* has been implicated in behaviors including spontaneous forward and backward movement, response to touch, chemotaxis, and learning and memory. Its expression in a group of neurons called the command interneurons controls forward and backward movement. Electrophysiological studies have determined that GLR-1 gates a fast, AMPA-like current. *glr-2*, but not *glr-1*, loss-of-function mutants can still form functional glutamate-gated channels, suggesting that in the absence of GLR-2, GLR-1 forms homomeric channels (Mellem et al. 2002, Brockie and Maricq 2006).There is evidence that GLR-1 forms heteromeric channels with GLR-2, but GLR-2 expression is not restricted to GLR-1-expressing neurons, so it may also be able to form homomers in a discrete population of neurons or heteromers with other GluR subunits (Mellem et al. 2002, Chang and Rongo 2005). Unlike in mammalian neurons, where GluA2 is frequently edited to be calcium impermeable, *glr-1* and *glr-2* are not edited, and so

AMPARs containing these subunits are all permeable to calcium (Strutz-Seebohm et al. 2003). Interestingly, *C. elegans* do not have voltage-gated sodium channels or action potentials, but rather neurotransmission occurs passively. *C. elegans* neurons are isopotential in nature and thus changes in membrane potential are not transmitted linearly, but rather occur instantaneously throughout the cell. As of yet, there is no known correlate of LTP, LTD, or synaptic scaling in *C. elegans*. This may be attributable to the relative difficulty of performing electrophysiology in these small animals. However, many studies have confirmed that *C. elegans* can perform associative learning, which depends on both *glr-1* and the transcription factor *crh*-1/CREB. Several studies have shown that the size of GLR-1 synaptic puncta changes in accordance with learning protocols, suggesting that, like in vertebrates, AMPARs may be a key locus for regulation of learning and memory (Stetak et al. 2009, Hadziselimovic et al. 2014).

Together with the relative simplicity of the *C. elegans* nervous system, the presence of a homologous glutamate neurotransmitter system makes this organism a powerful genetic model for studying basic mechanisms of glutamate neurotransmission. Indeed, AMPAR regulation and trafficking share many similarities with mammals and work in *C. elegans* has contributed much to our knowledge of these processes. Many of these insights have come from studies using GLR-1 tagged with GFP (GLR-1::GFP) to study GLR-1 localization and trafficking. This construct is functional, as it rescues behavioral phenotypes of *glr*-1 null mutants (Rongo et al. 1998). GLR-1::GFP forms puncta in the VNC that are closely opposed to presynaptic markers, suggesting that these puncta represent synapses (Rongo et al. 1998, Burbea et al. 2002), and the number of puncta is

similar to the number of glutamatergic inputs in the VNC enumerated by EM (White et al. 1986). Because GLR-1::GFP can be visualized *in vivo* in *C. elegans*, it has been an enormously useful research tool, particularly in mutagenic screens for genes that regulate GLR-1 trafficking.

C. elegans: GLR-1 trafficking

Canonical GLR-1 trafficking begins after the receptor is synthesized in the soma, whereupon it is trafficked to synapses by kinesin motor proteins, including KLP-4 and UNC-116. KLP-4 is a plus-end directed motor and member of the kinesin-3 family of motor proteins, homologous to drosophila KHC-73 and mammalian Kif13. *klp-4* loss-of-function mutants have decreased abundance of GLR-1 in the VNC and reduced anterograde movement of GLR-1 puncta, suggesting KLP-4 is necessary for normal trafficking from the cell body to the synapse (Monteiro et al. 2012). UNC-116, the homolog of mammalian Kif5, is also necessary for normal anterograde GLR-1 trafficking, and is involved in transporting GLR-1 to and from distal (posterior) synapses (Hoerndli et al. 2013).

At the synapse, membrane proteins interact with and regulate GLR-1 function. For example, SOL-1, a CUB domain-containing transmembrane protein, binds GLR-1 and regulates its conductance properties. SOL-1 was found in a screen for mutants that suppress the *lurcher* phenotype, which is caused by overexpression of a constitutively active GLR-1 channel (GLR-1 (A/T)) (Zheng et al. 2004). Because GLR-1 positively regulates reversal behavior, such that *glr-1* null animals exhibit fewer spontaneous

reversals than wild type animals, overexpression of constitutively active GLR-1 leads to a hyper-reversal phenotype (Zheng et al. 1999). Mutations in *sol-1* (suppressor-of-lurcher) suppress this phenotype by disrupting normal GLR-1 channel conductance (Zheng et al. 2004, Walker et al. 2006, Zheng et al. 2006). Since the discovery of *sol-1* in *C. elegans*, several CUB domain proteins have been identified in mammals that regulate kainate and NMDARs (Ng et al. 2009, Zhang et al. 2009).

Once at the synapse, GLR-1 undergoes a process of exo- and endocytosis to regulate its abundance in the postsynaptic membrane. In *C. elegans*, UNC-43/CaMKII, is required for both delivery of GLR-1 to synapses and membrane insertion (Rongo and Kaplan 1999, Hoerndli et al. 2015). Clathrin-mediated endocytosis removes GLR-1 from the synaptic membrane and into vesicles. This process is mediated by UNC-11/AP180, a clathrin-adaptin that, when mutated, prevents GLR-1 endocytosis and leads to receptor accumulation in the VNC (Burbea et al. 2002). Ubiquitin also mediates endocytosis of GLR-1. Ubiquitination occurs by the reversible conjugation of ubiquitin molecules onto lysine residues by E3 ubiquitin ligases (Mabb and Ehlers 2010). When all four cytoplasmic lysine resides of GLR-1 are mutated to arginines (GLR-1::4KR), GLR-1 ubiquitination is blocked and there is an increase in GLR-1 receptors at synapses in the VNC, suggesting that ubiquitination is required for GLR-1 endocytosis. Ubiquitinated GLR-1 accumulates in *unc-11* mutants, suggesting a model where GLR-1 is first ubiquitinated and then internalized from the synaptic membrane (Burbea et al. 2002). Although it is not clear which E3 ligase ubiquitinates GLR-1 in *C. elegans*, USP-46 has been shown to act as the deubiquitinating enzyme (DUB), and accordingly, *usp-46* loss-

of-function mutants have decreased synaptic GLR-1 in the VNC (Kowalski et al. 2011). While these and other studies show that GLR-1 is ubiquitinated and then endocytosed via clathrin-mediated endocytosis, there may also be clathrin-independent processes (Glodowski et al. 2007). Many of the molecules and mechanisms regulating GLR-1 are conserved in mammals, including ubiquitination of the receptor (Colledge et al. 2003, Patrick et al. 2003), specific ubiquitin ligases (Schwarz et al. 2010, Fu et al. 2011, Lin et al. 2011, Lussier et al. 2011), and the DUB, USP-46 (Scudder et al. 2014, Huo et al. 2015).

Electrophysiological experiments at neuron-neuron synapses in *C. elegans* are challenging due to the small soma of *C. elegans* neurons. Because of this difficulty, little is known about plasticity at these synapses, and even less about synaptic scaling. There is, however, evidence of homeostatic mechanisms regulating GLR-1 in response to activity. In particular, loss-of-function of *eat-4*, the vesicular glutamate transporter necessary for packaging glutamate into presynaptic vesicles, leads to an increase in glutamate-evoked currents and a corresponding increase in the abundance of synaptic GLR-1 protein (Grunwald et al. 2004). Mutation of *unc-11*/AP180 in *eat-4*/VGLUT mutants does not further increase the abundance of synaptic GLR-1, demonstrating that recycling of GLR-1 is required (Grunwald et al. 2004). These results suggest that in response to decreased glutamatergic signaling, neurons in *C. elegans* homeostatically increase synaptic GLR-1, at least partially through changes in GLR-1 recycling. It is unknown whether other features of synaptic scaling, such as CaMK signaling are involved in a scaling mechanism in *C. elegans*.

C. elegans: CaMK signaling

There is, however, strong evidence that a homologous CaMK signaling pathway exists and functions in *C. elegans*, as the genome contains a homologous CaMKK (*ckk-1*) and CREB (*crh-1*). While mammals express CaMKI and CaMKIV, *C. elegans* have only one gene that shares similarities to both of these kinases, *cmk-1*. Despite sharing slightly more sequence homology with CaMKI, CMK-1 is functionally more similar to CaMKIV: its expression is more nuclear than cytoplasmic, it is expressed in a distinct subset of cells (neurons) as opposed to ubiquitously, and it activates CREB (Eto et al. 1999, Kimura et al. 2002). Unlike in mammals, where cytoplasmic CaMK signaling accesses the nucleus by translocation of Ca^{2+}/CaM, CMK-1/CaMK itself appears to be the translocating agent in *C. elegans* (Eto et al. 1999, Cohen et al. 2015). There is no known role for *unc-43/*CaMKII in signaling to nuclear CaMKs in *C. elegans*. As in mammals, one of the key downstream targets of CaMK signaling is *crh-1*/CREB. *crh-1/*CREB shares 50% identify with vertebrate CREBs with conservation of the leucine zipper domain and the DNA binding domain. It is expressed ubiquitously throughout the animal (Mair et al. 2011). There is a phosphorylation site homologous to the Ser133 site in mammals that is necessary to activate CREB-mediated transcription (Kimura et al. 2002). Co-expression of CMK-1/CaMK with a CREB transcriptional fluorescent reporter leads to increased fluorescence which is dependent on the presence of endogenous CKK-1. This suggests that the CaMK pathway functions in *C. elegans* to regulate CREB-mediated transcription (Kimura et al. 2002).

In this thesis, I present data supporting the hypothesis that chronic changes in synaptic activity regulate transcription of *glr-1*, which is mediated by a CMK-1/CaMK signaling pathway. In Chapter 2, I show that mutants with altered GLR-1 synaptic abundance and/or altered GLR-1 activity have bidirectional changes in *glr-1* transcription. In Chapter 3, I show that the CMK-1/CaMK signaling pathway negatively regulates *glr-1* transcription, and I provide evidence that nuclear translocation of CMK-1/CaMK mediates *glr-1* transcriptional changes in response to changes in activity. In Chapter 4, I present ongoing work using a yeast-1-hybrid system to screen for transcription factors that regulate *glr-1* both basally and in the setting of homeostasis. This work demonstrates a novel pathway in *C. elegans* that responds to changes in neuronal activity by regulating *glr-1* transcription through CMK-1/CaMK signaling. This thesis establishes, for the first time, a direct connection between chronic changes in activity, CaMK signaling, and transcriptional regulation of AMPARs, laying the foundation for the discovery of novel transcriptional regulators involved in synaptic plasticity.

Materials and Methods

Strains

All strains were maintained at 20°C as previously described (Brenner 1974). The following strains were used in this study:

N2
FJ1211 *pzEx329* [Pglr-1::NLS-GFP::LACZ::glr-1 3'UTR]
FJ1217 *pzEx329; glr-1 (n2461)*
pzEx329; klp-4 (tm2114)
FJ1268 *pzEx354* [*Pnmr-1::NLS-GFP::LACZ::glr-1 3'UTR*]
FJ1284 *pzEx354; glr-1 (n2461)*
FJ1271 *pzEx354; klp-4 (tm2114)*
FJ1047 *pzIs29* [*Pglr-1::NLS-GFP::LACZ::unc-54 3'UTR*]
FJ1109 *pzIs29; glr-1 (n2461)*
FJ1073 *pzIs29; klp-4 (tm2114)*
pzIs29; usp-46 (ok2322)
FJ1148 *pzIs29; unc-11 (e47)*
FJ1266 *pzEx352* [*Pglr-1::NLS-mCherry::unc-54 3'UTR*]
FJ1297 *pzEx352; nuIs24*
FJ1313 *pzEx352; nuIs80*
MT6318 *eat-4 (n2474)*
FJ1322 *pzEx329; eat-4 (n2474)*
FJ1237 *pzIs29; eat-4 (n2474)*
FJ1316 *pzEx362* [*Pglr-1::HisCl1*]
pzIs29; *pzEx362* [*Pglr-1::HisCl1*]
PY1589 *cmk-1 (oy21)*
FJ1291 *pzEx329; ckk-1 (ok1033)*
FJ1159 *pzIs29; ckk-1 (ok1033)*
FJ1141 *pzIs29; cmk-1 (oy21)*
pzIs29; cmk-1 (ok287)
FJ1167 *pzIs29; crh-1 (tz2)*
FJ1288 *pzIs29; cbp-1 (ku258)*
FJ1244 *pzIs29; cmk-1 (oy21); pzEx333* [*Pglr-1::CMK-1*]
FJ1222 *pzIs29; pzEx333* [*Pglr-1::CMK-1*]
FJ1235 *pzIs29; cmk-1 (oy21); pzEx338* [*Pglr-1::CMK-1 (K52A)*]
FJ1142 *pzIs29; glr-1 (n2461); cmk-1 (oy21)*
FJ1214 *pzIs29; glr-1 (n2461); crh-1 (tz2)*
FJ1355 *pzIs29; cmk-1 (pg58)*
FJ1356 *pzIs29; glr-1 (n2461); cmk-1 (pg58)*
FJ1310 *pzIs29; unc-11 (e47); ckk-1 (ok1033)*
FJ1272 *pzEx356* [*Pglr-1::CMK-1::GFP*]
FJ1274 *pzEx356; ckk-1 (ok1033)*
FJ1273 *pzEx356; glr-1 (n2461)*
FJ1364 *pzEx356; unc-11 (e47)*
FJ1354 *pzIs29; glr-1 (n2461); pzEx370* [*Pglr-1::CMK-1::EGL-13 NLS*]

FJ1246 *pzEx342* [*Pnmr-1::NLS-GFP::LACZ::unc-54 3'UTR*]
pzEx342; klp-4 (tm2114)
FJ1247 *pzEx342; glr-1 (n2461)*
pzEx329; unc-11 (e47)

Constructs

Plasmids were generated using standard recombinant DNA techniques, and transgenic strains were created by plasmid microinjection.

Pglr-1::NLS-GFP::LACZ::unc-54 3'UTR was made by cloning 5.3 kb upstream of the *glr-1* transcription start site into pPD96.04 (Addgene, Fire Lab *C. elegans* Vector Kit) containing *NLS-GFP::LACZ* to generate plasmid FJ#119 and injected at 50 ng/ul to make *pzEx260*, which was integrated to make *pzIs29*.

Pglr-1::NLS-GFP::LACZ:unc-54 3'UTR (low expresser) was made by injecting the above plasmid at 1 ng/ul to make *pzEx356*.

Pglr-1::NLS-GFP::LACZ::*glr-1 3'UTR* was made by PCR of the *glr-1 3'UTR* from CR3 and cloning into pV6 with Sac1 and Spe1 to make pBM7 and then PCR of *NLS-GFP::LACZ* from *Pglr-1::NLS-GFP::LACZ::unc-54 3'UTR* and cloning into pBM7 with Nhe1. pBM12 was injected at 60 ng/ul to make *pzEx329*.

Pnmr-1::NLS-GFP::LACZ::glr-1 3'UTR was made by digesting Pnmr-1 from pKM05 and swapping into pBM12 for Pglr-1 with Sph1 and BamH1. pBM17 was injected at 50 ng/ul to make *pzEx354*.

Pnmr-1::NLS-GFP::LACZ::unc-54 3'UTR was made by digesting *Pnmr-1* from pKM05 and swapping into *Pglr-1::NLS-GFP::LACZ::unc-54 3'UTR* for *Pglr-1* with Sph1 and BamH1. pBM16 was injected at 50 ng/ul with *Pmyo-2::mCherry* at 10 ng/ul to make *pzEx342*.

Pglr-1::NLS-mCherry::unc-54 3'UTR was made by PCR of mCherry from *Pmyo2::mCherry* and, adding the SV40 NLS 5' and cloning into pV6. pBM26 was injected at 50 ng/ul.

Pglr-1::HisCl1 was made by digesting pNP403 (*Ptag-168::HisCl1::SL2::GFP*] with Nhe1 and Kpn1 and cloning into pV6. pBM29 was injected at 5 ng/ul with Pmyo2::mCherry at 10 ng/ul.

Pglr-1::CMK-1::GFP was made by PCR of *CMK-1::GFP* from *Pttx-1::CMK-1::GFP* (Sengupta lab) and cloning into pV6 with Kpn1 and Sac1. pBM15 was injected at 2.5 ng/ul with Pmyo2::mCherry at 10 ng/ul.

Pglr-1::CMK-1 was made by PCR of CMK- from *Pttx-1::CMK-1::GFP* (Sengupta lab) adding a 3' stop codon and cloning into pV6 with Nhe1 and Kpn1. pBM13 was injected at 25 ng/ul with *Pmyo2::mCherry* at 10 ng/ul.

Pglr-1::CMK-1 (K52A) was made by PCR of CMK-1 (K52A) from *Pttx-1::CMK-1* (K52A) (Sengupta lab) and cloning into pV6 with Nhe1 and Kpn1. pBM14 was injected at 25 ng/ul with Pmyo2::mCherry at 10 ng/ul.

Pglr-1::CMK-1::EGL-13 NLS was made by PCR of *CMK-1::EGL-13 NLS* from *Pttx-1::CMK-1::EGL-13 NLS* (Sengupta lab) and cloning into pV6 with Kpn1 and Sac1. pBM34 was injected at 25 ng/ul with Pttx-3::GFP at 50 ng/ul.

Epifluorescence Microscopy

GFP Reporter Quantitation. All GFP or mCherry reporter imaging experiments were performed with a Carl Zeiss Axiovert M1 microscope with a 100x Plan Aprochromat objective (1.4 numerical aperture) with GFP and RFP filter cubes. Images were acquired with an Orca-ER charge-coupled device camera (Hamamatsu), using MetaMorph, version 7.1 software (Molecular Devices). All L4 animals were immobilized with 30 mg/ml 2,3-butanedione monoxamine (Sigma-Aldrich, St. Louis, MO) for 6-8 minutes before imaging. To quantitate GFP or mCherry fluorescence, maximum intensity projections from Z-series stacks of 1 μm depth were taken from the PVC nucleus using MetaMorph software. Exposure settings were constant for each reporter. A region of interest was drawn around the nucleus and maximum pixel intensity was used for quantification. At least 20 animals were measured for each genotype and statistics were performed by Student's t-test (for two genotypes) or ANOVA with Tukey-Kramer post-hoc correction (greater than two genotypes). Control genotypes were always assayed on the same day to normalize for daily fluctuations in fluorescence.

CMK-1::GFP and GLR-1::GFP Quantitation. CMK-1::GFP and GLR-1::GFP quantitation in the VNC was performed with a Carl Zeiss Axiovert M1 microscope with a 100x Plan Aprochromat objective (1.4 numerical aperture) with GFP. Images were acquired with an Orca-ER charge-couple Orca-ER charge- coupled device camera (Hamamatsu), using MetaMorph, version 7.1 software (Molecular Devices). All L4 animals were immobilized with 30 mg/ml 2,3-butanedione monoxamine (Sigma-Aldrich, St. Louis, MO) for 6-8 minutes before imaging. To quantitate GFP, maximum intensity projections from Z-series stacks of 1 μm depth were taken from the anterior VNC using MetaMorph software. Exposure settings were constant for each transgene. FluoSphere yellow-green fluorescent beads (Invitrogen) were imaged daily to correct for day-to-day variation in microscope bulb intensity. Line scans of anterior VNC puncta were generated using MetaMorph version 6.0 and were then analyzed in Igor Pro (v5) using custom written software as previously described (Burbea et al. 2002). At least 20 animals were measured for each genotype and statistics were performed by ANOVA with Tukey-Kramer post-hoc correction. Control genotypes were always assayed on the same day to normalize for daily fluctuations in fluorescence

Confocal Microscopy

CMK-1::GFP Localization. Fluorescence imaging of CMK-1::GFP was performed using a Zeiss LSM510 confocal microscope with a 63X objective (NA1.4). Images were acquired with a photomultiplier tube using Zeiss LSM 510 software. All L4 animals were immobilized with 30 mg/ml 2,3-butanedione monoxamine as described above. Z-series

stacks were taken of PVC for each animal. Imaging settings were adjusted for each cell to optimize assessment of cytoplasmic vs. nuclear localization of CMK-1::GFP. Image acquisitions were taken blinded to genotype. Maximum projections of each image were used for scoring localization phenotypes. To confirm this scoring method, another experimenter blind to genotypes assessed localization for a subset of the images and similar results were obtained (data not shown). Statistics were performed using Chi-squared test with post-hoc corrections to assess significance vs. wild type.

Histamine Chloride

L4 wild type and animals expressing *Pglr-1::HisCl1* were transferred onto plates with and without 10 mM histamine as previously described (Pokala et al. 2014). At zero, one, and four hours, animals were picked off plates and the GFP reporter was imaged as described above. Each time point was normalized to the zero hour and then to the corresponding time point of animals no exposed to histamine. Statistics were performed using Student's t-test at each time point comparing animals on histamine to animals off histamine.

Behavior

Locomotion assays were performed as previously described (Juo et al. 2007, Kowalski et al. 2011). Briefly, wild type and animals expressing *Pglr-1::HisCl1* were placed on a plate with no food and allowed to acclimate for two minutes. Animals were then transferred to either a plate with or without 10 mM histamine (no food on either plate). Animals placed on histamine plates were exposed for 10 minutes. Animals were then

observed for five minutes while reversals were counted manually. Behavioral assays were performed by an experimenter blind to the genotypes being observed.

Real-time PCR

Total RNA was isolated from 10 10 cm plates per genotype of mixed-stage animals by lysing in Trizol (Invitrogen) and extracting with an RNeasy Fibrous Tissue Mini kit (Qiagen) with on-column DNAse treatment. For each genotype, at least three independent RNA preparations were made alongside a corresponding wild type (N2) preparation to control for variation introduced by each preparation. cDNA from these RNA preps was synthesized using Superscript III Reverse Transcriptase (Invitrogen). Real-time PCR was performed on the MX3000P real-time PCR machine (Tufts Center for Neuroscience Research) using the Brilliant SYBR Green QPCR Master Mix. The ΔΔCT method (Pfaffl 2001) was used to compute the relative amount of *glr-1* mRNA compared to two reference genes (*act*-1 and *ama*-1). Primers used for each gene: *glr-1*: F-CCGTTTAAACTTGCATTTGACC, R- ACAGACTGCGTTCACCATGT, *act-1* (DePina et al. 2011): F-CCAGGAATTGCTGATCGTATGCAGAA, R-TGGAGAGGGAAGCGAGGATAGA

ama-1 (Yan et al. 2009): F- ACTCAGATGACACTCAACAC, R-GAATACAGTCAACGACGGAG

SEM was calculated as previously described (Applied Biosystems). Statistical significance was determined using the Student's t-test on the geometric mean of the ΔCt values for each reference gene.

Yeast-One-Hybrid (Y1H)

Y1H was performed as described previously (Deplancke et al. 2004, Reece-Hoyes and Walhout 2012) with several modifications described in detail below. All yeast were grown at 30°C and maintained with yeast extract peptone dextrose media (YPD) or synthetic complete (Sc) selective media when appropriate.

Generation of Pglr-1 bait yeast strains. attB4 and attB1 sites were added to 2.4 kb of sequence upstream of the *glr-1* TSS by PCR to create a Gateway compatible PCR product. This PCR product was combined with pDONR P1-P4 in a Gateway BP reaction to create the *Pglr-1* (2.4 kb) entry clone. LR reaction of this entry clone with pDEST clones pMW#2 (HIS3 reporter plasmid) and pMW#3 (LACZ reporter plasmid) created the *Pglr-1* (2.4 kb) HIS3 and LACZ reporter plasmids. To create the *Pglr-1* (0.7 kb) reporter plasmids, the *Pglr-1* (0. 7kb) Gateway compatible clone was obtained from the *glr-1* promoterome (GE Dharmacon) and LP reaction with pMW#2 and pMW#3 created the *Pglr-1* (0.7 kb) HIS3 and LACZ reporter plasmids.

To create yeast strains from these plasmids, *Pglr-1* reporter plasmids were linearized and integrated (*Pglr-1* (2.4 kb) plasmids in one integration, *Pglr-1* (0.7 kb) plasmids in another) into yeast strain YM2471 according to Reese-Hoyes and Walhout (Reece-Hoyes and Walhout 2012). 12-14 colonies from each integration were streaked onto a new agar plate and then replica-plated to 3-AT plates for the HIS3 assays and a YPD plate with a nitrocellulose filter placed on top for the X-gal assay (see below for description of X-gal assays). Integrants with the lowest auto-activation were selected for use in the Y1H, and

15% glycerol in YPD stocks were frozen and stored at -80°C. PCR sequencing of the integrants confirmed the presence of the HIS3 and LACZ reporter.

X-gal assay. Yeast were replicated onto nitrocellulose membranes placed on 150 mm YPD agar plates and allowed to grow for 2-3 days. For each plate to be assayed two Whatman filters were placed into an empty 150 mm Petri dish with 15 mL X-gal solution (15 mL Z-buffer, 36.6 ul B-mercapto-ethanol, 233 ul 4% (w/v) X-gal). The nitrocellulose membrane was frozen for 10 seconds in liquid nitrogen and then placed onto the X-gal-soaked Whatman filters. These plates were then incubated at 37°C and results were assessed at 24 hours.

Screening the transcription factory library. The *C. elegans* transcription factor yeast library was obtained from GE Dharmacon. This library contains 755 putative TFs arrayed across eight 96-well plates. To screen a plate against the *Pglr-1* baits, yeast TFs were grown for 1-2 days in selective media (Sc –Trp) in 96-well plates and the *Pglr-1* baits were grown in selective media (Sc – His, - Ura). 100 ul of bait was then mixed with 100 ul of TF in a 96-well plate (one plate for each bait). Yeast were allowed to mate overnight. 5 ul of the mating solution was plated onto selective media (Sc- His, - Trp, - Ura). These plates were allowed to grow for 2-3 days and then replicated plated onto fresh selective plates and a YPD plate with a nitrocellulose membrane. Plates were grown for 2-3 days before performing the X-gal assay as described above on the nitrocellulose membrane.

Acknowledgements

I would like to thank the following for strains and reagents: Cori Bargmann for *HisCl1*, Piali Sengupta for CMK-1::GFP, CMK-1 (K52A), and CMK-1::EGL-13-NLS, Miriam Goodman and Dominic Glauser for *cmk-1 (pg58)*, Maria Grunwald and Josh Kaplan for *nuIs80*, Albertha Walhout for Y1H reagents, and the CGC for strains.

Chapter 2

A bidirectional feedback mechanism negatively couples synaptic levels and activity of GLR-1 to *glr-1* transcription

Attributes

All experiments in Chapter 2 were performed by Benjamin Moss, except for Figure 2-6A, which was performed by Lidia Park.

Previous data suggests that trafficking mutants with reduced GLR-1 abundance at synapses in the ventral nerve cord (VNC) exhibit reciprocal increases in *glr-1* mRNA levels. Specifically, animals with mutations in the deubiquitinating enzyme USP-46, which removes ubiquitin from GLR-1 and protects it from degradation, exhibit decreased levels of GLR-1 in the VNC and a compensatory three-fold increase in *glr-1* transcript levels as measured by real-time quantitative PCR (RT-qPCR) (Kowalski et al. 2011). Similarly, mutations in the kinesin motor KLP-4/KIF13, which positively regulates GLR-1 trafficking to the VNC, result in decreased levels of GLR-1 in the VNC and a compensatory two fold increase in *glr-1* transcript levels (Monteiro et al. 2012). I hypothesized that GLR-1 levels or function at synapses in the VNC are monitored and coupled via a negative feedback mechanism to *glr-1* transcript levels.

glr-1 transcription is negatively coupled to GLR-1 levels in the ventral nerve cord

Increased *glr-1* transcript in *klp-4* and *usp-46* mutants could be due to increased transcription, increased mRNA stability, or a combination of the two. To investigate the molecular mechanisms involved in this feedback pathway, I generated transgenic animals expressing different combinations of a nuclear-localized GFP reporter (NLS-tagged GFP fused to LACZ) under control of the *glr-1* promoter (*Pglr-1*) and/or the *glr-1* 3' untranslated region (UTR). The *glr-1* promoter includes 5.3 kilobases (kb) of sequence upstream of the transcription start site (TSS) (Rongo et al. 1998), and including it in the construct allows monitoring of transcriptional activity at the *glr-1* promoter. The *glr-1* 3'UTR includes 100 base pairs (bp) as predicted by modENCODE (Mangone et al. 2010). Including the 3'UTR allows regulation and monitoring of transcript stability.

I first validated this *glr-1* reporter under control of both *Pglr-1* and the *glr-1* 3'UTR by testing if GFP fluorescence was altered in *klp-4* trafficking mutants. Briefly, I measured the maximum fluorescence intensity of GFP in the nucleus of the *glr-1*-expressing interneuron PVC in wild type and *klp-4 (tm2114)* loss-of-function mutants (see Materials and Methods). I found that GFP fluorescence increased in *klp-4* mutants (Fig. 2-1A), consistent with previous RT-qPCR results (Monteiro et al. 2012). Because *klp-4* mutants have reduced GLR-1 at synapses in the VNC, this data implies that decreased synaptic GLR-1 may trigger a compensatory feedback mechanism resulting in increased *glr-1* transcript. To directly test if loss of GLR-1 itself could trigger the feedback pathway, I measured the GFP reporter under control of *Pglr-1* and the *glr-1* 3'UTR in *glr-1 (n2461)* null mutants. I found that GFP fluorescence increased in *glr-1* mutants to a similar extent as in *klp-4* mutants (Fig. 2-1B). These data suggest that decreased GLR-1 protein or function is sufficient to trigger a compensatory feedback mechanism negatively coupling GLR-1 to its own transcript levels. These data also indicate that the *glr-1* promoter and/or 3'UTR are sufficient to mediate the feedback mechanism.

To determine the respective contributions of *Pglr-1* and the *glr-1* 3'UTR to the feedback mechanism, I generated additional GFP reporter transgenes consisting of NLS-GFP-LACZ under the control of either the *glr-1* or *nmr-1* promoters combined with either the *glr-1* or *unc-54* 3'UTRs. The *nmr-1* promoter provides an alternative promoter to *glr-1* that is also well expressed in PVC interneurons (Brockie et al. 2001). The *unc-54* 3'UTR is a permissive 3'UTR that is commonly used for stable gene expression in *C. elegans*

Figure 2-1

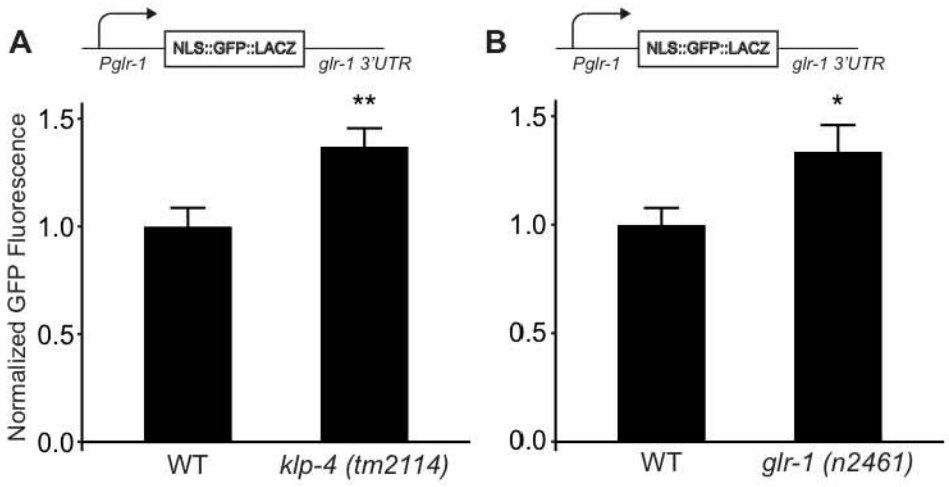
A
Pglr-1
NLS::GFP::LACZ
glr-1 3'UTR
Normalized GFP Fluorescence
1.5
1.0
0.5
0.0
**
WT
klp-4 (tm2114)
B
Pglr-1
NLS::GFP::LACZ
glr-1 3'UTR
1.5
1.0
0.5
0.0
*
WT
glr-1 (n2461)

Figure 2-1. Mutants with decreased synaptic GLR-1 have increased expression of a GFP reporter containing the *glr-1* promoter and the *glr-1* 3'UTR

(A-B) *Pglr-1::nlsGFP::LACZ::glr-1 3'UTR* mean GFP fluorescence in wild type (n=42 (A), n=40 (B)), *klp-4 (tm2114)* (n=46) **(A)**, and *glr-1 (n2461)* (n=42) **(B)** animals normalized to wild type. Maximum GFP fluorescence was measured in the tail neuron PVC. Error bars are SEM. Student's t test was used to compare means. * $p < .05$, ** $p < .01$.

(Fire et al. 1990). I crossed these GFP reporter transgenes into several genetic backgrounds and measured GFP fluorescence in the nucleus of PVC interneurons as described above. When GFP fluorescence was measured from a GFP reporter under control of the *nmr-1* promoter and the *glr-1* 3'UTR, I observed no significant change in fluorescence in either *klp-4 (tm2114)* or *glr-1(n2461)* mutants (Fig. 2-2A and 2-2B). This suggests that the *glr-1* 3'UTR is not sufficient to mediate the feedback mechanism. On the other hand, when GFP fluorescence was measured from the reporter transgene containing *Pglr-1* and the *unc-54* 3'UTR (hereafter referred to as the *glr-1* transcriptional reporter), I observed a small but significant increase in fluorescence in both *klp-4* and *glr-1* mutants (Fig. 2-3A and 2-3B). Importantly, the *unc-54* 3'UTR is not differentially regulated by the feedback mechanism because a GFP reporter containing the *nmr-1* promoter and the *unc-54* 3'UTR was unaltered in *klp-4* and *glr-1* mutants (Fig. 2-4A and 2-4B). Together, these data indicate that *Pglr-1* is sufficient to mediate the feedback mechanism, and suggest that neurons respond to decreased GLR-1 levels or function in the VNC by increasing *glr-1* transcription.

To confirm that mutants with decreased synaptic GLR-1 protein have increased *Pglr-1* activity, I tested the same *glr-1* transcriptional reporter in additional mutants. The *glr-1* transcriptional reporter was also increased in *usp-46 (ok2232)* loss-of-function mutants (Fig. 2-5A), consistent with previous RT-qPCR results (Kowalski et al. 2011) (see above). Cyclin-dependent-kinase-5 (CDK-5) is a serine/threonine kinase that regulates synaptic GLR-1 levels and *cdk-5* loss-of-function animals have decreased synaptic GLR-1 (Juo et al. 2007). One downstream mediator of CDK-5 is KLP-4, which was identified

Figure 2-2

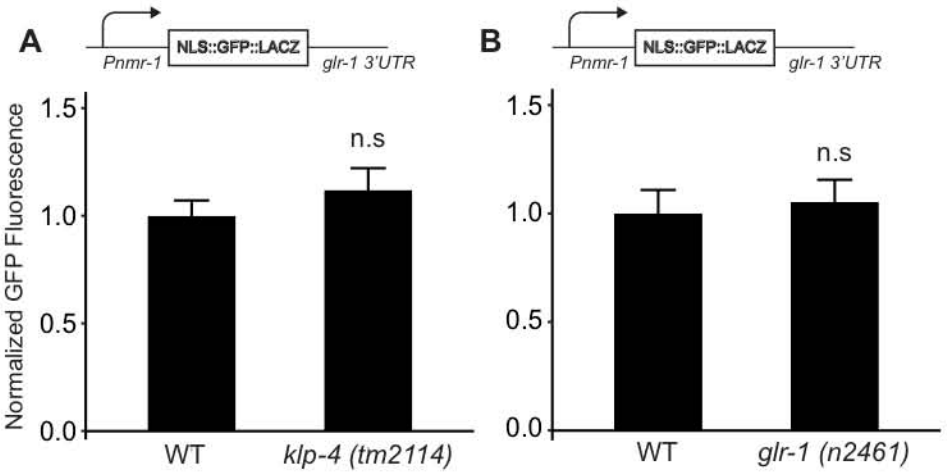
A
Pnmr-1
NLS::GFP::LACZ
glr-1 3'UTR
B
Pnmr-1
NLS::GFP::LACZ
glr-1 3'UTR
Normalized GFP Fluorescence
1.5
1.0
0.5
0.0
n.s
n.s
WT
klp-4 (tm2114)
WT
glr-1 (n2461)

Figure 2-2. The *glr-1* 3'UTR is not sufficient for increased GFP reporter expression in mutants with decreased synaptic GLR-1

(A-B) *Pnmr-1::nlsGFP::LACZ::glr-1 3'UTR* mean GFP fluorescence in wild type (n=76 (A), n=35 (B)), *klp-4 (tm2114)* (n=58) **(A)**, and *glr-1 (n2461)* (n=40) **(B)** animals normalized to wild type. Maximum GFP fluorescence was measured in the tail neuron PVC. Error bars are SEM. Student's t test was used to compare means. n.s. denotes no significant difference ($p > .05$).

Figure 2-3

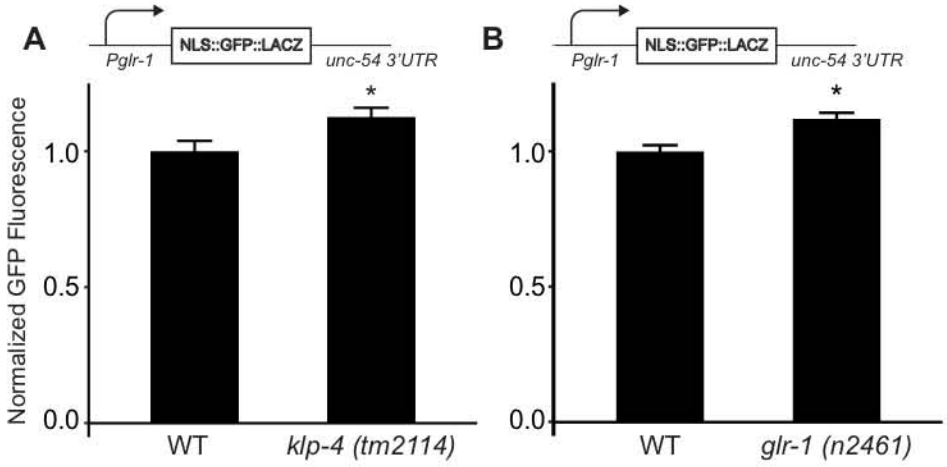
A
Pglr-1
NLS::GFP::LACZ
unc-54 3'UTR
Normalized GFP Fluorescence
1.0
0.5
0.0
*
WT
klp-4 (tm2114)
B
Pglr-1
NLS::GFP::LACZ
unc-54 3'UTR
1.0
0.5
0.0
*
WT
glr-1 (n2461)

Figure 2-3. Mutants with decreased synaptic GLR-1 have increased *glr-1* transcription

(A-B) *Pglr-1::nlsGFP::LACZ::unc-54 3'UTR* mean GFP fluorescence in wild type, *klp-4 (tm2114)* **(A)**, and *glr-1 (n2461)* **(B)** animals normalized to wild type. Maximum GFP fluorescence was measured in the tail neuron PVC for 20 animals for each genotype. Error bars are SEM. Student's t test was used to compare means. * $p < .05$.

Figure 2-4

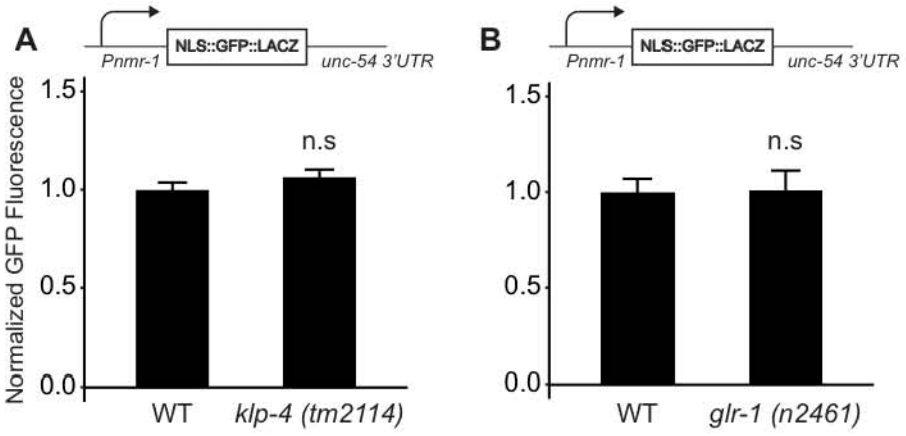
A
Pnmr-1
NLS::GFP::LACZ
unc-54 3'UTR
Normalized GFP Fluorescence
1.5
1.0
0.5
0.0
n.s
WT
klp-4 (tm2114)
B
Pnmr-1
NLS::GFP::LACZ
unc-54 3'UTR
1.5
1.0
0.5
0.0
n.s
WT
glr-1 (n2461)

Figure 2-4. The *nmr-1* promoter and the *unc-54* 3'UTR are not differentially regulated in mutants with decreased synaptic GLR-1.

(A-B) *Pnmr-1::nlsGFP::LACZ::unc-54 3'UTR* mean GFP fluorescence in wild type (n=39 (A), n=42 (B)), *klp-4 (tm2114)* (n=41) **(A)**, and *glr-1 (n2461)* (n=34) **(B)** animals normalized to wild type. Maximum GFP fluorescence was measured in the tail neuron PVC. Error bars are SEM. Student's t test was used to compare means. n.s. denotes no significant difference ($p > .05$).

in a screen for mutants that suppress the CDK-5 overexpression phenotype of increased synaptic GLR-1 (Monteiro et al. 2012). If KLP-4 functions as a target of CDK-5 to regulate GLR-1, then, like *klp-4* mutants, *cdk-5* mutants should have increased *Pglr-1* activity. Indeed, I found a similar fold change in GFP fluorescence in *cdk-5* (*gm336)* mutants (Fig. 2-5B). Together, these data indicate that *Pglr-1* is sufficient to mediate the feedback mechanism, and suggest that neurons respond to decreased GLR-1 levels or function in the VNC by increasing *glr-1* transcription.

I next investigated whether the feedback mechanism is bidirectional by testing if increased GLR-1 in the VNC triggers a decrease in *glr-1* transcription. UNC-11/AP180 is a clathrin adaptin involved in endocytosis of GLR-1 and the receptor accumulates at the plasma membrane in the VNC of *unc-11* mutants (Burbea et al. 2002). I found that fluorescence of the GFP reporter under control of *Pglr-1* and the *glr-1* 3'UTR decreased in *unc-11(e47)* null mutants (Fig. 2-6A). I observed a similar reduction of the *glr-1* transcriptional reporter in *unc-11* mutants (Fig. 2-6B), suggesting that *Pglr-1* is sufficient to mediate decreased *glr-1* transcription in response to increased GLR-1. Together, these results suggest that *glr-1* transcription responds in a compensatory and reciprocal manner to bidirectional changes in GLR-1 levels in the VNC.

Decreased glutamatergic activity increases *glr-1* transcription

Since changes in GLR-1 levels in the VNC can alter *glr-1* transcription, I performed several experiments to test if changes in glutamate signaling are sufficient to trigger the transcriptional feedback mechanism. First, I tested whether reductions in glutamatergic

Figure 2-5

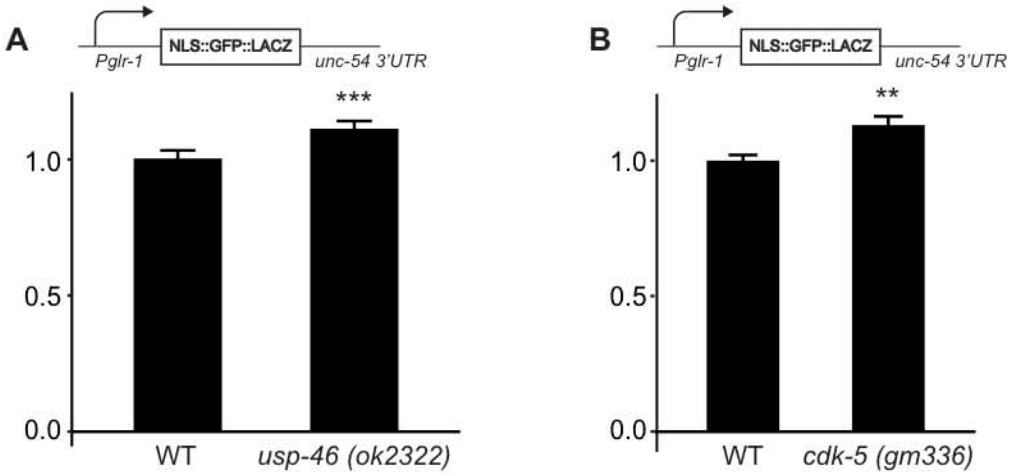
A
Pglr-1
NLS::GFP::LACZ
unc-54 3'UTR
***
1.0
0.5
0.0
WT
usp-46 (ok2322)
B
Pglr-1
NLS::GFP::LACZ
unc-54 3'UTR
**
1.0
0.5
0.0
WT
cdk-5 (gm336)

Figure 2-5. GLR-1 trafficking mutants with decreased synaptic GLR-1 have increased *glr-1* transcription

(A-B) *Pglr-1::nlsGFP::LACZ::unc-54 3'UTR* mean GFP fluorescence in wild type, *usp-46(ok2322)* **(A)**, and *cdk-5 (gm336)* **(B)** animals normalized to wild type. Maximum GFP fluorescence was measured in the tail neuron PVC for 31 animals for each genotype. Error bars are SEM. Student's t test was used to compare means. ** $p < .01$, *** $p < .001$.

Figure 2-6

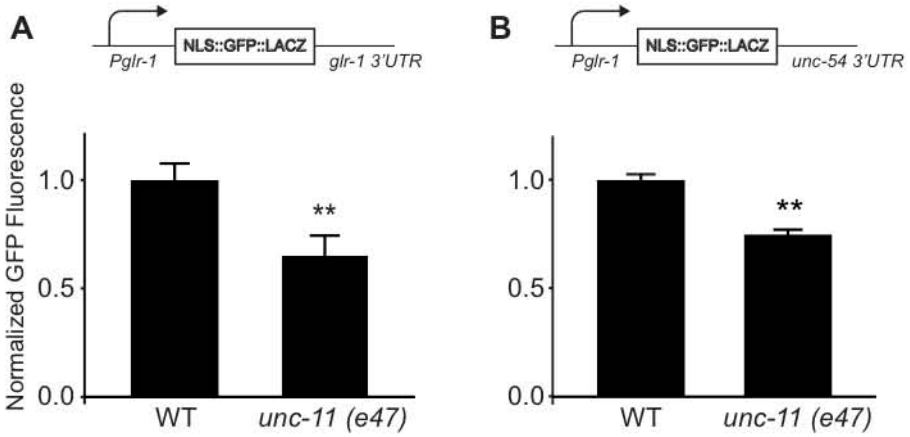
A
Pglr-1
NLS::GFP::LACZ
glr-1 3'UTR
Normalized GFP Fluorescence
1.0
0.5
0.0
**
WT
unc-11 (e47)
B
Pglr-1
NLS::GFP::LACZ
unc-54 3'UTR
1.0
0.5
0.0
**
WT
unc-11 (e47)

Figure 2-6. *unc-11*/AP180 mutants with increased synaptic GLR-1 have decreased *glr-1* transcription

(A) *Pglr-1::nlsGFP::LACZ::glr-1 3'UTR* mean GFP fluorescence in wild type (n=39) and *unc-11 (e47)* (n=24) animals normalized to wild type. **(B)** *Pglr-1::nlsGFP::LACZ::unc-54 3'UTR* mean GFP fluorescence in wild type (n=41) and *unc-11 (e47)* (n=41) animals normalized to wild type. Maximum GFP fluorescence was measured in the tail neuron PVC. Error bars are SEM. Student's t test was used to compare means. ** $p < .01$.

transmission could trigger the feedback mechanism by analyzing *glr-1* expression in *eat-4* synaptic transmission mutants. EAT-4 is a vesicular glutamate transporter (VGLUT) responsible for loading glutamate into synaptic vesicles (Bellocchio et al. 1998, Lee et al. 1999). Loss of *eat-4*/VGLUT results in defects in glutamatergic transmission (Berger et al. 1998, Lee et al. 1999) and a compensatory increase in synaptic GLR-1 in the VNC (Grunwald et al. 2004). I found that *eat-4 (n2474)* loss-of-function mutants exhibit increased endogenous *glr-1* mRNA levels compared to wild type controls by RT-qPCR (Fig. 2-7A). In support of this data, I found that *eat-4* mutants also exhibit increased GFP fluorescence from the reporter under control of *Pglr-1* and the *glr-1* 3'UTR (Fig. 2-7B). Furthermore, *Pglr-1* was sufficient to mediate this effect because GFP fluorescence still increased in *eat-4* mutants expressing the *glr-1* transcriptional reporter (Fig. 2-7C). Together, these data suggest that chronic decreases in glutamate signaling (Fig. 2-7) or postsynaptic glutamate receptors (Figs. 2-1 to 2-5) are sufficient to trigger the transcriptional feedback pathway.

I tested two additional synaptic activity mutants to confirm that decreased synaptic activity triggers increased *Pglr-1* activity. UNC-2 is a voltage-dependent calcium channel (VGCC) expressed presynaptically and *unc-2*/VGCC loss-of-function mutants have reduced neurotransmitter release (Richmond et al. 2001). Reduced neurotransmitter release in *unc-2* mutants trigger a similar fold increase in the *glr-1* transcriptional reporter (Fig. 2-8A). The presynaptic protein UNC-13/MUNC13 binds the N-terminus of syntaxin and functions during synaptic vesicle priming. Like *unc-2* mutants, *unc-13* mutants have reduced neurotransmitter release (Richmond et al. 2001). I tested whether *unc-13* mutants

Figure 2-7

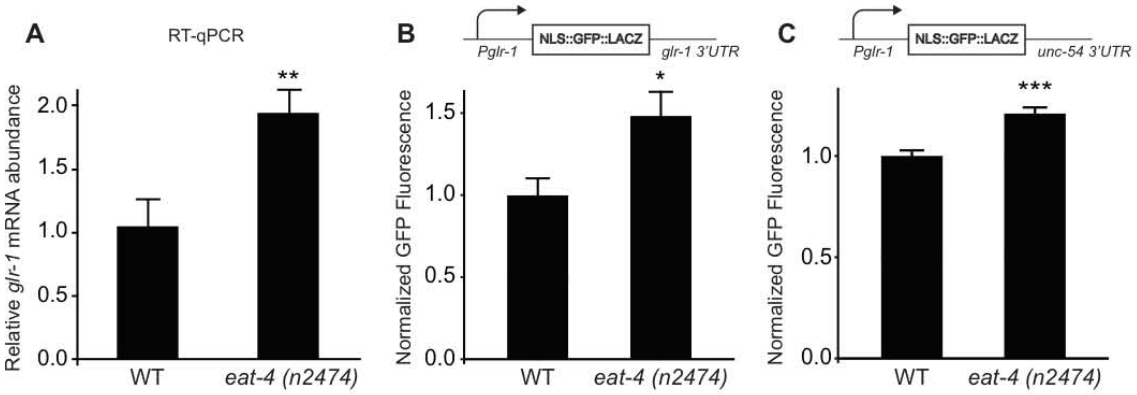
A
RT-qPCR
Relative glr-1 mRNA abundance
2.0
1.5
1.0
0.5
0.0
**
WT
eat-4 (n2474)
B
Pglr-1
NLS::GFP::LACZ
glr-1 3'UTR
Normalized GFP Fluorescence
1.5
1.0
0.5
0.0
*
WT
eat-4 (n2474)
C
Pglr-1
NLS::GFP::LACZ
unc-54 3'UTR
Normalized GFP Fluorescence
1.0
0.5
0.0
***
WT
eat-4 (n2474)

Figure 2-7. Decreased glutamatergic transmission increases *glr-1* expression

(A) Real-time qPCR in wild type and *eat-4* (*n2474*) animals comparing *glr-1* expression in four biological replicates normalized to two references genes (*act-1* and *ama-1*). ΔCt values were compared using Student's t-test. **(B)** *Pglr-1::nlsGFP::LACZ::glr-1 3'UTR* mean GFP fluorescence in wild type (n=45) and *eat-4 (n2474)* (n=40) animals normalized to wild type **(C)**. *Pglr-1::nlsGFP::LACZ::unc-54 3'UTR* mean GFP fluorescence in wild type (n=37) and *eat-4 (n2474)* (n=45) animals normalized to wild type. Maximum GFP fluorescence was measured in the tail neuron PVC. Error bars are SEM. Student's t test was used to compare means. * $p < .05$, ** $p < .01$, *** $p < .001$.

Figure 2-8

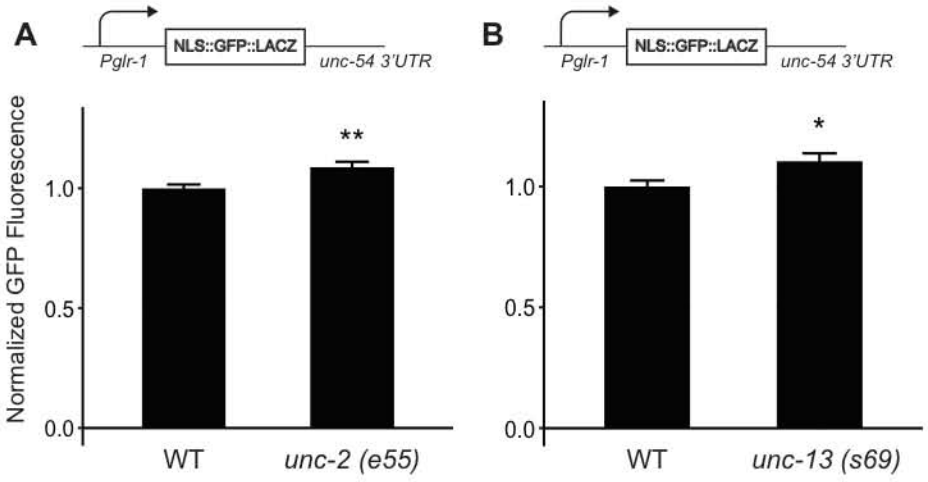
A
Pglr-1
NLS::GFP::LACZ
unc-54 3'UTR
Normalized GFP Fluorescence
1.0
0.5
0.0
**
WT
unc-2 (e55)
B
Pglr-1
NLS::GFP::LACZ
unc-54 3'UTR
1.0
0.5
0.0
*
WT
unc-13 (s69)

Figure 2-8. Decreased synaptic activity increases *glr-1* transcription

(A-B) *Pglr-1::nlsGFP::LACZ::unc-54 3'UTR* mean GFP fluorescence in wild type, *unc-2 (e53)* **(A)**, and *unc-13 (s69)* **(B)** animals normalized to wild type. Maximum GFP fluorescence was measured in the tail neuron PVC for 45 animals for each genotype. Error bars are SEM. Student's t test was used to compare means. * $p < .05$, ** $p < .01$.

have increased *Pglr-1* activity and, again, found a similar fold increase in the *glr-1* transcriptional reporter as in *eat-4*/VGLUT and *unc-2*/VGCC mutants (Fig. 2-8B). Together, these results suggest that reductions in presynaptic release of neurotransmitter (*unc-2*/VGCC and *unc-13*/MUNC13) and specifically in release of glutamate (*eat-4*/VGLUT), are sufficient to trigger increased *Pglr-1* activity.

I hypothesized that decreased presynaptic glutamate release leads to decreased activation of GLR-1, decreased GLR-1-gated currents, and ultimately decreased postsynaptic activity. Thus, I next aimed to test whether specifically decreasing GLR-1-gated currents triggers increased *Pglr-1* activity. SOL-1 encodes a GLR-1 auxiliary protein that is required for GLR-1-dependent glutamate-gated currents and normal *glr-1*-dependent locomotion (Zheng et al. 2004). While GLR-1 function is disrupted in *sol-1* loss-of-function mutants, GLR-1 is normally expressed and localized at synapses in the VNC (Zheng et al. 2004). *sol-1* loss-of-function mutants thus make it possible to specifically test whether decreases in postsynaptic glutamate-gated currents are sufficient to trigger the feedback mechanism. If decreased postsynaptic activity is sufficient to trigger increased *glr-1* transcription, then *sol-1* mutants should have similar increases as *glr-1, klp-4*, and *eat-4*. Contrary to this hypothesis, I found that *sol-1 (ak63)* loss-of-function mutants exhibit no change in fluorescence of the *glr-1* transcriptional reporter (Fig. 2-9A).

Despite having decreased GLR-1-mediated currents, *sol-1* mutants have intact NMDA-mediated currents (Zheng et al. 2004). I hypothesized that the influx of ions through

Figure 2-9

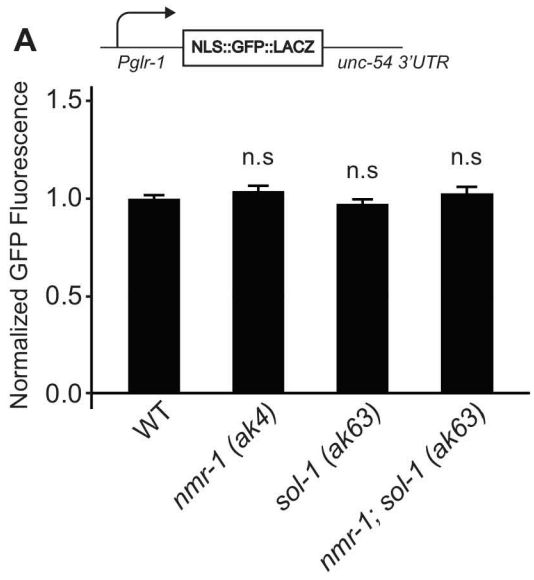
A
Pglr-1
NLS::GFP::LACZ
unc-54 3'UTR
Normalized GFP Fluorescence
1.5
1.0
0.5
0.0
n.s
n.s
n.s
WT
nmr-1 (ak4)
sol-1 (ak63)
nmr-1; sol-1 (ak63)

Figure 2-9. *sol-1*, *nmr-1*, or *sol-1; nmr-1* loss-of-function does not affect *glr-1* transcription

(A) *Pglr-1::nlsGFP::LACZ::unc-54 3'UTR* mean GFP fluorescence in wild type (n=100), *nmr-1 (ak4)* (n=64), *sol-1 (ak63)* (n=39), and *nmr-1; sol-1* (n=48) animals normalized to wild type. Maximum GFP fluorescence was measured in the tail neuron PVC. Error bars are SEM. ANOVA with Tukey-Kramer post hoc test was used to compare means. n.s. denotes no significant difference ($p > .05$).

NMDA receptors could be suppressing an increase in *Pglr-1* activity. To test this, I assayed the *glr-1* transcriptional reporter in *nmr-1* (the sole *C. elegans* homolog of NMDA receptor subunit NR1) single mutants and *nmr-1; sol-1* double mutants. *nmr-1* mutants completely abolish the slower component of the glutamate-gated current in the AVA interneuron, and in the absence of GLR-1 and GLR-2, most of the residual glutamate-gated current is dependent on NMR-1 (Mellem et al. 2002). Thus, *sol-1; nmr*-1 double mutants should abolish most current through ionotropic GluRs. However, like *sol-1* single mutants, *nmr-1; sol-1* double mutants did not have an increase in *Pglr-1* activity (Fig. 2-9A). This result suggests that blocking glutamate receptor current postsynaptically is not sufficient to increase *glr-1* transcription. However, because glutamate-gated currents have only been measured in AVA interneurons it is not known to what extent SOL-1 functions in the particular neuron in which the GFP reporter measurements are recorded (PVC). Further electrophysiological experiments would be required to confirm that *sol-1* loss of function disrupts GLR-1 currents in PVC.

To more directly test whether changes in activity specifically in GLR-1-expressing cells (including PVC) lead to increased *Pglr-1* activity, I used a recently developed genetic tool that allows for repression of neuronal activity by activation of an exogenous histamine chloride channel (HisCl1) from *Drosophila* (Pokala et al. 2014) (*C. elegans* do not express histamine-gated channels). I generated transgenic animals expressing HisCl1 in *glr-1*-expressing neurons (*Pglr-1::HisCl1*) and verified the efficacy of this silencing approach by measuring GLR-1-dependent locomotion reversal behavior. The frequency of spontaneous reversals is regulated by glutamatergic signaling, and mutants with

reduced glutamatergic signaling (e.g., *glr-1* or *eat-4* mutants) exhibit decreased reversal frequencies (Zheng et al. 1999, Brockie et al. 2001, Burbea et al. 2002). I found that exposure of animals expressing HisCl1 to exogenous histamine for 10 minutes led to a dramatic decrease in spontaneous reversal frequency compared to wild type controls (Fig. 2-10A). This data suggests that activation of HisCl1 channels specifically in *glr-1*-expressing neurons suppresses their activity and impacts GLR-1-dependent locomotion behavior. In order to test whether direct inhibition of *glr-1*-expressing neurons could increase *glr-1* transcription, I exposed HisCl1-expressing animals to histamine for one and four hours and then measured the *glr-1* transcriptional reporter. Fluorescence at each time point was normalized to HisCl1-expressing animals in the absence of histamine (see Materials and Methods). I found a significant ($p<0.01$) increase in GFP reporter fluorescence after one and four hours (Fig. 2-10B). In contrast, wild type animals not expressing HisCl1 showed no increase in *Pglr-1* activity when exposed to histamine (Fig. 2-10C). I did, however, observe a significant reduction in *Pglr-1* activity in wild type animals (i.e. not expressing HisCl1) after four hours of histamine exposure (Fig. 2-10C), suggesting that the increased *Pglr-1* activity observed in HisCl1-expressing animals may be underestimated. Together, these results suggest that decreasing neuronal activity specifically in *glr-1*-expressing neurons can trigger the feedback mechanism to increase *glr-1* transcription.

Increased glutamatergic activity decreases *glr-1* transcription

Because increased GLR-1 in the VNC of *unc-11*/AP180 mutants is correlated with decreased *Pglr-1* activity (Fig. 2-6), I investigated whether directly increasing GLR-1

Figure 2-10

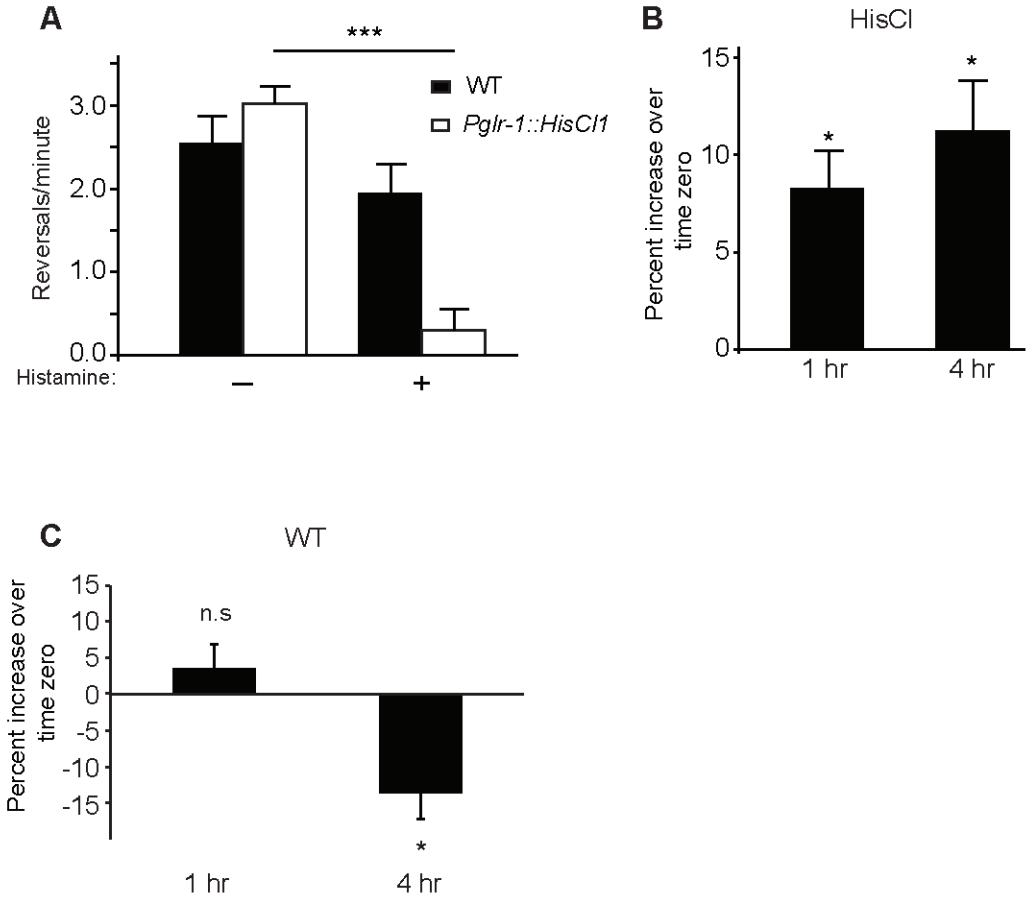
A
***
WT
Pglr-1::HisCl1
Reversals/minute
3.0
2.0
1.0
0.0
Histamine:
–
+
B
HisCl
Percent increase over time zero
15
10
5
0
*
*
1 hr
4 hr
C
WT
Percent increase over time zero
15
10
5
0
-5
-10
-15
n.s
*
1 hr
4 hr

Figure 2-10. Suppression of activity in *glr-1*-expressing neurons increases *glr-1* transcription

(A) Reversals were counted for five minutes in wild type and HisCl1 (*Pglr-1::HisCl1*) animals off and on plates containing 10 mM histamine. Student's t-tests were used to compare differences between conditions. n=8 for all conditions **(B)** HisCl1 animals were placed on plates with 10 mM histamine for one and four hours and normalized to unexposed animals. n = 30 animals per condition **(C)** Wild type animals were placed on plates with 10 mM histamine for one and four hours and normalized to unexposed animals. n=15 animals per condition. For reporter imaging maximum fluorescence was measured in the tail neuron PVC. Mean fluorescences normalized to the zero time point for each genotype were compared by Student's t-test. Error bars are SEM. * $p < .05$, *** $p < .001$. n.s. denotes no significant difference ($p > .05$)

function could regulate the transcriptional feedback mechanism. I increased GLR-1 activity in *glr-1*-expressing interneurons by expressing a mutant version of GLR-1, GLR-1(A/T)::YFP (*nuIs80*) that contains an alanine to threonine substitution in the pore domain, which results in a constitutively active channel with increased conductance (Zheng et al. 1999). Animals expressing GLR-1(A/T) exhibit a dramatic increase in spontaneous reversals consistent with increased glutamatergic signaling (Zheng et al. 1999, Zheng et al. 2004, Kowalski et al. 2011). Because GLR-1(A/T)::YFP fluorescence could not be distinguished from the NLS-GFP-LACZ fluorescence, I constructed a red fluorescent version of the *glr-1* transcriptional reporter (*Pglr-1::NLS-mCherry::unc-54 3'UTR*). First, I tested this reporter to confirm it responds to the feedback mechanism. *glr-1 (n2461)* mutants had a similar fold change increase in red fluorescence using this reporter (Fig. 2-11A) as green fluorescence using the NLS-GFP-LACZ reporter (Fig. 2-3B), indicating that it could be used to test *glr-1* transcriptional responses to GLR-1(A/T)::YFP. Using this red reporter, *Pglr-1* activity decreased in GLR-1(A/T)-expressing animals compared to wild type controls or animals overexpressing wild type GLR-1::GFP (*nuIs24*) (Fig. 2-11B). These data are consistent with the idea that increased GLR-1 function triggers the feedback pathway to reduce *glr-1* transcription. Together, these data show that increasing or decreasing glutamatergic signaling results in reciprocal, compensatory changes in *glr-1* transcription.

Figure 2-11

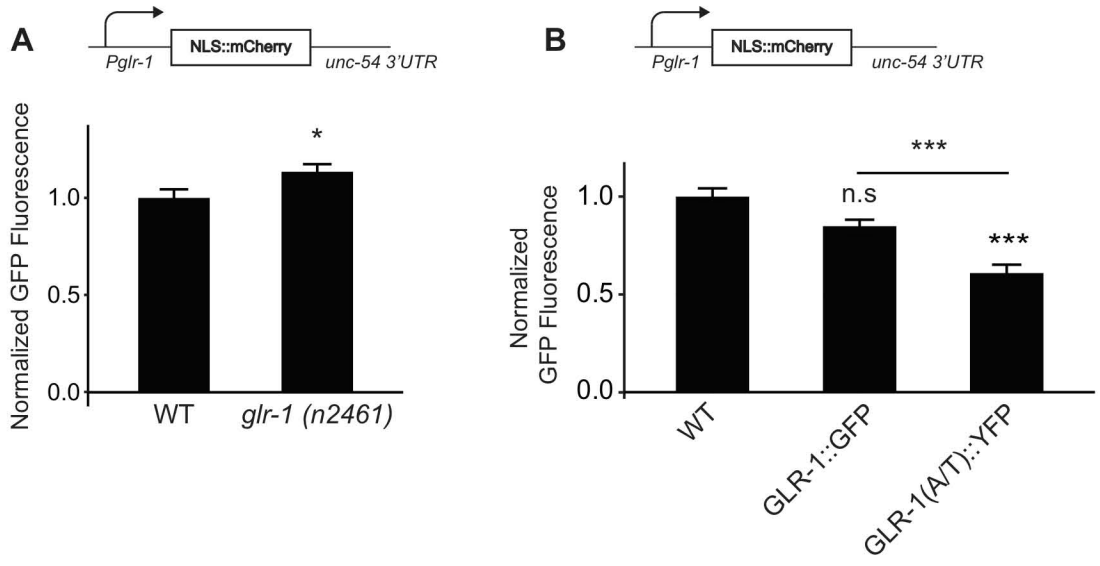
A
Pglr-1
NLS::mCherry
unc-54 3'UTR
Normalized GFP Fluorescence
1.0
0.5
0.0
*
WT
glr-1 (n2461)
B
Pglr-1
NLS::mCherry
unc-54 3'UTR
Normalized GFP Fluorescence
1.0
0.5
0.0
***
n.s
***
WT
GLR-1::GFP
GLR-1(A/T)::YFP

Figure 2-11. Increased GLR-1 activity decreases *glr-1* transcription

(A-B) *Pglr-1::nls-mCherry::unc-54 3'UTR* mean mCherry fluorescence in wild type (n=43 (A), n=46 (B)), *glr-1 (n2461)* (n=40) **(A)**, *nuIs24* (GLR-1::GFP) (n=47) **(B)**, and *nuIs80* (GLR-1(A/T)::YFP) (n=44) **(B)** animals normalized to wild type. Maximum mCherry fluorescence was measured in the tail neuron PVC. Error bars are SEM. Student's t-test (A) or ANOVA with Tukey-Kramer post hoc test (B) were used to compare means. * $p < .05$, *** $p < .001$. n.s. denotes no significant difference ($p > .05$)

Chapter 3

A CMK-1/CaMK signaling pathway mediates the *glr-1* transcriptional feedback mechanism

Attributes
All experiments in Chapter 3 were performed by Benjamin Moss

I next investigated the signaling mechanism involved in communicating information about GLR-1 levels or activity at the synapse to the nucleus in order to regulate *glr-1* transcription. There are several well-studied synapse-to-nucleus signaling mechanisms, and I focused on the CMK-1/CaMK pathway (Fig. 3-1A). CaMKI and IV are important mediators of calcium-dependent signaling mechanisms involved in neuronal development and function (Wayman et al. 2008). In addition, CaMKIV has been shown to mediate AMPAR-dependent homeostatic synaptic scaling which is blocked by pharmacological inhibitors of transcription (Ibata et al. 2008, Goold and Nicoll 2010). In *C. elegans*, CMK-1, the homolog of CaMKI and CaMKIV (Eto et al. 1999), is widely expressed in the nervous system (Satterlee et al. 2004), and has been shown to function in specific sensory neurons to mediate experience-dependent thermotaxis at physiological temperatures and avoidance of noxious heat (Satterlee et al. 2004, Schild et al. 2014, Yu et al. 2014). Despite these known roles for CMK-1/CaMK in mediating synaptic scaling and experience-dependent plasticity, it is unclear which downstream targets are involved. In this chapter, I explore the role of the CMK-1/CaMK signaling pathway (Fig. 3-1A) in regulating *glr-1* transcription.

The CMK-1/CaMK signaling pathway regulates *glr-1* transcription

To test whether CMK-1/CaMK is involved in regulating *glr-1* transcription, I first measured endogenous *glr-1* mRNA levels in *cmk-1 (oy21)* loss-of-function mutants using RT-qPCR. I found increased *glr-1* mRNA levels relative to two reference genes (*act-1* and *ama-1*) in *cmk-1 (oy21)* mutants (Fig. 3-2A), suggesting that CMK-1/CaMK negatively regulates *glr-1* transcript levels. Consistent with this result, loss-of-function

Figure 3-1

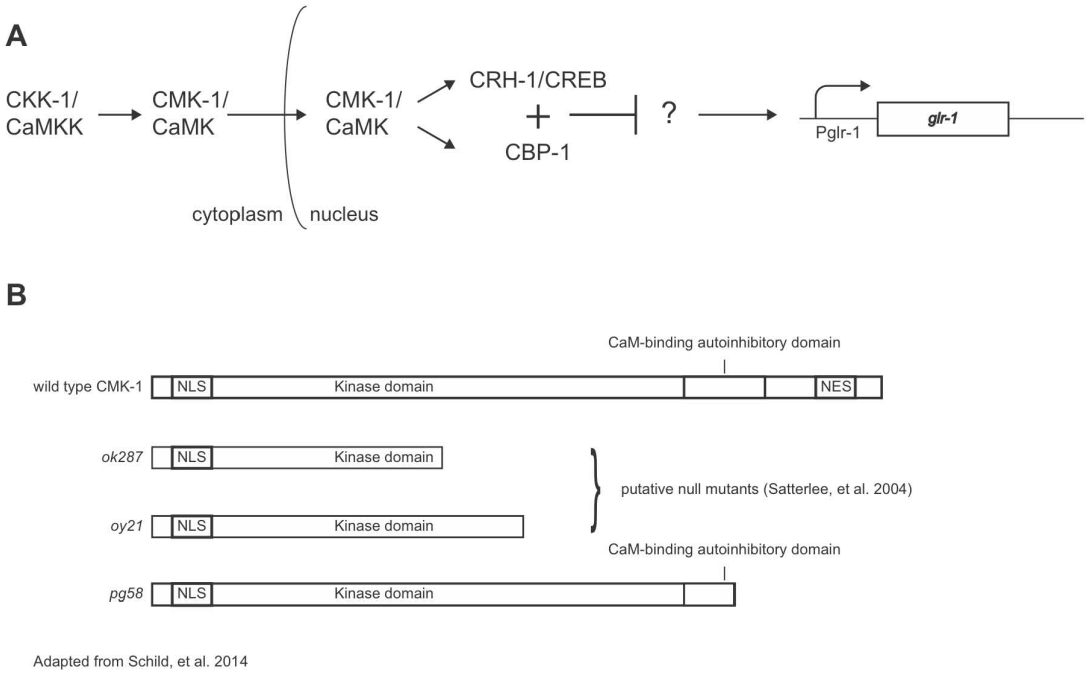

Adapted from Schild, et al. 2014

Figure 3-1. CMK-1/CaMK signaling pathway and CMK-1 alleles

(A) Schematic of a simplified CMK-1/CaMK signaling pathway in *C. elegans*. CKK-1/CaMKK is the upstream kinase that phosphorylates CMK-1/CaMK. Phosphorylation of CMK-1/CaMK induces its nuclear translocation. Once in the nucleus, CMK-1/CaMK can phosphorylate downstream targets including CRH-1/CREB and CBP-1 to regulate gene expression. Data presented in this study (see below) suggests that the CMK-1/CaMK pathway inhibits a downstream activator of *glr-1* transcription (or activates a downstream repressor), leading to decreased *glr-1* transcription. **(B)** Schematic of the *cmk-1* alleles used in this study (adapted from Schild, et al. 2014).

mutations in *ckk-1*/CaMKK, the upstream activator of CMK-1/CaMK (Fig. 3-1A), resulted in increased GFP fluorescence from a reporter under control of *Pglr-1* and *glr-1* 3'UTR (Fig. 3-2B). I next tested whether *Pglr-1* was sufficient to mediate the effects of the CMK-1/CaMK pathway using the *glr-1* transcriptional reporter. I found that *Pglr-1* activity increased in *ckk-1 (ok1033)* loss-of-function mutants and two independent loss-of-function alleles of *cmk-1* (*oy21* and *ok287*, see Fig. 3-1B for diagrams of *cmk-1* alleles used in this study) (Fig. 3-2C, 3-2D, and 3-2E). These results indicate that the CMK-1/CaMK signaling pathway acts basally to repress *glr-1* transcription. Expression of *cmk-1* cDNA specifically in GLR-1 neurons rescued the increase in the *glr-1* transcriptional reporter observed in *cmk-1 (oy21)* loss-of-function mutants (Fig. 3-2F), whereas expression of a kinase-dead version of CMK-1(K52A) (Kimura et al. 2002) did not rescue (Fig. 3-2G). These results suggest that CMK-1/CaMK functions in a kinase-dependent manner specifically in *glr-1*-expressing neurons to repress *glr-1* transcription.

CaMKI and CaMKIV in mammals, and CMK-I in *C. elegans,* have been shown to phosphorylate the transcription factor cyclic AMP response element (CRE) binding protein (CREB) to regulate gene expression (Sheng et al. 1991, Enslen et al. 1994, Matthews et al. 1994, Sun et al. 1994, Eto et al. 1999, Kimura et al. 2002). Thus, I tested whether mutations in *crh-1*, the *C. elegans* homolog of CREB, affected *glr-1* transcription. I found that fluorescence of the *glr*-1 transcriptional reporter increased in *crh-1 (tz2)* loss-of-function mutants (Fig. 3-3A), consistent with a role for CREB as a downstream target of CMK-1/CaMK in regulating *glr-1* transcription. Additionally, since CREB is known to function together with the transcriptional co-activator CREB binding

Figure 3-2

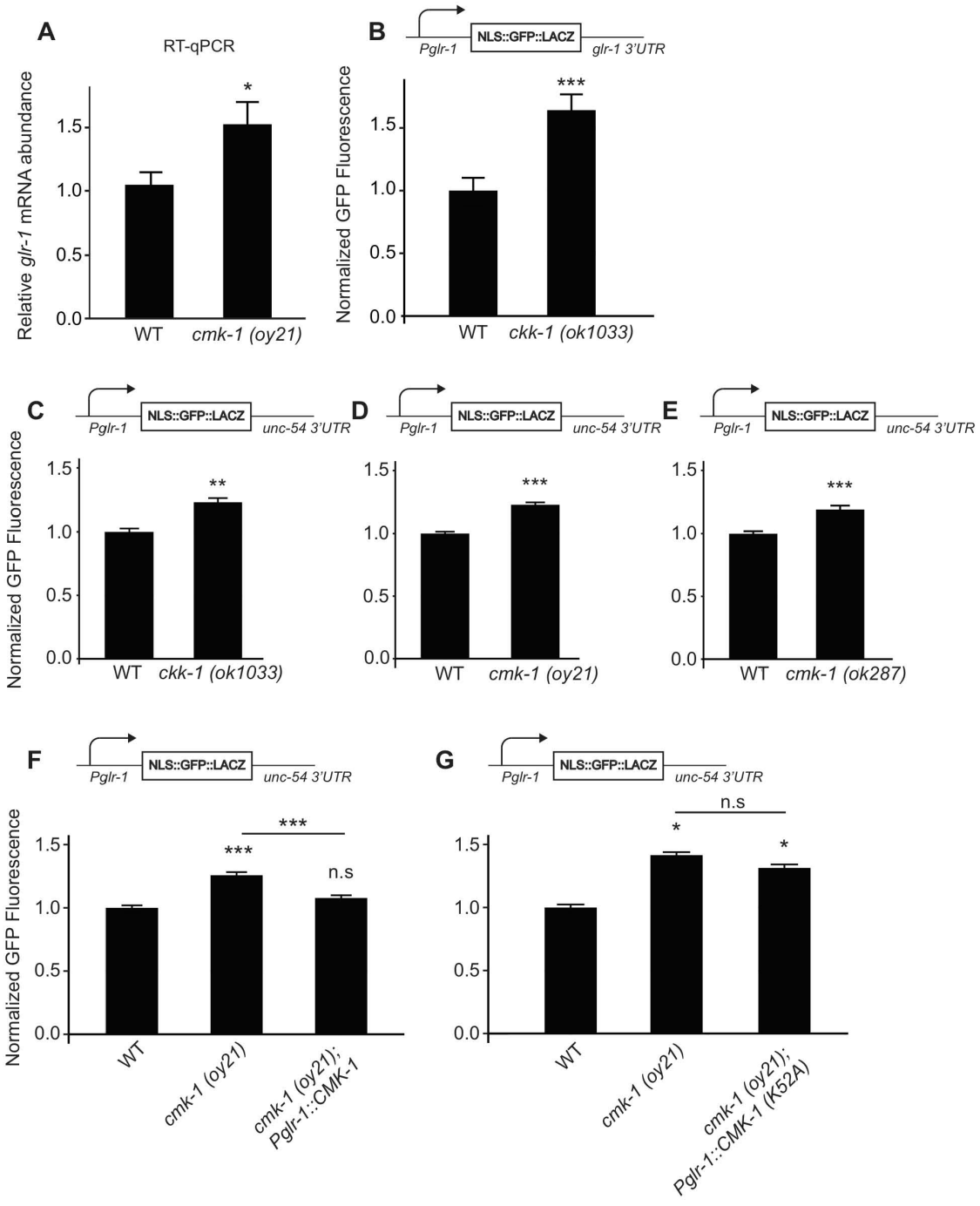
A
RT-qPCR
Relative glr-1 mRNA abundance
1.5
1.0
0.5
0.0
*
WT
cmk-1 (oy21)
B
Pglr-1
NLS::GFP::LACZ
glr-1 3'UTR
Normalized GFP Fluorescence
***
WT
ckk-1 (ok1033)
C
Pglr-1
NLS::GFP::LACZ
unc-54 3'UTR
Normalized GFP Fluorescence
**
WT
ckk-1 (ok1033)
D
Pglr-1
NLS::GFP::LACZ
unc-54 3'UTR
***
WT
cmk-1 (oy21)
E
Pglr-1
NLS::GFP::LACZ
unc-54 3'UTR
***
WT
cmk-1 (ok287)
F
Pglr-1
NLS::GFP::LACZ
unc-54 3'UTR
Normalized GFP Fluorescence
***
***
n.s
WT
cmk-1 (oy21)
cmk-1 (oy21); Pglr-1::CMK-1
G
Pglr-1
NLS::GFP::LACZ
unc-54 3'UTR
n.s
*
*
WT
cmk-1 (oy21)
cmk-1 (oy21); Pglr-1::CMK-1 (K52A)

Figure 3-2. The CMK-1/CaMK signaling pathway regulates *glr-1* transcription

(A) Real-time qPCR in wild type and *cmk-1 (oy21)* animals comparing *glr-1* expression in four biological replicates normalized to two references genes (*act-1* and *ama-1*). ΔCt values were compared using Student's t-test. **(B)** *Pglr-1::nlsGFP::lacZ::glr-1 3'UTR* mean GFP fluorescence in wild type (n=45) and *ckk-1 (ok1033)* (n=48) animals normalized to wild type. **(C-E)** *Pglr-1::nlsGFP::LACZ::unc-54 3'UTR* mean GFP fluorescence in wild type, *ckk-1 (ok1033)* **(C)** *cmk-1 (oy21)* **(D)**, and *cmk-1 (ok287)* **(E)** animals. n=45 for all genotypes **(F)** A *cmk-1* cDNA rescue construct was expressed under the *glr-1* promoter (*Pglr-1::CMK-1*) and *Pglr-1::nlsGFP::LACZ::unc-54 3'UTR* mean GFP fluorescence was measured in wild type, *cmk-1 (oy21)*, and *cmk-1 (oy21)*; *Pglr-1::CMK-1* animals normalized to wild type. n=64 for all genotypes **(G)** A kinase-dead *cmk-1 (K52A)* cDNA rescue construct was expressed under the *glr-1* promoter (*Pglr-1::CMK-1*) and *Pglr-1::nlsGFP::LACZ::unc-54 3'UTR* mean GFP fluorescence was measured in wild type (n=41), *cmk-1 (oy21)* (n=28), and *cmk-1 (oy21)*; *Pglr-1::CMK-1 (K52A)* (n=44) animals normalized to wild type. Mean fluorescences normalized to wild type were compared by Student's t-test (B-E) or by ANOVA with Tukey-Kramer post hoc tests (F-G). Error bars are SEM. * $p < .05$, ** $p < .01$, *** $p < .001$.

Figure 3-3

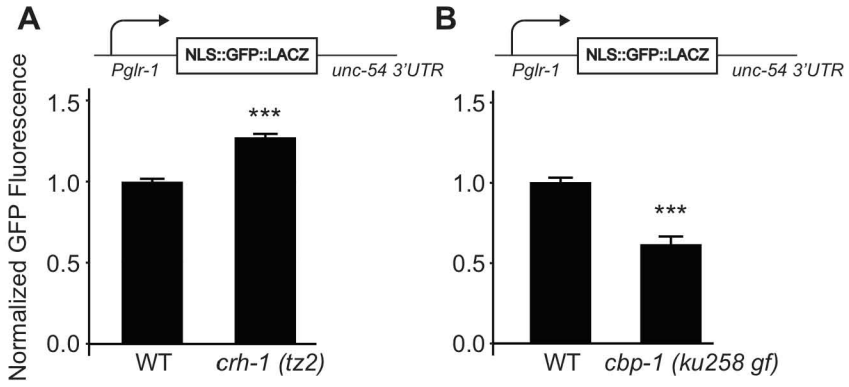
A
Pglr-1
NLS::GFP::LACZ
unc-54 3'UTR
Normalized GFP Fluorescence
1.5
1.0
0.5
0.0
***
WT
crh-1 (tz2)
B
Pglr-1
NLS::GFP::LACZ
unc-54 3'UTR
1.5
1.0
0.5
0.0
***
WT
cbp-1 (ku258 gf)

Figure 3-3. CRH-1/CREB and CBP negatively regulate *glr-1* transcription

(A-B) *Pglr-1::nlsGFP::LACZ::unc-54 3'UTR* mean GFP fluorescence in wild type (n=44 (A), n=43 (B)), *crh-1 (tz2)* (n=44) **(A)** and *cbp-1 (ku258 gf)* (n=37) **(B)** animals normalized to wild type. Maximum GFP fluorescence was measured in the tail neuron PVC. Error bars are SEM. Student's t test was used to compare means. *** $p < .001$.

protein (CBP-1)/p300 which can also be phosphorylated by CaMKIV (Wayman et al. 2008), I took advantage of a gain-of-function allele in *cbp-1 (ku258 gf)* (Eastburn and Han 2005) to test if *cbp-1* was involved in regulating *glr-1* transcription. I found that *cbp-1 (ku258 gf)* mutants exhibited decreased fluorescence of the *glr*-1 transcriptional reporter (Fig. 3-3B). Together, these results indicate that the CMK-1/CaMK signaling axis (Fig. 3-1A), including CKK-1/CaMKK, CMK-1/CaMK, CRH-1/CREB and CBP-1/p300 acts to repress *glr-1* transcription.

The CMK-1/CaMK signaling pathway mediates the *glr-1* transcriptional feedback mechanism

I generated a series of genetic double mutants between *glr-1* and various CMK-1/CaMK pathway mutants to test whether the negative feedback mechanism triggered by loss of *glr-1* was mediated by CMK-1/CaMK signaling. Since my data indicate that the CMK-1/CaMK signaling pathway represses *glr-1* transcription, I hypothesized that decreased GLR-1 signaling triggers an increase in *glr-1* transcription by deactivating the CMK-1/CaMK pathway. In this case, I would expect *glr-1*; *cmk-1* double mutants to have non-additive effects on the *glr-1* transcriptional reporter. Alternatively, if *cmk-1* functions in an independent pathway to regulate *glr-1* transcription, I would expect *glr-1*; *cmk-1* double mutants to have an additive effect on the *glr-1* transcriptional reporter. I found that *glr-1 (n2461)*; *cmk-1 (oy21)* double mutants exhibited a non-additive increase in the *glr-1* transcriptional reporter that is indistinguishable from either single mutant (Fig. 3-4A). This result suggests that the *glr-1*-triggered feedback mechanism and *cmk-1* function in the same pathway to increase *glr-1* transcription. In support of this finding, I found that

Figure 3-4

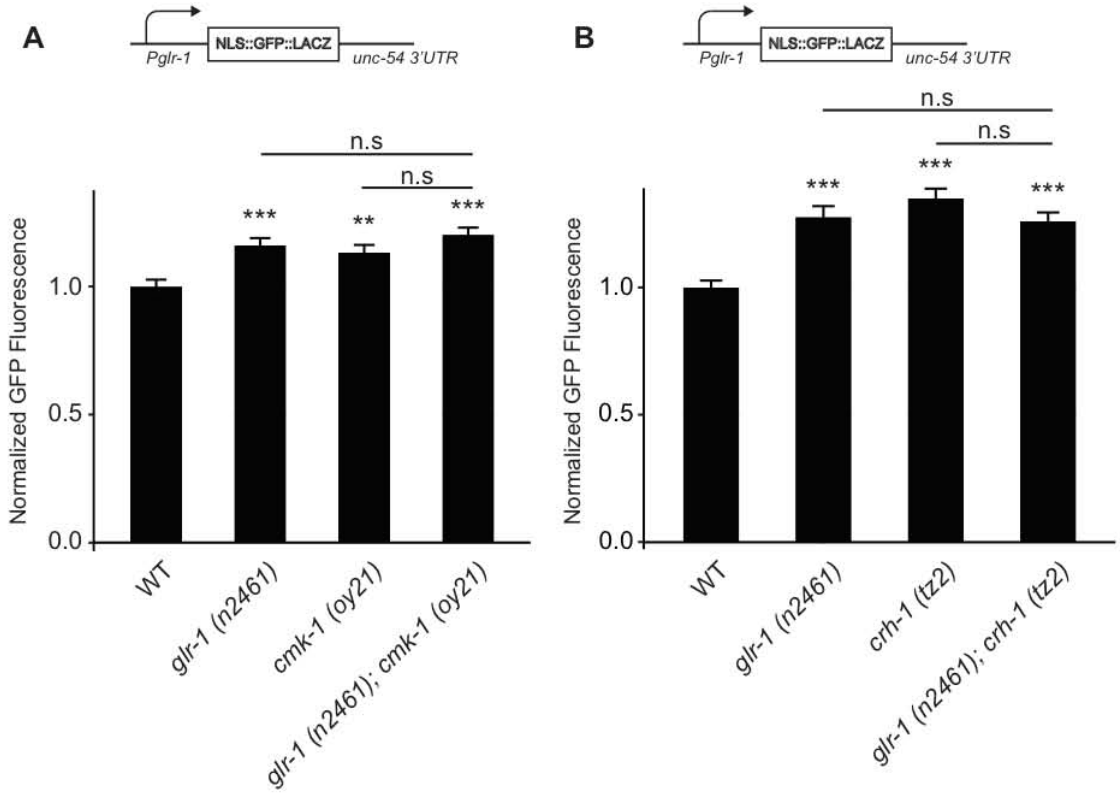
A
Pglr-1
NLS::GFP::LACZ
unc-54 3'UTR
n.s
n.s
***
**
***
Normalized GFP Fluorescence
1.0
0.5
0.0
WT
glr-1 (n2461)
cmk-1 (oy21)
glr-1 (n2461); cmk-1 (oy21)
B
Pglr-1
NLS::GFP::LACZ
unc-54 3'UTR
n.s
n.s
***
***
***
Normalized GFP Fluorescence
1.0
0.5
0.0
WT
glr-1 (n2461)
crh-1 (tz2)
glr-1 (n2461); crh-1 (tz2)

Figure 3-4. The CMK-1/CaMK signaling pathway mediates increased *glr-1* transcription in the *glr-1* transcriptional feedback mechanism

(A) *Pglr-1::nlsGFP::LACZ::unc-54 3'UTR* mean GFP fluorescence in wild type (n=40), *glr-1 (n2461)* (n=40), *cmk-1 (oy21)* (n=41), and *glr-1 (n2461); cmk-1 (oy21)* (n=35) animals normalized to wild type. **(B)** *Pglr-1::nlsGFP::LACZ::unc-54 3'UTR* mean GFP fluorescence in wild type, *glr-1 (n2461), crh-1 (tz2),* and *glr-1 (n2461); crh-1 (tz2)* animals normalized to wild type. n=44 for all genotypes. Maximum GFP fluorescence was measured in the tail neuron PVC. Error bars are SEM. ANOVA with Tukey-Kramer post hoc test was used to compare means. ** $p < .01$, *** $p < .001$. n.s. denotes no significant difference ($p > .05$).

glr-1 (n2461); crh-1 (tz2) double mutants also exhibited a non-additive increase in the *glr*-1 transcriptional reporter that was identical to either single mutant (Fig. 3-4B), suggesting that CRH-1/CREB also functions in the same pathway to negatively regulate *glr-1* transcription.

To provide further support for a role for CMK-1/CaMK in the *glr-1* transcriptional feedback mechanism, I tested whether a recently isolated gain-of-function (*gf*) allele of *cmk-1*, *pg58*, could suppress the increase in *glr-1* transcription observed in *glr-1* mutants. *cmk-1 (pg58 gf)* contains a premature stop codon at W305 resulting in a truncated version of CMK-1 (1-304) (Fig. 3-1B). *pg58* is missing most of its regulatory domain and a putative nuclear export sequence and has been shown to accumulate in the nucleus (Schild et al. 2014). Interestingly, I found that although *cmk-1(pg58 gf)* did not reduce the *glr*-1 transcriptional reporter alone, this gain-of-function allele completely blocked the increase in the *glr*-1 transcriptional reporter triggered by loss of *glr-1* (Fig. 3-5A). Together, these data suggest that CMK-1/CaMK signaling mediates the *glr-1* transcriptional feedback mechanism.

I also used genetic double mutant analysis to test whether the CMK-1/CaMK signaling pathway is required for decreased transcription triggered by increased GLR-1. As described above, GLR-1 levels increase in the VNC of *unc-11/AP180* endocytic mutants (Burbea et al. 2002) resulting in a compensatory reduction in *glr-1* transcription (Fig. 1-6). I hypothesized that accumulation of GLR-1 at synapses in the VNC of *unc-11* mutants results in increased GLR-1 signaling leading to activation of the CMK-1/CaMK pathway

Figure 3-5

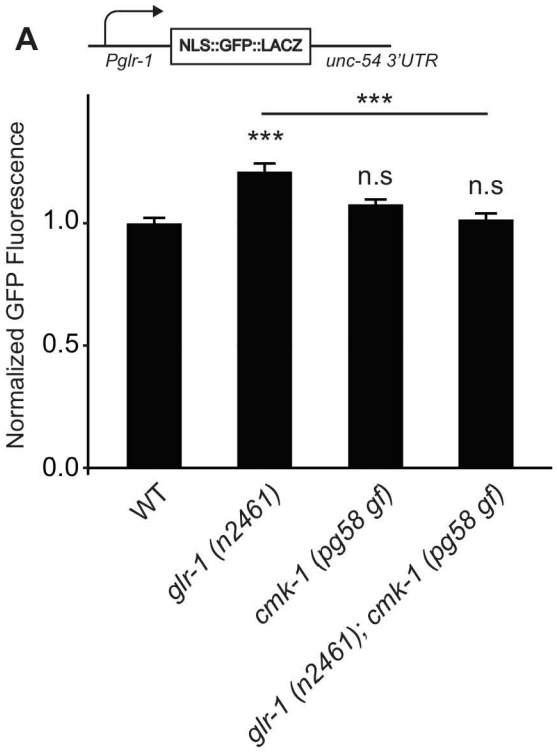
A
Pglr-1
NLS::GFP::LACZ
unc-54 3'UTR
Normalized GFP Fluorescence
1.0
0.5
0.0
***
***
n.s
n.s
WT
glr-1 (n2461)
cmk-1 (pg58 gf)
glr-1 (n2461); cmk-1 (pg58 gf)

Figure 3-5. A gain-of-function CMK-1 allele suppresses the *glr-1* transcriptional feedback mechanism

(A) *Pglr-1::nlsGFP::LACZ::unc-54 3'UTR* mean GFP fluorescence in wild type, *glr-1 (n2461), cmk-1 (pg58 gf),* and *glr-1 (n2461); cmk-1 (pg58 gf)* animals normalized to wild type. Maximum GFP fluorescence was measured in the tail neuron PVC. Error bars are SEM. ANOVA with Tukey-Kramer post hoc test was used to compare means. *** $p < .001$. n.s. denote no significant difference ($p > .05$).

and repression *glr-1* transcription. I found that *ckk-1 (ok1033)*; *unc-11 (e47)* double mutants resulted in fluorescence of the *glr-1* transcriptional reporter at a value that was in between *unc-11* and *ckk-1* single mutants (Fig. 3-6A). These data are consistent with the idea that the repression of *glr-1* transcription observed in *unc-11* mutants is mediated in part by CKK-1. Alternatively, CKK-1/CaMKK may function in parallel with UNC-11/AP180 to reduce *glr-1* transcription.

Given that the CMK-1/CaMK pathway regulates *glr-1* transcription and mRNA levels, I next tested whether this pathway regulates GLR-1 protein levels at synapses. I measured the distribution of an integrated GLR-1::GFP transgene (*nuIs25*) in the anterior VNC of wild type, *cmk-1*, and *crh-1* mutants. GLR-1::GFP localizes to puncta in the VNC of wild type animals and these puncta are closely opposed to presynaptic markers, suggesting that GLR-1::GFP localizes to postsynaptic sites. GLR-1::GFP is functional, as it rescues the behavioral locomotion deficits of *glr-1* null mutants (Rongo et al. 1998, Burbea et al. 2002). I found a trend towards increased GLR-1::GFP puncta intensities in *cmk-1* mutants and a significant increase in puncta intensities in *crh-1* mutants (Fig. 3-7A) with no significant changes in puncta width (Fig. 3-7B). It is possible that, while CRH-1 loss-of-function is sufficient to increase synaptic GLR-1 expression, regulators of GLR-1 synaptic protein expression that are parallel to or downstream of CMK-1/CaMK are able to compensate for *cmk-1* loss-of-function. Together these data suggest that the CMK-1/CaMK signaling pathway regulates *glr-1* gene expression and may, through CREB, affect the abundance of synaptic GLR-1.

Figure 3-6

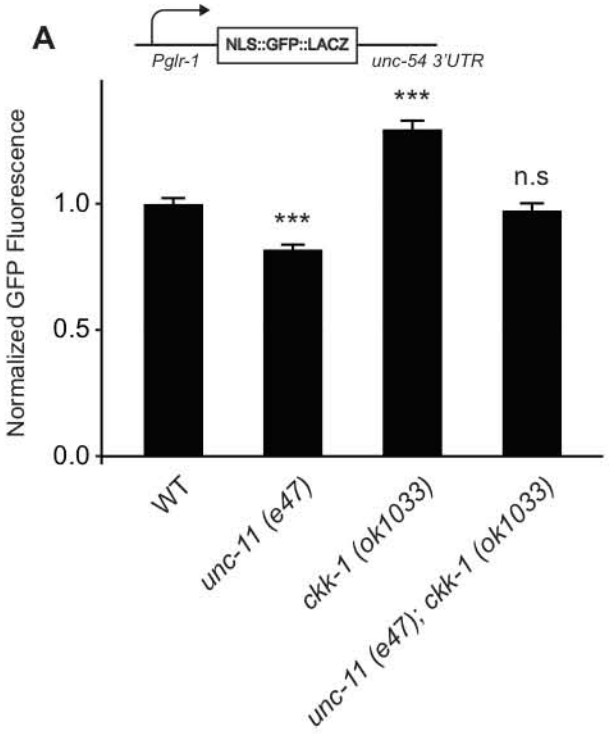
A
NLS::GFP::LACZ
Pglr-1
unc-54 3'UTR
Normalized GFP Fluorescence
1.0
0.5
0.0
***
***
n.s
WT
unc-11 (e47)
ckk-1 (ok1033)
unc-11 (e47); ckk-1 (ok1033)

Figure 3-6. The CMK-1/CaMK signaling pathway may partially mediate decreased *glr-1* transcription in the *glr-1* transcriptional feedback mechanism

(A) *Pglr-1::nlsGFP::LACZ::unc-54 3'UTR* mean GFP fluorescence in wild type (n=44), *unc-11 (e47)* (n=36), *ckk-1 (ok1033)* (n=44), and *unc-11 (e47); ckk-1 (ok1033)* (n=42) animals normalized to wild type. Maximum GFP fluorescence was measured in the tail neuron PVC. Error bars are SEM. ANOVA with Tukey-Kramer post hoc test was used to compare means. *** $p < .001$. n.s. denotes no significant difference ($p > .05$).

Figure 3-7

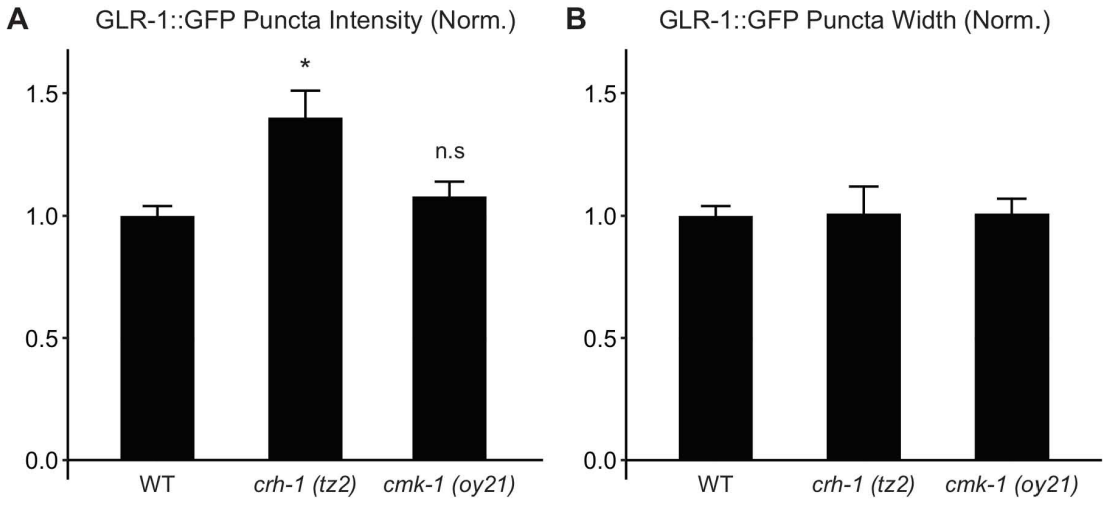
A
GLR-1::GFP Puncta Intensity (Norm.)
*
n.s
1.5
1.0
0.5
0.0
WT
crh-1 (tz2)
cmk-1 (oy21)
B
GLR-1::GFP Puncta Width (Norm.)
1.5
1.0
0.5
0.0
WT
crh-1 (tz2)
cmk-1 (oy21)

Figure 3-7. GLR-1 abundance is increased in the VNC of in *crh-1*/CREB loss-of-function mutants

(A) Quantification of normalized GLR-1::GFP puncta intensities. **(B)** Quantification of normalized GLR-1::GFP puncta widths. n=32 for all genotypes. Error bars are SEM. Differences between genotypes were compared by ANOVA with Tukey-Kramer post hoc tests. * $p < .05$. n.s. denotes no significant difference ($p > .05$).

The GLR-1 feedback mechanism regulates the subcellular localization of CMK-1

CaM kinases are well-known mediators of activity-dependent gene expression and specific isoforms have been shown to translocate between the cytoplasm and nucleus (Wayman et al. 2008, Ma et al. 2014). For example, in mammalian neuronal cultures, homeostatic increases in synaptic GluRs are correlated with a reduction in activated CaMKIV in the nucleus (Ibata et al. 2008). In *C. elegans*, CMK-1/CaMK can shuttle between the cytoplasm and nucleus to regulate thermosensory behaviors (Schild et al. 2014, Yu et al. 2014). Thus, I tested whether changes in the subcellular localization of CMK-1/CaMK were correlated with alterations in *glr-1* transcription. I expressed GFP-tagged CMK-1 (CMK-1::GFP) (Satterlee et al. 2004) in interneurons under control of *Pglr-1* and used confocal microscopy to determine the relative subcellular localization of CMK-1::GFP in the cytoplasm versus nucleus of PVC neurons (see Materials and Methods). The subcellular localization of CMK-1::GFP is regulated by changes in physiological temperature and noxious heat (Schild et al. 2014, Yu et al. 2014), and CMK-1::GFP can rescue heat avoidance behavioral defects in *cmk-1* mutants suggesting that the tagged protein is functional (Schild 2014). Since CKK-1 phosphorylation of CMK-1/CaMK has been shown to promote the nuclear accumulation of CMK-1::GFP in sensory neurons (Schild et al. 2014, Yu et al. 2014), I first analyzed the subcellular localization of CMK-1::GFP in GLR-1-expressing interneurons in *ckk-1* (*ok1033*) loss-of-function mutants. I found that *ckk-1* mutants exhibited increased cytoplasmic CMK-1/CaMK (Fig. 3-8A), consistent with previous studies (Schild et al. 2014, Yu et al. 2014).

To test whether the subcellular localization of CMK-1/CaMK is regulated by the *glr-1* transcriptional feedback mechanism, I analyzed the distribution of CMK-1::GFP in *glr-1* mutants. Similar to *ckk-1* mutants, I found that *glr-1* (*n2461*) mutants exhibited increased cytoplasmic CMK-1::GFP (Fig. 3-8A). These results are consistent with the idea that decreased synaptic GLR-1 results in increased retention of CMK-1/CaMK in the cytoplasm and relief of repression of *glr-1* transcription. On the other hand, I found mutants with increased GLR-1 in the VNC, such as *unc-11(e47)*/AP180 endocytic mutants (Burbea et al. 2002), exhibited increased CMK-1::GFP in the nucleus compared to wild type controls (Fig. 3-8A). Together, these data suggest that increased or decreased GLR-1 in the VNC results in increased or decreased accumulation, respectively, of CMK-1/CaMK in the nucleus.

To specifically test whether nuclear localization of CMK-1/CaMK is sufficient to repress the increase in *glr-1* transcription triggered by loss of glutamatergic signaling, I expressed a constitutively nuclear-localized version of CMK-1/CaMK containing an exogenous NLS (*Pglr-1::CMK-1::EGL-13-NLS*) in GLR-1-expressing neurons. CMK-1::EGL-13-NLS was shown to be five-fold enriched in the nucleus where it can rescue *cmk-1* null mutants for several thermosensory defects (Yu et al. 2014). I found that expression of constitutively nuclear CMK-1/CaMK was sufficient to block the increase in the *glr-1* transcriptional reporter observed in *glr-1* (*n2461*) mutants (Fig. 3-8B). These data suggest that nuclear localization of CMK-1/CaMK represses *glr-1* transcription and provides further evidence that the CMK-1/CaMK signaling pathway mediates the *glr-1* transcriptional feedback mechanism.

Figure 3-8

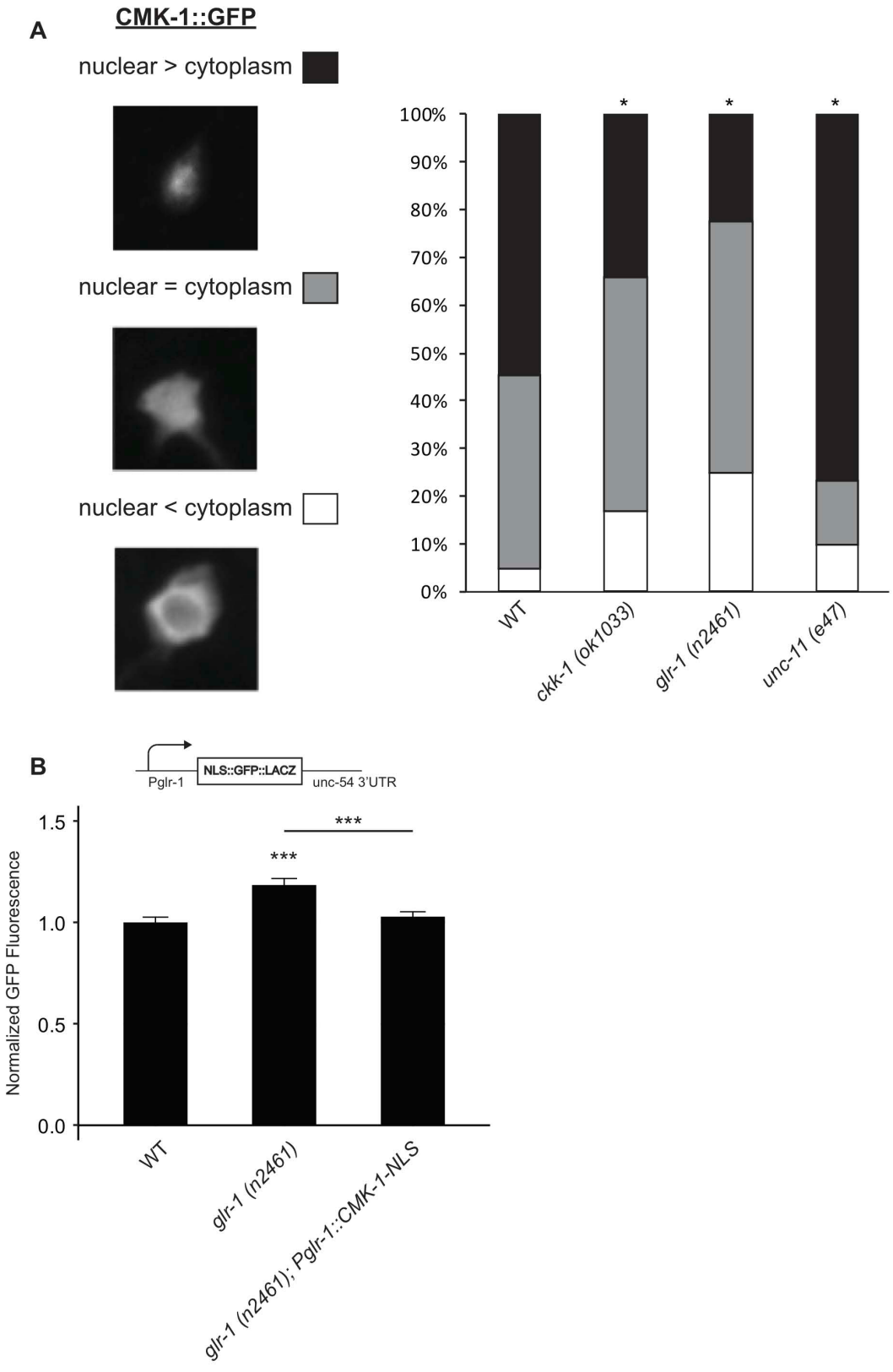
A
CMK-1::GFP
nuclear > cytoplasm
nuclear = cytoplasm
nuclear < cytoplasm
100%
90%
80%
70%
60%
50%
40%
30%
20%
10%
0%
*
*
*
WT
ckk-1 (ok1033)
glr-1 (n2461)
unc-11 (e47)
B
Pglr-1
NLS::GFP::LACZ
unc-54 3'UTR
Normalized GFP Fluorescence
1.5
1.0
0.5
0.0
***
***
WT
glr-1 (n2461)
glr-1 (n2461); Pglr-1::CMK-1-NLS

Figure 3-8. The subcellular localization of CMK-1 is altered in the *glr-1* transcriptional feedback mechanism

(A) CMK-1::GFP was expressed under the *glr-1* promoter (*Pglr-1::CMK-1::GFP*) and visualized in PVC neurons using confocal microscopy. Each cell was qualitatively assessed by a blinded scorer as either more nuclear than cytoplasmic (nuclear > cytoplasm), equal distribution between cytoplasm and nucleus (nuclear = cytoplasm), or less nuclear than cytoplasmic (nuclear < cytoplasm). Wild type (n=64), *ckk-1 (ok1033)* (n=47), *glr-1 (n2461)* (n=40), and *unc-11 (e47)* (n=30) animals were scored. Comparison to wild type was made using Chi-squared post hoc test. **(B)** Nuclear-localized CMK-1 was expressed under the *glr*-1 promoter (*Pglr-1::CMK-1::EGL-13-NLS*) and *Pglr1::nlsGFP::LACZ::unc-54 3'UTR* measured in wild type (n=19), *glr-1 (2461)* (n=21), and *glr-1* (n2461); *Pglr-1::CMK-1::EGL-13-NLS* (n=21) animals normalized to wild type. Maximum GFP fluorescence was measured in the tail neuron PVC. Error bars are SEM. ANOVA with Tukey-Kramer post hoc test was used to compare means. * $p < .05$, *** $p < .001$.

A transcriptional response to synaptic activity requires a signal from the synapse to the nucleus. I tested whether CMK-1/CaMK may signal between the synapse and the nucleus in response to changes in activity. Specifically, CMK-1/CaMK may translocate from synapse to nucleus in response to increases in activity and from nucleus to synapse in response to decreases in activity. To test this possibility, I measured fluorescence intensity of CMK-1::GFP at puncta in the anterior VNC in wild type (Fig. 3-9A) and *ckk-1* mutants. I found an increase in fluorescence in *ckk-1* mutants (Fig. 3-9B) suggesting that when CMK-1/CaMK is not phosphorylated, its abundance increases at synapses in the VNC. Next I measured peak fluorescence in *glr-1* and *unc-11* mutants to test whether decreased or increased GLR-1 levels, respectively, affect CMK-1/CaMK localization to puncta in the VNC. I found increased puncta fluorescence in *glr-1* mutants and a trend towards decreased puncta fluorescence in *unc-11* mutants (Fig. 3-9B). Levels of CMK-1::GFP in the cord in between puncta were also significantly increased in *ckk-1* and *glr-1* mutants, and trended towards decreased values in *unc-11* mutants (Fig. 3-9C), suggesting that CMK-1/CaMK may be regulated at both synapses and neuronal processes in response to the feedback mechanism. Together, these data suggest a model where, in response to changes in levels or activity of GLR-1, CMK-1/CaMK translocates between synapses or neuronal processes and the nucleus in order to regulate *glr-1* transcription (see model, Fig. 3-10).

Calcineurin mediates the *glr-1* transcriptional feedback pathway

Calcineurin is a ubiquitous phosphatase that responds to synaptic calcium influx and is critical for initiating activity-dependent signaling cascades (Goold and Nicoll 2010).

Figure 3-9

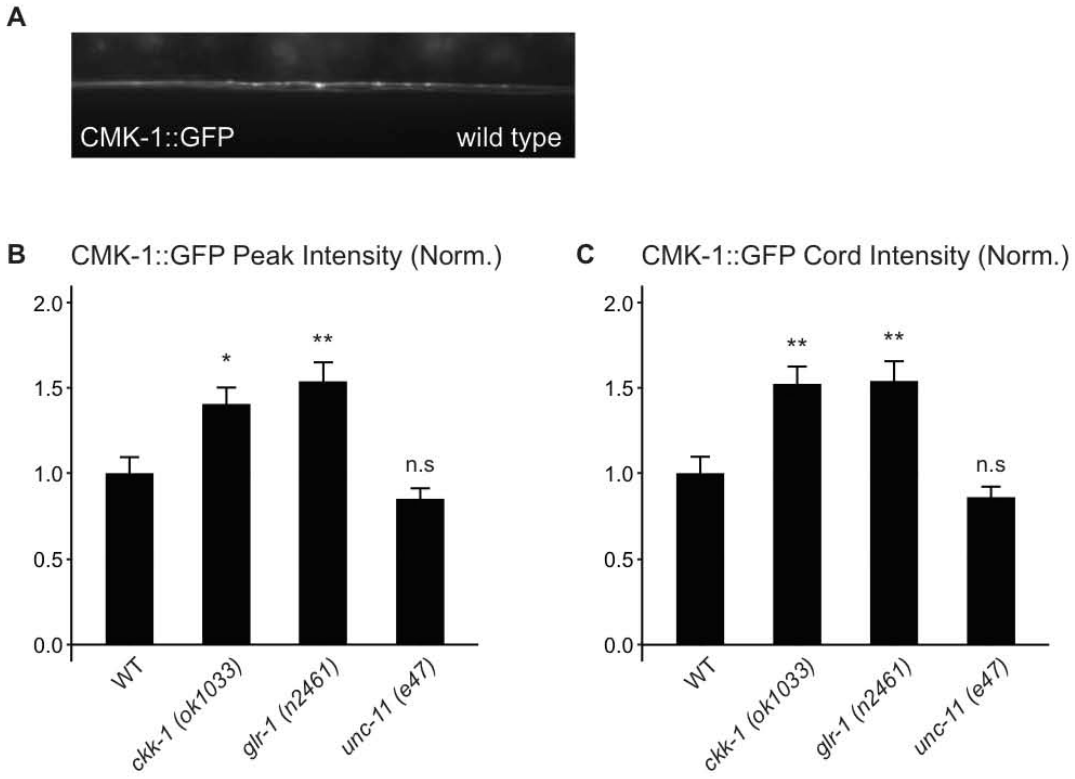
A
CMK-1::GFP
wild type
B
CMK-1::GFP Peak Intensity (Norm.)
2.0
1.5
1.0
0.5
0.0
*
**
n.s
WT
ckk-1 (ok1033)
glr-1 (n2461)
unc-11 (e47)
C
CMK-1::GFP Cord Intensity (Norm.)
2.0
1.5
1.0
0.5
0.0
**
**
n.s
WT
ckk-1 (ok1033)
glr-1 (n2461)
unc-11 (e47)

Figure 3-9. CMK-1 abundance in the VNC is altered in the *glr-1* transcriptional feedback mechanism

(A) Representative image of CMK-1::GFP puncta in the VNC of a wild type animal **(B)** Quantification of normalized CMK-1::GFP puncta intensities. **(C)** Quantification of normalized CMK-1::GFP cord intensities. Shown are the means and SEM for wild type (n=35), *ckk-1 (ok1033)* (n=46), *glr-1 (n2461)* (n=42), and *unc-11 (e47)* (n=26). Differences between genotypes were compared by ANOVA with Tukey-Kramer post hoc test. * $p < .05$, ** $p < .01$. n.s. denotes no significant difference ($p > .05$).

Figure 3-10

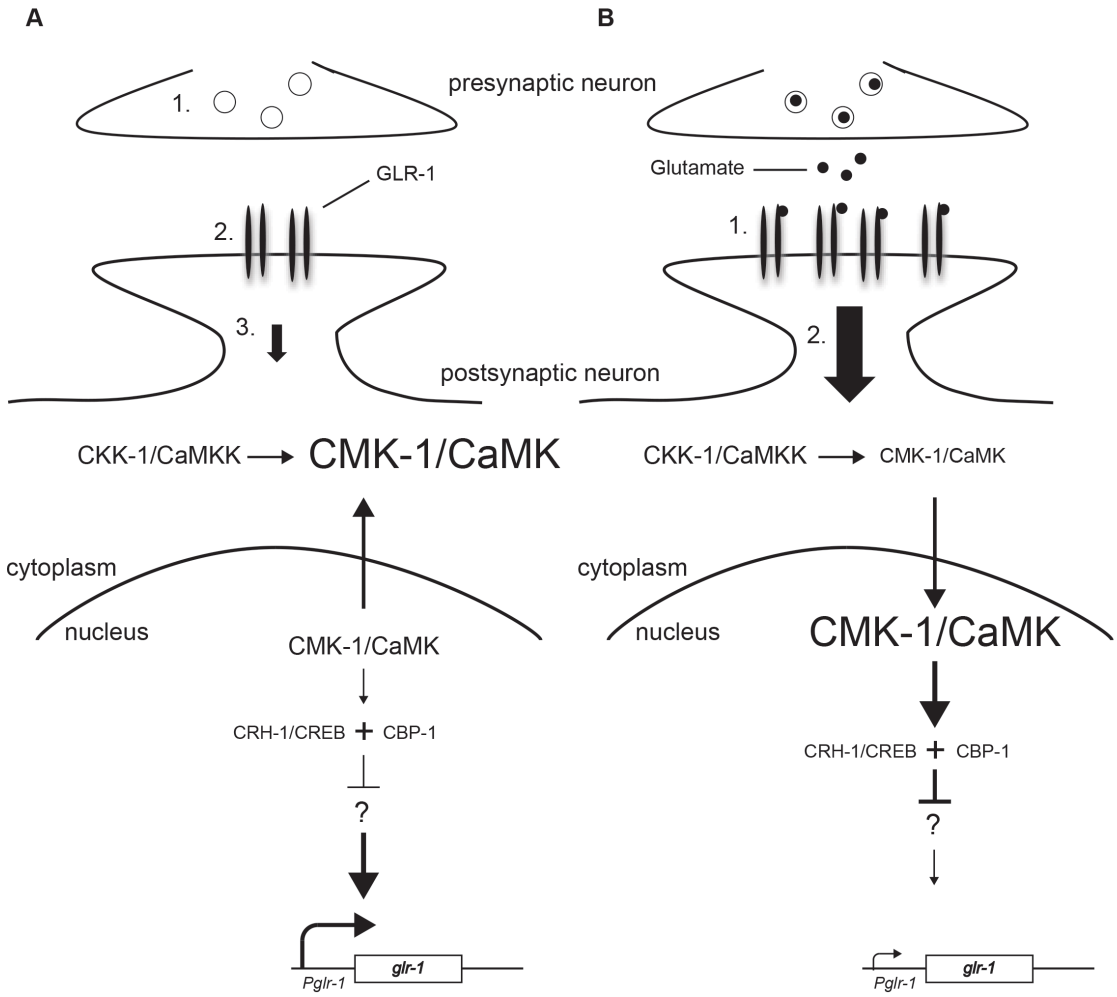
A
B
presynaptic neuron
1.
GLR-1
2.
3.
postsynaptic neuron
Glutamate
1.
2.
CKK-1/CaMKK
CMK-1/CaMK
CKK-1/CaMKK
CMK-1/CaMK
cytoplasm
nucleus
CMK-1/CaMK
CRH-1/CREB
CBP-1
?
glr-1
Pglr-1
cytoplasm
nucleus
CMK-1/CaMK
CRH-1/CREB
CBP-1
?
glr-1
Pglr-1

Figure 3-10. Model: CMK-1/CaMK mediates a feedback mechanism coupling synaptic GLR-1 with *glr-1* transcription.

(A) Increased cytoplasmic CMK-1/CaMK leads to relief of repression of *glr-1* transcription in response to 1) decreased glutamate release, 2) decreased levels of synaptic GLR-1, or 3) decreased postsynaptic activity. **(B)** Increased nuclear CMK-1/CaMK leads to repression of *glr-1* transcription in response to 1) increased levels of synaptic GLR-1 or 2) increased GLR-1 activity.

Calcineurin acts in opposition to the CaMK enzymes by dephosphorylating downstream targets such as GluA1. Dephosphorylation by calcineurin leads to AMPAR internalization and decreased synaptic efficacy (Baumgartel and Mansuy 2012). Furthermore, calcineurin has a known role in synaptic scaling. TTX treatment leads to reduced calcineurin and calcineurin knockdown induces CP-AMPAR-dependent scaling. This suggests a model where chronic activity-blockade inactivates calcineurin, allowing for increased synaptic AMPAR expression (Kim 2014). *C. elegans* calcineurin is encoded by two genes, *cna-1/tax-6* (containing the phosphatase domain) and *cnb-1* (containing the regulatory domain). Loss-of-function of the calcineurin phosphatase domain (*cna-1/tax-6 (p675)*) had no effect on basal *glr-1* transcription but suppressed the increase in transcription in *glr-1* null mutants (Fig. 3-11A), suggesting that *cna-1* is necessary for the feedback mechanism, but not for basal *glr-1* transcription. On the other hand, *cnb-1 (jh703)* mutants missing the regulatory domain had decreased *glr-1* transcription basally, which was not increased in *cnb-1; glr-1* double mutants (Fig. 3-11B). Thus, calcineurin appears to be necessary for the transcriptional increases seen in the feedback mechanism. The regulatory domain may also be necessary for basal *glr-1* transcription, perhaps through interactions with an alternate phosphatase. This positive regulatory role for calcineurin on GLR-1 is in contrast to mammalian calcineurin which negatively regulates AMPARs during synaptic scaling.

Figure 3-11

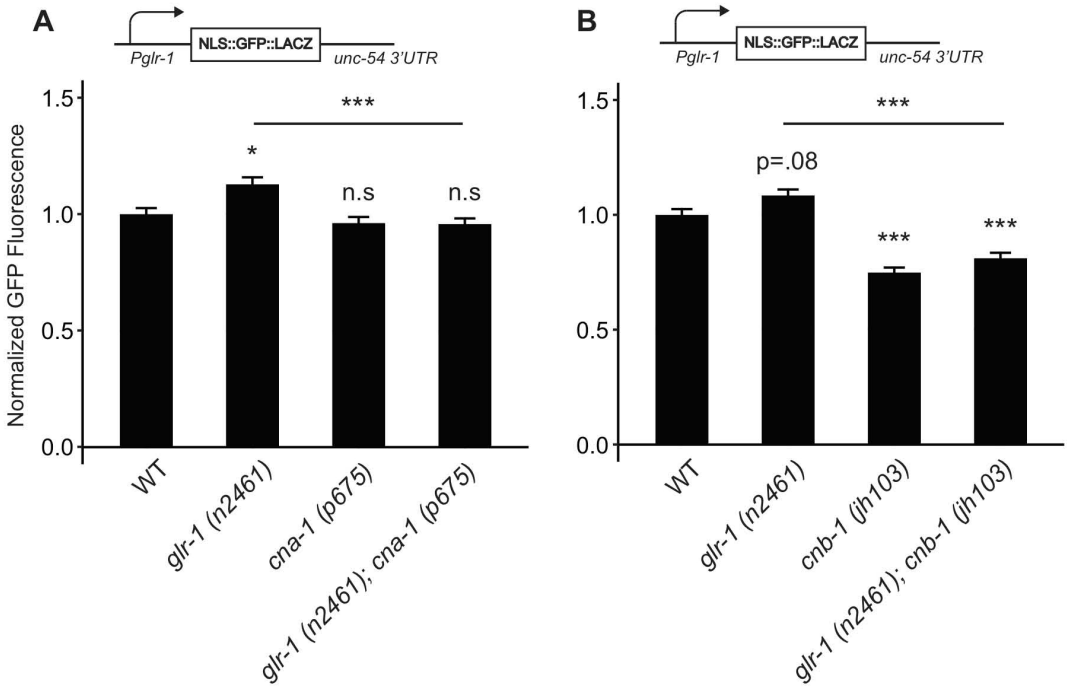
A
Pglr-1
NLS::GFP::LACZ
unc-54 3'UTR
Normalized GFP Fluorescence
1.5
1.0
0.5
0.0
***
*
n.s
n.s
WT
glr-1 (n2461)
cna-1 (p675)
glr-1 (n2461); cna-1 (p675)
B
Pglr-1
NLS::GFP::LACZ
unc-54 3'UTR
1.5
1.0
0.5
0.0
***
p=.08
***
***
WT
glr-1 (n2461)
cnb-1 (jh103)
glr-1 (n2461); cnb-1 (jh103)

Figure 3-11. Calcineurin mediates increased *glr-1* transcription in the *glr-1* transcriptional feedback mechanism

(A) *Pglr-1::nlsGFP::LACZ::unc-54 3'UTR* mean GFP fluorescence in wild type (n=40), *glr-1 (n2461)* (n=40), *cna-1 (p675)* (n=40), and *glr-1 (n2461); cna-1 (p675)* (n=34) animals normalized to wild type. **(B)** *Pglr-1::nlsGFP::LACZ::unc-54 3'UTR* mean GFP fluorescence in wild type (n=40), *glr-1 (n2461)* (n=37), *cnb-1 (jh103)* (n=40), and *glr-1 (n2461); cnb-1 (jh103)* (n=39) animals normalized to wild type. Maximum GFP fluorescence was measured in the tail neuron PVC. Error bars are SEM. ANOVA with Tukey-Kramer post hoc test was used to compare means. ** $p < .01$, *** $p < .001$. n.s. denotes no significant difference ($p > .05$)

Chapter 4

A yeast-1-hybrid screen for transcription factors that regulate *glr-1* basally and in the feedback mechanism

Attributes

Experiments in Chapter 4 were performed by Benjamin Moss and Lidia Park. Experiments Figures 4-2 and 4-3 were performed by Benjamin Moss. Experiments in Figure 4-5 were performed by Lidia Park. Experiments in Figures 4-4 and 4-6 were performed by Benjamin Moss and Lidia Park.

Chapters 2 and 3 present data describing a feedback mechanism mediated by CMK-1/CaMK that responds to changes in neuronal activity by regulating *glr-1* transcription. Little is known about transcription of GluRs in response to changes in activity, and there are no validated transcription factors (TFs) for GLR-1. Thus, I aimed to identify TFs that regulate GLR-1, particularly those involved in the feedback mechanism. To do this, I am performing a yeast-1-hybrid (Y1H) on the *glr-1* promoter using a yeast library of *C. elegans* TFs.

The Y1H, like its predecessor, the yeast-two-hybrid, takes advantage of interactions between a protein's DNA binding domain (DB) and an activating domain (AD). In the yeast-two-hybrid a bait protein is fused to the DB and a prey protein is fused to the AD. If these two hybrid proteins interact in the yeast system, the proximity of the DB and AD form a functional TF which leads to expression of a reporter. In a Y1H assay, the AD is fused to a TF, and since transcription factors inherently have DBs, the DB is not required (Fig. 4-1A). The AD of GAL4 is commonly used, as it was found that addition of this AD allows any TF, activator or repressor, to activate expression of a downstream reporter. Thus, this system allows for identification of both activator and repressor TFs (Reece-Hoyes and Marian Walhout 2012).

Deplancke, et al. established a Y1H system that utilizes a *C. elegans* TF library based on the *C. elegans* ORFeome (Deplancke et al. 2004). This library contains 755 plasmid-encoded TFs fused with the GAL4p AD, representing an estimated 80% of known *C. elegans* TF open reading frames (Vermeirssen et al. 2007). DNA promoter regions of

Figure 4-1

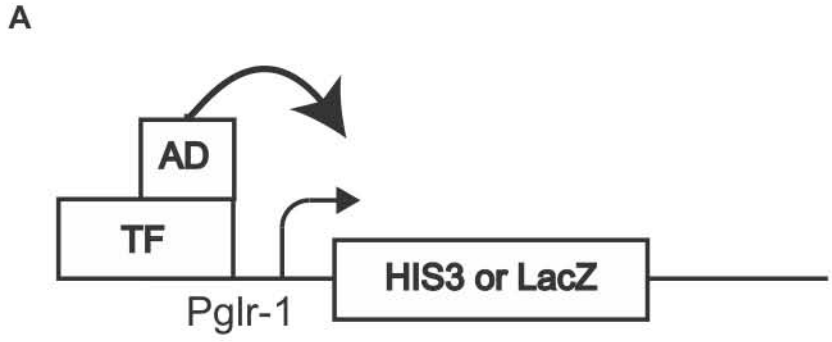

Figure 4-1. Yeast-one-hybrid model

(A) When a transcription factor (TF) prey interacts with a promoter bait (*Pglr-1*), the AD domain of the transcription factor triggers expression of HIS3 and LACZ reporters. HIS3 expression allows for growth of yeast containing bait-prey interactions on media containing 3-AT, an inhibitor of the His3p enzyme. Yeast containing bait-prey interactions exhibit expression of LACZ which causes these yeast to turn blue when treated with X-gal.

interest are cloned into two different reporter plasmids whose expression is induced by binding of the TF-GAL4p protein. One reporter, HIS3, allows for growth on medium containing 3-AT, an inhibitor of the His3p enzyme. In the second reporter, B-galactosidase encodes for the LACZ protein which turns colorless X-gal blue. Both of these reporters contain minimal promoters that have low levels of baseline expression even without activation by the TF-AD prey. The use of two reporters decreases the rate of technical false positives (Reece-Hoyes and Marian Walhout 2012).

Design of *Pglr-1* baits

While classically only very short DNA segments (~30 bp) were used for Y1H assays, Deplancke et. al. developed a system using promoters up to 2.4 kb (Deplancke et al. 2004). However, all of the *Pglr-1* transcriptional reporters described above in Chapters 2 and 3 contain 5.3 kb of promoter (the stretch of DNA from the *glr-1* TSS until the next upstream gene). Thus, for the Y1H, I shortened *Pglr-1* to 2.4 kb upstream of the *glr-1* TSS. Because longer promoters typically induce higher background noise (auto-activation), I also utilized a shorter promoter in order to reduce auto-activation. I constructed a *Pglr-1* bait from the Gateway compatible *C. elegans* promoterome (Dupuy et al. 2004), which contains ~700 bp of *Pglr-1* upstream of the TSS.

Assessment of baits using GFP transcriptional reporters

Since the entire 5.3 kb of *Pglr-1* used in the GFP reporter assays is too large to function as a Y1H bait, I tested whether shorter 2.4 kb and 0.7 kb baits could still mediate the feedback mechanism in vivo. Either a region containing 2.4 kb or 0.7 kb upstream of the

glr-1 TSS was swapped into the *glr-1* transcriptional reporter and animals expressing transgenic extrachromosomal arrays were maintained (as opposed to the 5.3 kb *glr-1* transcriptional reporter, which was integrated into the genome). These reporters were then crossed into various mutants to test their efficacy in mediating the feedback pathway. For the 2.4 kb promoter, *cmk-1* mutants exhibited a significant increase in GFP fluorescence, while *crh-1* mutants trended towards an increase (Fig. 4-2A). Because this construct was expressed as an array, the variation in fluorescence between animals was much higher than in the integrant, possibly accounting for why the increase in *crh-1* mutants did not reach statistical significance.

While our lab had previously used the 2.4 kb promoter to express transgenes in *glr-1*-expressing neurons, it was unknown if the 0.7 kb promoter would be sufficient for expression in the same cells. However, as in the 5.3 kb and 2.4 kb reporters, the 0.7 kb reporter did lead to expression in a group of neurons in the head as well as in the PVC interneurons (data not shown). Interestingly, GFP fluorescence was highly variable in animals expressing the 0.7 kb reporter, making it challenging to define imaging parameters that were able to capture the full range of expression. As can be seen from the scatter plots of GFP fluorescence (Fig. 4-3B), while many animals had very low fluorescence of the reporter, other animals were overexposed at the same imaging settings. This made quantification of the strain problematic, though, when analyzed, I observed no significant increase in fluorescence in *glr-1* or *ckk-1* mutants (Fig. 4-3A). While this result suggests that the 0.7 kb promoter does not mediate the feedback

Figure 4-2

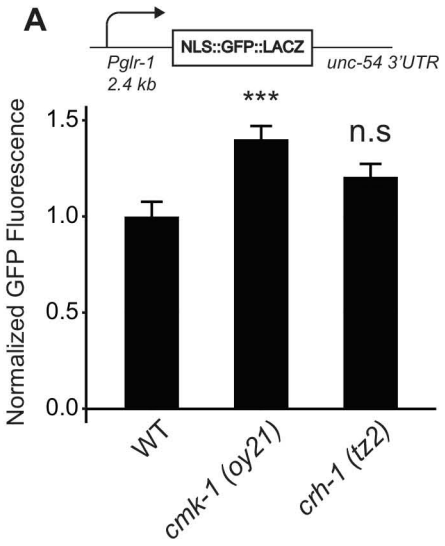
A
NLS::GFP::LACZ
Pglr-1
2.4 kb
unc-54 3'UTR
***
n.s
Normalized GFP Fluorescence
1.5
1.0
0.5
0.0
WT
cmk-1 (oy21)
crh-1 (tz2)

Figure 4-2. 2.4 kb of promoter upstream of the *glr-1* transcription start site is sufficient to mediate the *glr-1* transcriptional feedback mechanism.

(A) *Pglr-1 (2.4 kb)::nlsGFP::LACZ::unc-54 3'UTR* normalized GFP fluorescence in wild type, *cmk-1 (oy21)*, and *crh-1 (tz2)* animals normalized to wild type. Maximum GFP fluorescence was measured in the tail neuron PVC for 40 for each genotype. Error bars are SEM. ANOVA with Tukey-Kramer post hoc test was used to compare means. *** $p < .001$. n.s. denotes no significant difference ($p > .05$)

Figure 4-3

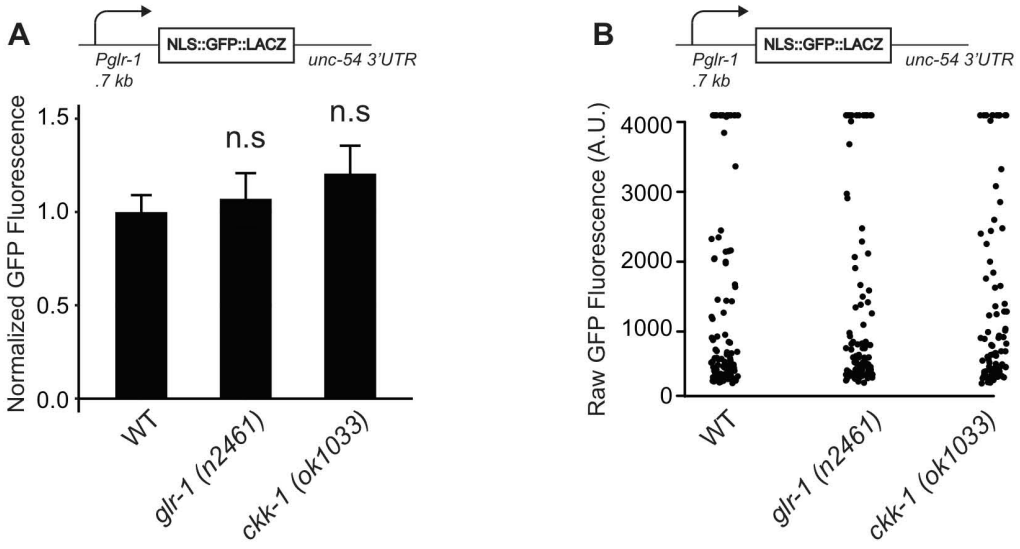
A
Pglr-1
.7 kb
NLS::GFP::LACZ
unc-54 3'UTR
Normalized GFP Fluorescence
1.5
1.0
0.5
0.0
n.s
n.s
WT
glr-1 (n2461)
ckk-1 (ok1033)
B
Pglr-1
.7 kb
NLS::GFP::LACZ
unc-54 3'UTR
Raw GFP Fluorescence (A.U.)
4000
3000
2000
1000
0
WT
glr-1 (n2461)
ckk-1 (ok1033)

Figure 4-3. 0.7 kb of promoter upstream of the *glr-1* transcription start site is not sufficient to mediate the *glr-1* transcriptional feedback mechanism

(A) *Pglr-1 (2.4 kb)::nlsGFP::LACZ::unc-54 3'UTR* mean GFP fluorescence in wild type (n=114), *glr-1 (n2461)* (n=115), and *ckk-1 (ok1033)* (n=92) animals normalized to wild type. Error bars are SEM. ANOVA with Tukey-Kramer post hoc test was used to compare means. Maximum GFP fluorescence was measured in the tail neuron PVC. *** $p < .001$. n.s. denotes no significant difference ($p > .05$)

mechanism, both mutants trended towards an increase, and the high variability within strains could obfuscate meaningful results.

Together these results suggest that the 2.4 kb promoter is sufficient to mediate the feedback mechanism, but the 0.7 kb promoter likely is not. This potentially provides a way to screen positive hits from the Y1H as likely candidates for mediating the feedback mechanism. TFs involved in mediating the feedback mechanism should activate the 2.4 kb promoter reporter in the Y1H but not the 0.7 kb promoter reporter. Future experiments with additional mutants (e.g., *glr-1* and *eat-4*) will be tested to confirm whether the 2.4 kb promoter can also respond to decreased synaptic GLR-1 and decreased glutamatergic activity.

Construction of Y1H baits

After Gateway cloning *Pglr-1* (2.4kb) and *Pglr-1* (0.7kb) into the HIS3 and LACZ reporter plasmids, these bait constructs were integrated into the Y1H yeast strain YM4271. A handful of integrants were tested for auto-activation in the X-gal and 3-AT assays. For the 3-AT assay, integrants were patched onto plates with concentrations of 0 mM, 20 mM, 50 mM, and 80 mM 3-AT. Higher activation of the HIS3 bait allows for growth on higher concentrations of 3-AT, which inhibits production of histamine. Several controls from the Walhout lab were used in these assays. PB0507.1 corresponds to the promoter for the clone B0507.1, which has low auto-activation and positively interacts with the TF, CES-1, in the Y1H assay (Reece-Hoyes et al. 2009). Thus, PB0507.1 can be used as a positive control bait that expresses low levels of auto-activation in the 3-AT and

X-gal assays (Fig. 4-4A and 4-4B). Control 4 and control 5 (Ct4 and Ct5) are control yeast strains that contain robust bait-prey interactions. Thus, they serve as positive controls for the X-gal and 3-AT assays and express robust activation— stronger blue color in the presence of X-gal and stronger growth on high concentrations of 3-AT— of both reporters (Fig. 4-4A and 4-4B).

For the *Pglr-1* (2.4 kb) bait, while there is less growth on the 80 mM plates for the integrants, there appears to be much more auto-activation than for the PB0507.1 bait, which shows very little growth in the absence of the positive interacting prey CES-1, on 20 mM and 80 mM 3-AT. Because of this high background, integrants were chosen based on the X-gal assay, and all subsequent experiments were performed using the X-gal reporter (The 3-AT assay was repeated for the 0.7 kb promoter, but similar problems were encountered). For the X-gal assay the 2.4 kb and 0.7 kb integrants with the lowest blue signal were selected for the Y1H assay (Figure 4-4B and 4-4C, red boxes). While the level of background in the X-gal assay for both the 2.4 kb and 0.7 kb promoter was significantly more pronounced than for the PB0507.1 bait, it was significantly less than for Ct4. This suggests that while the *Pglr-1* baits may have a high level of background, positive interactions as strong as Ct4 should still be detectable.

Screening controls

I next optimized a system in which to perform the Y1H screen (see Materials and Methods). Previous protocols (Deplancke et al. 2004, Reece-Hoyes and Walhout 2012) were designed for screening a cDNA library of TF preys. I modified these protocols for

Figure 4-4

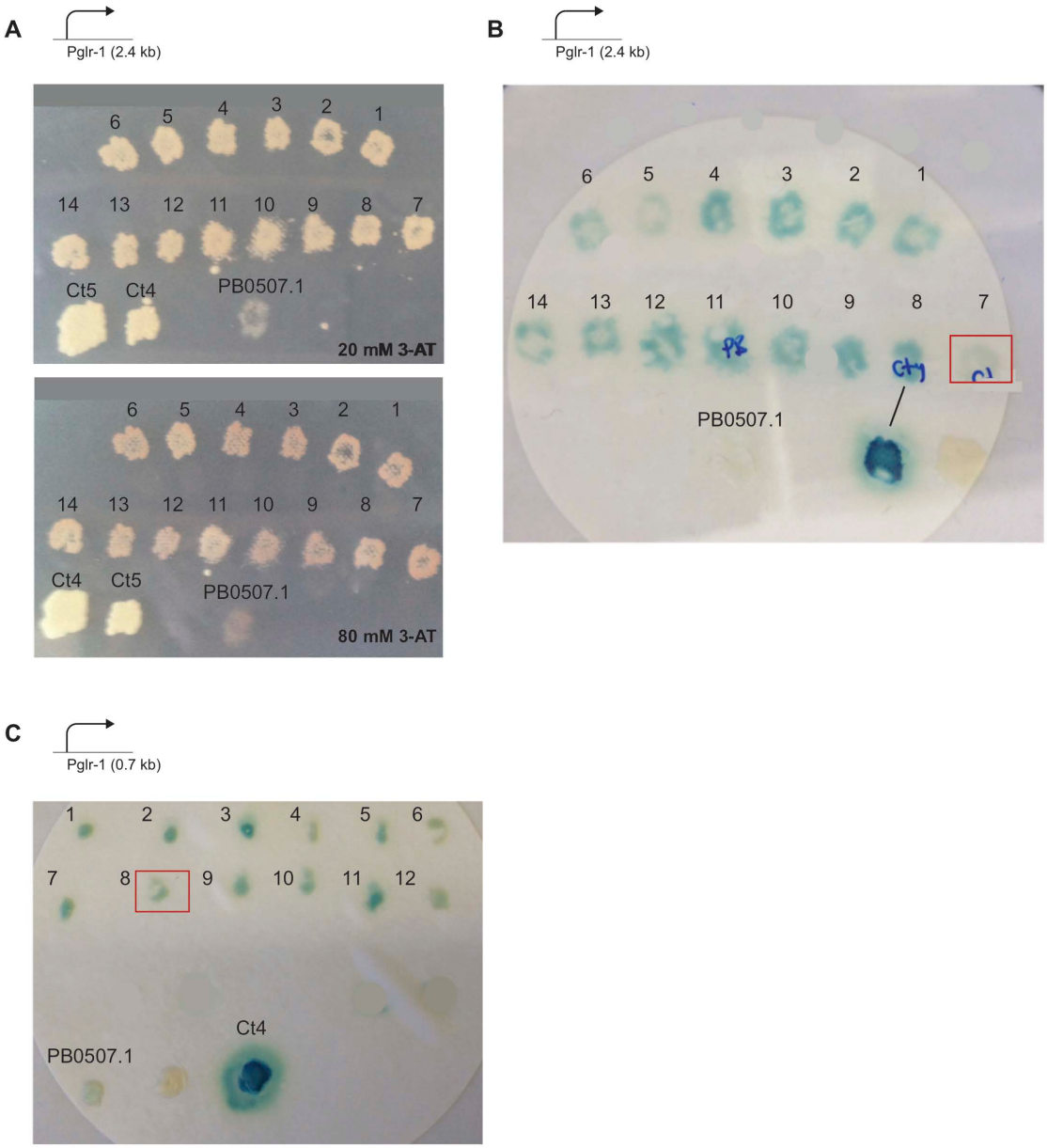
A
Pglr-1 (2.4 kb)
6 5 4 3 2 1
14 13 12 11 10 9 8 7
Ct5 Ct4
PB0507.1
20 mM 3-AT
6 5 4 3 2 1
14 13 12 11 10 9 8 7
Ct4 Ct5
PB0507.1
80 mM 3-AT
B
Pglr-1 (2.4 kb)
6 5 4 3 2 1
14 13 12 11 10 9 8 7
PB0507.1
C
Pglr-1 (0.7 kb)
1 2 3 4 5 6
7 8 9 10 11 12
Ct4
PB0507.1

Figure 4-4. Selection of *Pglr-1* bait integrants

(A) 3-AT assay of *Pglr-1* (2.4 kb) integrants. *Pglr-1* (2.4 kb) HIS3 and LACZ reporter plasmids were integrated into the Y1H yeast strain YM2471 and integrants were assayed for growth on 3-AT. High levels of growth indicate high auto-activation of the HIS3 reporter. **(B)** X-gal assay of *Pglr-1* (2.4 kb) integrants. The integrant with the least blue signal (#7) after 24 hours of incubation with X-gal was selected for the Y1H screen. **(C)** X-gal assay of *Pglr-1* (0.7 kb) integrants. The integrant with the least blue signal (#8) after 24 hours of incubation with X-gal was selected for the Y1H screen.

screening a library of yeast TFs arrayed across eight 96-well plates. Briefly, yeast TFs were grown in 96-well plates of selective liquid media and then mated overnight in non-selective media in a 96-well plate format to the *Pglr-1* (2.4 kb) and *Pglr-1* (0.7 kb) baits. These matings were spotted in duplicate onto selective media agar plates, so that only progeny of TF-bait matings would grow. Matings were then replicate-plated to nitrocellulose membranes placed on selective agar media, allowed to grow for several days, and then the X-gal assay was performed on the nitrocellulose membranes.

After testing a time course for the X-gal assay I determined that positive hits could be visualized at 24 hours. I tested this method using the known interaction of PB0507.1 bait and CES-1 TF prey (Reece-Hoyes et al. 2009). As a negative control for PB0507.1, I used SKN-1, which has no known association with PB0507.1. I also tested the *Pglr-1* baits with these two TFs. However, one of the persistent problems with the Y1H screen is the lack of positive control prey for the *Pglr-1* baits as there are no TFs validated to interact with *Pglr-1*. I used SKN-1, as this was the only positive hit from an *in silico* search for TF-binding sites within *Pglr-1* (TRANSFAC, BioBase). I first tested the baits alone to measure background auto-activation and found significant auto-activation for the *Pglr-1* baits and very minimal auto-activation for PB0507.1 (Fig. 4-5A). Next I performed matings to the TFs, SKN-1 and CES-1, as described above (except in tubes, not 96-well plates). The controls for the X-gal assay, Ct4 and Ct5, show strong X-gal staining (Fig 4-5B). Importantly, PB0507.1 shows very little staining for mating with SKN-1, but turns blue when mated to CES-1 (Fig. 4-5B), confirming that I can detect bait-prey interactions with this protocol. Both CES-1 and SKN-1 matings with both of the

Figure 4-5

A

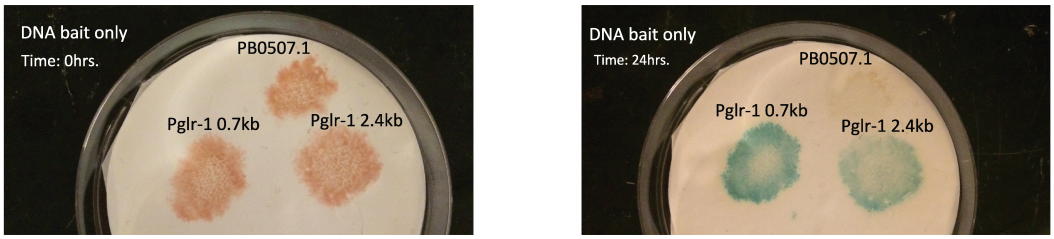
DNA bait only
Time: 0hrs.
PB0507.1
Pglr-1 0.7kb
Pglr-1 2.4kb
DNA bait only
Time: 24hrs.
PB0507.1
Pglr-1 0.7kb
Pglr-1 2.4kb

B

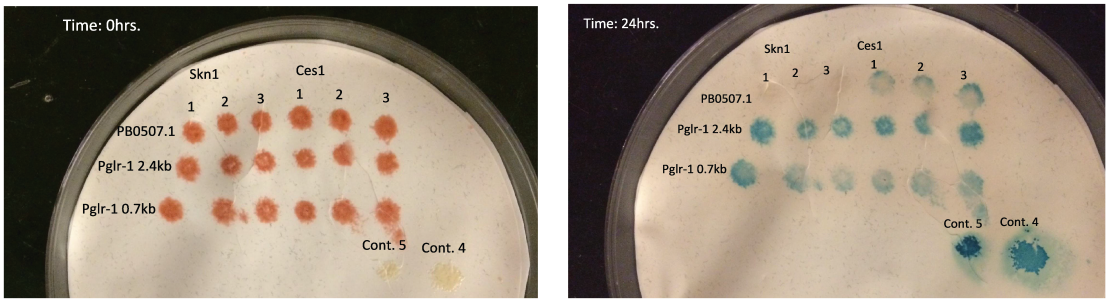
Time: 0hrs.
Skn1
Ces1
1 2 3 1 2 3
PB0507.1
Pglr-1 2.4kb
Pglr-1 0.7kb
Cont. 5
Cont. 4
Time: 24hrs.
Skn1
Ces1
1 2 3 1 2 3
PB0507.1
Pglr-1 2.4kb
Pglr-1 0.7kb
Cont. 5
Cont. 4

Figure 4-5. Detection of known positive interactions with the modified yeast-one-hybrid (Y1H)

(A) DNA baits were tested for auto-activation after 24 hours in the X-gal assay. **(B)** Baits PB0507.1, *Pglr-1* (2.4 kb), and *Pglr-1* (0.7 kb) were tested for interactions with the transcription factors SKN-1 and CES-1 in the X-gal assay. Cont. 4 and Cont 5. are positive controls for the X-gal assay. PB0507.1 interacts with CES-1 and all other interactions are negative.

Pglr-1 baits exhibited relatively strong staining, but not visibly stronger than the unmated baits, suggesting no interaction with either of these proteins (Fig. 4-5B). While auto-activation is not as strong as the staining for Ct4 and Ct5, it is also possible that auto-activation of the *Pglr-1* baits is too strong to detect an interaction.

Preliminary results

Despite high levels of auto-activation, I have begun screening the Y1H library. Auto-activation may increase false negatives, but, given the number of positive hits from published Y1H screens (DePlancke 2004), it is likely that even with highly auto-activated baits, some interactions may still be detectable. Figure 4-6 shows an example of results from screening plate 1 and identification of a candidate interaction. This screen was performed with the *Pglr-1* (2.4 kb) bait. Following the protocol described above, Ct4 and Ct5 turn dark blue in the X-gal assay, while the bait only sample does not turn blue at all. (Fig. 4-6A). In the X-gal assay of samples from plate 1, sample 2A turned darker blue than the other samples, suggesting an interaction between this TF and the *Pglr-1* (2.4kb) promoter. To confirm this result, 2A and three other samples (3F, another potential hit which turned slightly bluer than the rest of the samples, and 7A and 8B as negative controls) were re-mated to the *Pglr-1* (2.4 kb) bait and the X-gal assay was repeated with five mating replicates per sample. This confirmed that 2A turned bluer than the negative controls and suggests it as a preliminary hit for the Y1H screen. 3F did not turn bluer than the negative controls, so is unlikely to be a hit. These data suggest that the Y1H can detect preliminary hits.

Figure 4-6

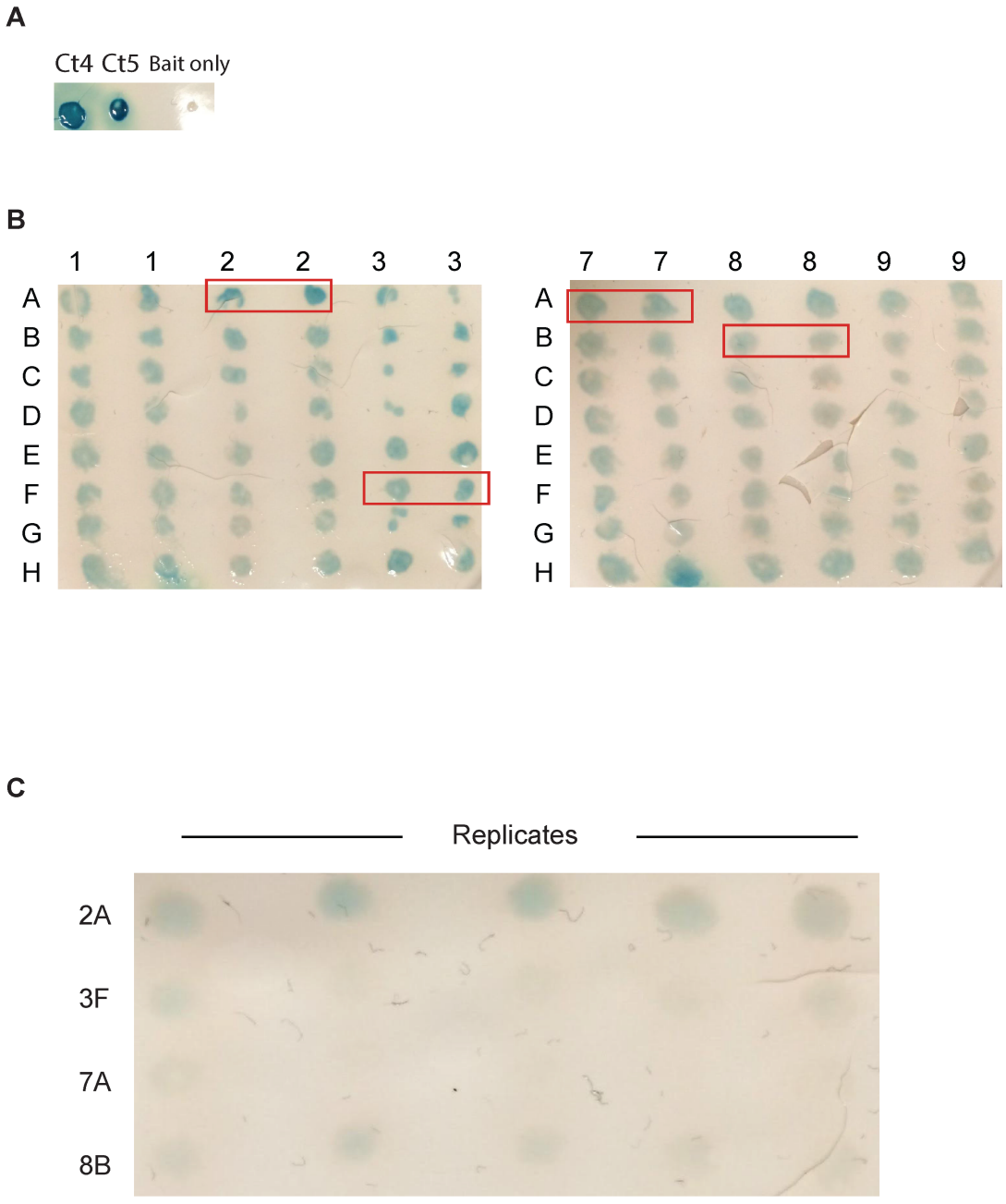
A
Ct4 Ct5 Bait only
B
1 1 2 2 3 3
A
B
C
D
E
F
G
H
7 7 8 8 9 9
A
B
C
D
E
F
G
H
C
Replicates
2A
3F
7A
8B

Figure 4-6. Detection of a candidate hit from the *Pglr-1* (2.4 kb) yeast-one-hybrid (Y1H) screen.

(A) Ct4 and Ct5, positive controls for the X-gal assay, are positive in the modified Y1H screening protocol, while the *Pglr-1* (2.4 kb) bait-only control is negative. **(B)** Two plates from the *Pglr-1* (2.4 kb) Y1H screen of the transcription factor TF library plate 1. Each TF is run in duplicate in the X-gal assay. Column numbers and row letters refer to the 96-well plate from the TF library. Samples were assessed after 7 hours of incubation with X-gal. 2A is a candidate hit. All samples that were re-tested are in black boxes. **(C)** TF samples from **(B)** were re-mated to *Pglr-1* (2.4 kb) bait and tested in quintuplet in the X-gal assay.

Sample 2A is the gene *elt-2* (erythroid-like transcription factor family), homologous to vertebrate GATA transcription factors required for cardiac and endoderm development. ELT-2 has known roles in differentiation of the intestine and in the intestinal innate immune response. Future studies will determine if this hit is biologically relevant by obtaining available mutants for this gene and testing these mutants in the *glr1* transcriptional reporter. Screening of the remainder of the TF library is ongoing and additional hits will be assessed in a similar manner.

Chapter 5

Discussion

Regulation of AMPARs underlies the homeostatic responses to chronic changes in neuronal activity during synaptic scaling. While many mechanisms have been proposed to explain how changes in activity regulate AMPARs, the precise details of this process remain unknown. Synaptic scaling is dependent on transcription and mediated by calcium signaling through CaMKs, specifically CaMKIV. In this thesis, I investigate a novel feedback mechanism, which responds to chronic, bidirectional changes in the levels and activity of the *C. elegans* AMPAR, GLR-1, by regulating *glr-1* transcription. I also show that a CMK-1/CaMK signaling pathway basally regulates *glr-1* transcription and present evidence that this same pathway mediates the feedback mechanism. Specifically, the feedback mechanism triggers CMK-1/CaMK translocation between the cytoplasm and nucleus, altering CMK-1's ability to regulate transcription. Together, these results highlight, for the first time, a direct connection between CMK-I/CaMK signaling, *glr-1* transcription, and chronic changes in activity.

Chronic changes in either GLR-1 levels or GLR-1 activity regulate *glr-1* transcription

GluR transcription

In Chapter 2, I present evidence that changes in levels or activity of GLR-1 regulate *glr-1* transcription. Little is known about regulation of GluR transcription and even less about transcriptional regulation in response to chronic or acute changes in activity. Previous work has focused on regulatory elements in GluR promoters that control cell-specific expression of these receptors. For example, an RE1/neuron restrictive-silencing element (NRSE)-like sequence is present in the promoter of GluA2. In non-neuronal cells, when this NRSE is bound by the transcriptional repressor RE1-silencing transcription factor

(REST), co-repressors and histone deacetylases are recruited to the GluA2 promoter to repress transcription (Myers et al. 1998, Huang et al. 1999). REST and the NRSE sequence also play a role in transcriptional responses to extracellular events, as the NRSE has also been implicated in BDNF-mediated induction of GluA2 promoter activity. Additionally, several studies have examined alterations in GluA2 expression in response to acute insults to the brain. Under these circumstances, epigenetic mechanisms and transcription factors regulate GluA2 transcription. For example, in status epilepticus GluA2 mRNA is downregulated by reduced H4 acetylation of GluA2 and in ischemia induction of REST gene expression downregulates GluA2 (Huang et al. 2002, Calderone et al. 2003). A functional ortholog of REST exists in *C. elegans*, spr-4 (suppressor of presenilin defect) (Lakowski et al. 2003) — future studies are warranted to examine whether this gene regulates *C. elegans* GluRs.

Several studies have examined GluA2 transcriptional regulation in response to activity changes in cultured visual cortical neurons. Acute block of activity by TTX in cultured neurons leads to decreased GluA2 mRNA expression, while acute depolarization leads to increased GluA2 mRNA expression. These bidirectional changes are mediated by the transcription factor NRF-1 (Wong-Riley and Jacobs 2002, Dhar et al. 2009). Although it is possible that neurons employ different mechanisms in response to acute versus chronic changes in activity, it would be interesting to test whether NRF-1 is also implicated in responses to chronic activity.

Regulation of AMPAR transcription in response to chronic changes in activity remains largely unexplored. There is, however, evidence that GluA1 and GluA3 synthesis and transcription are increased during late-phase LTP and this increase is dependent on PKA signaling (Mahanty and Sah 1998). Furthermore, several lines of evidence suggest that AMPAR transcription is regulated by synaptic scaling. However, direct investigation of AMPAR transcriptional responses to synaptic scaling has not been shown. AMPAR protein and mRNA levels are altered during scaling up and scaling down (Ju et al. 2004, Aoto et al. 2008, Qiu et al. 2012) and synaptic scaling depends on transcription (Seeburg et al. 2008, Gainey et al. 2009, Han and Stevens 2009, Goold and Nicoll 2010). Despite the evidence that AMPAR expression is regulated in scaling and that scaling is dependent on transcription, direct regulation of AMPAR transcription by chronic activity changes has not been shown. Chapter 2 shows, for the first time, direct transcriptional regulation of an AMPAR in response to chronic changes in activity.

DNA methylation has recently been proposed to regulate AMPAR expression in synaptic scaling (Meadows et al. 2015, Yu et al. 2015). These studies suggest that in scaling up, there is a decrease in DNA methylation, whereas in scaling down there is an increase. As methylation is typically associated with gene repression, this would correspond to increased gene expression in scaling up and decreased gene expression in scaling down. Though originally believed to be non-existent, there is now evidence of DNA methylation in *C. elegans* (Greer et al. 2015). Future studies could explore whether DNA methylation plays a role in the feedback mechanism regulating *glr-1* transcription by testing whether DNA methylation mutants suppress or enhance the feedback mechanism.

The role of the glr-1 3'UTR

Though data presented in Chapters 2 and 3 provides the first evidence of a direct mechanistic link between synaptic scaling and AMPAR transcription, the GluA1 3'UTR has previously been implicated in scaling up. The GluA1 3'UTR is necessary for upregulation of surface GluA1 receptors upon treatment of neurons in culture with TTX and APV, and this upregulation is mediated by regulation of miRNAs (Letellier et al. 2014). In Chapter 2 of this study, however, I find that the 3'UTR is not sufficient for increased reporter expression in the setting of decreased synaptic GLR-1 (Fig. 2-2). This lack of 3'UTR-dependent regulation could be due to differences in miRNA regulation of AMPARs in *C. elegans* and mammals. miRNA regulation of the GluA1 3'UTR in response to chronic changes in activity may not be conserved in *C. elegans,* as the *glr-1* 3'UTR lacks any conserved miRNA binding sites (based on both TargetScan and PicTar miRNA prediction software). However, although I showed that the *glr-1* 3'UTR alone is insufficient to increase reporter fluorescence in the feedback mechanism, a reporter containing both the *glr-1* 3'UTR and *Pglr-1* did result in an increased response in *glr-1*, *klp-4*, *eat-4*, and *ckk-1* mutants compared to the *glr*-1 transcriptional reporter. This suggests that there may be a synergistic effect of the promoter and 3'UTR. 3'UTRs contain many regulatory elements that may act in tandem with other regions of the gene, including introns and 5'UTRs (Szostak and Gebauer 2013). For example polyA binding protein brings the 3' end of mRNAs in contact with the 5' end, allowing for regulatory elements that bind the 3'UTR to alter translation (Szostak 2012). This is just one way in which reporters containing the *glr-1* 3'UTR may allow different regulatory proteins to interact, altering levels of the GFP reporter. If a set of more complex GFP reporters were

tested containing various sequences of regulatory regions (including the promoter, 5'UTR, introns, and 3'UTR), these might help to discern whether or not regions in the *glr-1* 3'UTR contribute to increased expression of the GFP reporter.

Addressing the small magnitude change of the transcriptional reporter

The fold change effect of the *glr-1* transcriptional reporter was smaller than that observed with RT-qPCR (e.g. approximately 2-fold change in *glr-1* RT-qPCR vs. approximately 1.15-fold change for the *glr-1* transcriptional reporter in *klp-4* mutants), and addition of the *glr-1* 3'UTR, while increasing the effect (approximately 1.4-fold in *klp-4* mutants), still did not match the RT-qPCR result. I considered two testable hypotheses for this discrepancy. First, the GFP reporter— in which multiple copies of exogenous *Pglr-1* are expressed in addition to endogenous *Pglr-1*— could be diluting the transcriptional machinery and attenuating effects on *glr-1* transcription. Second, there could be a ceiling effect of the GFP reporter that occludes large fold changes. For example, if the cell can only maintain a set amount of GFP protein in the nucleus, then it would be impossible to measure increases of GFP fluorescence larger than this set amount.

To address the first hypothesis, I injected the *glr*-1 transcriptional reporter construct into animals at a 50-fold lower concentration than was injected to create the transcriptional reporter used above. I measured GFP fluorescence in *cdk-5* mutants and found that the low-expressing transcriptional reporter had the same fold increase as the 50-fold higher expressing reporter (1.13 fold). Although this increase did not reach statistical significance, this data suggests that dilution of the transcriptional machinery cannot

explain the difference between transcriptional reporter and RT-qPCR fold changes. To address the second hypothesis, I performed RT-qPCR on the GFP reporter itself. If the small fold changes in GFP fluorescence are due to a ceiling effect of the protein itself, then this ceiling effect should not apply to the transcript and there should be a larger increase measured by RT-qPCR (assuming there is not a similar ceiling effect for the transcript). RT-qPCR measurements of GFP from the *glr-1* transcriptional reporter in *klp-4* mutants showed a similar fold change increase compared to wild type as the GFP fluorescence fold change (*gfp* RT-qPCR: 1.23, GFP fluorescence: 1.15). Although the RT-qPCR result did not reach statistical significance, this result suggests that the small effect size is not due to a ceiling effect of the protein. It is possible that another factor, such as the lack of critical regulatory elements (e.g. introns or enhancers) in the *glr-1* transcriptional reporter, is responsible for the disparity between the RT-qPCR result and the GFP reporter results.

Another way to test whether inherent properties of the GFP protein limit the fold change in fluorescence would be to express the transcriptional reporter with a destabilized GFP. Addition of PEST sequences to GFP have been shown to cause faster protein degradation (Li et al. 1998, Corish and Tyler-Smith 1999), and so GFP-PEST could be used in future studies to test whether buildup of GFP protein limits the observable fold change increase. Lastly, it is possible that the small effect size of the transcriptional reporter compared to the RT-qPCR is a true biological difference—that is, there may be larger increases in endogenous *glr-1* mRNA transcript than there are in *Pglr-1* activity in response to the feedback mechanism, even with the addition of the *glr-1* 3'UTR. This makes sense if the

feedback mechanism employs multiple strategies or regulatory elements to increase *glr-1* mRNA that are not represented in the fluorescent reporter transgenes. Such a *Pglr*-1 and *glr-1* 3'UTR independent mechanism could be a distal enhancer element or intronic regulatory sequence.

Changes in glutamatergic activity regulate glr-1 transcription

In Chapter 2, I utilized two complementary approaches to investigate whether altered glutamatergic transmission is sufficient to trigger changes in *glr-1* transcription based on the *glr-1* transcriptional reporter: synaptic transmission mutants and suppression of activity via ectopic expression of a histamine-gated chloride channel (HisCl). First I used synaptic transmission mutants; either with general defects in synaptic transmission (*unc-2*/VGCC and *unc-13*/MUNC13) or with specific defects in glutamatergic transmission (*eat-4*/VGLUT). *unc-2* and *unc-13* mutants exhibit decreased release of neurotransmitter (Richmond et al. 2001), and had a corresponding increase in fluorescence of the *glr-1* transcriptional reporter, suggesting that decreased release of neurotransmitter leads to increased *glr-1* transcription (Fig. 2-8). While consistent with the hypothesis that defects in synaptic activity trigger the feedback mechanism, I wanted to more specifically test glutamatergic deficits. *eat-4* mutants exhibit specific decreases in glutamate-gated currents (Grunwald et al. 2004), accompanied by an increase in synaptic GLR-1::GFP in the VNC. Here, I show that there is also an increase in *glr-1* mRNA and transcription in *eat-4* mutants (Fig. 2-7).

The increase in GLR-1 in response to decreased glutamatergic transmission has been likened to a homeostatic feedback mechanism (Grunwald et al. 2004). Similar to synaptic scaling in mammals, synaptic GLR-1 in *C. elegans* is upregulated in response to blockade of glutamatergic transmission and this upregulation is multiplicative across synapses (Grunwald et al. 2004). One key difference between synaptic scaling in mammals and the homeostatic response in *eat-4* mutants is the calcium-permeability of the regulated receptors. Neither GLR-1 nor GLR-2 subunits undergo the editing seen in mammalian glutamate receptors which confers calcium impermeability. Thus, synaptic scaling in mammals can take advantage of CP-AMPARs to regulate calcium influx at the postsynaptic membrane whereas *C. elegans* does not appear to have this degree of control. For example, in mammals, TTX-induced scaling non-selectively upregulates AMPARs, increasing expression of calcium-impermeable receptors, but when APV is added to block NMDARs, GluA1 and CP-AMPARs are specifically upregulated (see above). In *C. elegans*, *eat-4* mutants may be comparable to blocking both action potentials (because *eat-4* mutants have decreased glutamate-dependent behaviors suggesting decreased firing of these neurons) and NMDARs, leading to upregulation of calcium-permeable receptors. Therefore, in *C. elegans,* upregulation of synaptic GLR-1 could be a response to decreased calcium influx through GLR-1.

The homeostatic increase in synaptic GLR-1 in *eat-4* mutants has been proposed to be dependent on endocytosis and recycling of GLR-1. This is demonstrated by the finding that *unc-11; eat-4* double mutants had similar, non-additive increases in GLR-1 compared to *unc-11* single mutants (Grunwald et al. 2004). This result suggests that *eat-4*

loss-of-function increases synaptic GLR-1 by the same mechanism as *unc-11* loss-of-function—that is, by decreased endocytosis. Endocytosis has also been implicated in mammalian synaptic scaling. For example, chronic TTX treatment leads to decreased Arc/Arg3.1 which causes decreased AMPAR endocytosis. This results in an increase in synaptic AMPAR insertion and facilitates synaptic scaling (Shepherd et al. 2006). There are other possible explanations for the *eat-4; unc-11* non-additive phenotype. For example, there may be a ceiling effect in either *unc-11* or *eat-4* mutants that prevents a further increase in VNC GLR-1. Another relevant explanation is that decreased transcription of *glr-1* in *unc-11* mutants masks an additive increase in synaptic GLR-1 in *eat-4; unc-11* mutants.

Interestingly, this same study (Grunwald et al. 2004) investigated whether *eat-4* mutants have increased expression of *glr-1* by testing a transcriptional reporter and performing western blots. Contrary to my findings, no changes in *glr-1* gene expression were observed in *eat-4* mutants. This data was based on a less sensitive transcriptional reporter (*Pglr-1::GFP)* that relied on measurements of soluble, diffuse GFP in an arbitrary region of the VNC. Localization of GFP to the nucleus in the *glr-1* transcriptional reporter was important in the current study for increasing the accuracy and sensitivity of the fluorescence measurements. The western blot analysis suggested no changes in total protein of GLR-1::GFP. It is possible that the western blot is either not sensitive or cell-type specific enough to detect small fold changes in gene expression. An additional possibility is that even though transcriptional activity of *Pglr-1* and *glr-1* mRNA may have been increased, posttranscriptional or posttranslational mechanisms could have

limited the increase in protein. Further studies will be needed to clarify whether double mutants between *eat-4* and genes in the feedback pathway interact to regulate levels of GLR-1 in the VNC. For example, experiments showing that *cmk-1 gf* mutants suppress the increase in GLR-1 in *eat-4* would suggest that the transcriptional feedback pathway does regulate GLR-1 in the VNC, although other downstream targets of CMK-1/CaMK could also be responsible.

If decreased glutamate release in *eat-4* mutants ultimately leads to increased *glr-1* transcription by reducing calcium influx through GLR-1, then other mutants that decrease calcium influx through GLR-1 should also trigger increased fluorescence of the *glr-1* transcriptional reporter. SOL-1 is an auxiliary protein that is necessary for normal glutamate-gated currents through GLR-1, but, importantly, is not necessary for normal expression or localization of GLR-1 (Zheng et al. 2004, Walker et al. 2006, Zheng et al. 2006). Thus, if GLR-1 activity is sufficient to regulate transcription, *sol-1* mutants should show increased expression of the *glr-1* transcriptional reporter. Contrary to my hypothesis, *sol-1* mutation had no effect on the *glr-1* transcriptional reporter (Fig. 2-9). To investigate whether the absence of a phenotype for *sol-1* mutants was due to calcium influx through or activity of other glutamate receptors, I tested the transcriptional reporter in *sol-1*; *nmr-1* double mutants. *nmr-1* mutants completely abolish the slower component of the glutamate-gated current in the AVA interneuron. In the absence of GLR-1, most of the residual glutamate-gated current is dependent on NMR-1 (Mellem et al. 2002). Thus I hypothesized that a *sol-1*; *nmr-1* double mutant should have decreased calcium influx

through GLR-1 and NMR-1 receptors. However, *sol-1; nmr-1* double mutants also had no effect on the *glr-1* transcriptional reporter (Fig. 2-9).

There are several possible explanations for these findings. The first is that previous studies of SOL-1 and NMR-1 function were performed in the AVA interneuron. While there is evidence that SOL-1 is expressed in PVC (Wang et al. 2012), there is no direct evidence that the same electrophysiological properties exist in PVC. To be more in line with SOL-1's known function in AVA, future studies could measure the transcriptional reporter in AVA in *sol-1* mutants. Additionally, the expression of alternative glutamate receptors in PVC that are not regulated by *sol-1* could allow for postsynaptic glutamatergic activity in the absence of *sol-1*. *C. elegans* also expresses several mGluRs, and glutamate activation of these receptors could also activate the feedback mechanism or could have compensatory roles in *sol-1* mutants. Finally, it is possible that decreased influx of calcium and positive ions through GluRs is insufficient to trigger the feedback mechanism.

An additional approach to investigating whether decreased glutamatergic signaling triggers the *glr-1* transcriptional feedback mechanism was to specifically suppress activity in GLR-1 expressing neurons. I took advantage of a recent genetic tool that allows exogenous suppression of activity by ectopic expression of a histamine-gated chloride channel (HisCl). HisCl activation induced a more pronounced reduction in spontaneous reversals (Fig. 2-10A) than has been reported for any of the GLR-1 trafficking mutants (Burbea et al. 2002, Kowalski et al. 2011, Monteiro et al. 2012),

suggesting robust suppression of GLR-1 neuronal activity. Interestingly, this robust suppression of activity led to an increase in *glr-1* transcription that was similar to the increase observed in GLR-1 trafficking mutants (Fig. 2-10B). A possible explanation for the smaller-than-expected increase in *glr-1* transcription is that extended exposure to histamine may activate compensatory mechanisms affecting either *glr-1* transcription or GFP expression. Along these lines, wild type animals exposed to histamine displayed a surprising reduction in the *glr-1* transcriptional reporter after four hours. This suggests that the increase in fluorescence in HisCl-expressing animals is somewhat attenuated by exposure to histamine. In the future, it would be interesting to measure *glr-1* mRNA levels to see if there is also a weaker effect on the *glr-1* transcript in response to strong activity suppression.

CMK-1/CaMK mediates the GLR-1 feedback mechanism

In Chapter 3, I present evidence that a CaMK signaling pathway regulates *glr-1* transcription and mediates the feedback mechanism. Several studies have reported a role for CaMK signaling and transcription in regulating GluRs in response to synaptic scaling (Ibata et al. 2008, Goold and Nicoll 2010). Interestingly, while CaMKIV is a known regulator of transcription, it is not clear if CaMKIV specifically regulates gene transcription in the setting of synaptic scaling. Nor is it clear which genes may be regulated by CaMKIV in response to chronic changes in activity. We show that the CaMKIV homolog in *C. elegans*, CMK-1, represses GLR-1 transcription. This is consistent with previous reports describing decreased activated nuclear CaMKIV in the

setting of synaptic scaling up (Ibata et al. 2008), and suggests that nuclear CMK-1/CaMK directly or indirectly regulates *glr-1* transcription.

CMK-1/CaMK translocates between the cytoplasm and the nucleus to regulate glr-1 transcription

CMK-1/CaMK translocates between the cytoplasm and the nucleus in several different models of experience-dependent plasticity. In one model, CMK-1/CaMK is necessary for thermotaxis towards cultivation temperature. Here, after prolonged exposure to high temperatures, CMK-1/CaMK acts in the AFD sensory neuron to regulate gene expression and increase intracellular cGMP levels. Accordingly, exposure to high temperatures causes CMK-1/CaMK to shift to the nucleus (Yu et al. 2014). Another study implicates CMK-1/CaMK in reduced thermal avoidance typically observed in animals grown at higher cultivation temperatures (Schild et al. 2014). As with thermotaxis towards the cultivation temperature, thermal avoidance depends on CMK-1/CaMK shifting between the cytoplasm and the nucleus. A truncated allele of CMK-1/CaMK that is localized to the nucleus (because it lacks a nuclear export signal) phenocopies the thermal avoidance seen in animals grown at higher cultivation temperatures. Similarly, attaching an NLS to wild type CMK-1/CaMK phenocopies the truncated allele. Interestingly, the fact that expressing wild type CMK-1/CaMK rescues the truncated CMK-1/CaMK allele suggests a cytoplasmic function of CMK-1/CaMK in addition to its known nuclear role of regulating transcription. These two studies highlight two features of *C. elegans* CMK-1/CaMK signaling. First, CMK-1/CaMK translocation between the cytoplasm and nucleus is critical for regulation of experience-dependent thermosensory behaviors.

Second, several functions of CMK-1/CaMK are dependent on phosphorylation by the upstream kinase CKK-1. Interestingly, CMK-1/CaMK may also have phosphorylation independent functions, as a kinase-dead form of CMK-1/CaMK can rescue CMK-1/CaMK regulation of a downstream transcriptional target GCY-8 in AFD (Satterlee et al. 2004). The data I present in Chapter 3 provide further evidence for the importance of CMK-1/CaMK phosphorylation and subcellular localization in regulating gene expression.

While CMK-1/CaMK functions as the translocating agent that triggers nuclear signaling in the CaMK signaling pathway in *C. elegans*, a recent study in mammalian cultured neurons suggests that this function may not be conserved between species (Ma et al. 2014, Cohen et al. 2015). In response to acute depolarization with KCl, CaM is bound to γCaMKII. γCaMKII dephosphorylation by calcineurin reveals an NLS site, which allows translocation of the CaM/ γCaMKII to the nucleus. In the nucleus, CaM can activate the CaMK cascade to drive CREB-mediated gene transcription via CaMKIV phosphorylation. Thus, in models of acute depolarization, CaM/ γCaMKII is the translocating agent in the CaMKIV signaling pathway, not CaMKIV (Ma et al. 2014). It remains to be determined if this is also true of CaMKIV signaling in response to the chronic changes activity that occur during synaptic scaling. There is ample evidence in *C. elegans* that CMK-1 translocates between the cytoplasm and the nucleus (Yu et al. 2014, Schild et al. 2014), so it is unlikely that a homologous mechanism involving a γCaMKII chaperone functions in *C. elegans.*

Bidirectional regulation of glr-1 transcription by the CMK-1/CaMK pathway

In Chapter 2, I present evidence that increases or decreases in GLR-1 levels or activity have reciprocal effects on *glr-1* transcription. In Chapter 3, I present evidence that the CMK-1/CaMK signaling pathway mediates increased *glr-1* transcription (Fig. 3-4). However, it is less clear if the CMK-1/CaMK signaling pathway also mediates decreased *glr-1* transcription. Basally, *cbp-1 (gf)* mutants, but not *cmk-1 (gf)* mutants, have decreased fluorescence of the *glr-1* transcriptional reporter (Figs. 3-3B and 3-5A), suggesting that upstream kinases in addition to CMK-1/CaMK may regulate CBP-1 in mediating its effects on *glr-1* transcription. Furthermore, *unc-11; ckk-1* double loss-of-function mutations had a phenotype intermediate between the single mutants (Fig. 3-6). This result can be interpreted several ways. First, *unc-11* and *ckk-1* may function in separate pathways to regulate *glr-1* transcription. Second, in the presence of *unc-11* loss-of-function, *ckk-1* loss-of-function may be insufficient to fully activate the downstream CMK-1/CaMK signaling pathway. Third, if *unc-11* triggers additional pathways that regulate *glr-1* transcription besides the CMK-1/CaMK pathway, *ckk-1* may only be able to partially rescue the *unc-11* phenotype. In support of the latter hypothesis, CMK-1::GFP was increased in the nucleus of *unc-11* mutants (Fig. 3-8A), suggesting that *unc-11* does partially go through the CMK-1/CaMK pathway to regulate *glr-1* transcription. As *unc-11* is involved in clathrin-mediated endocytosis of several membrane proteins it is likely that multiple downstream pathways are affected when its function is disrupted. Future studies investigating double mutants between *unc-11* and more downstream elements of the CMK-1/CaMK pathway (*e.g., cmk-1* or *crh-1*/CREB) will aid in

clarifying this interaction. Additionally, GLR-1(A/T) double mutants with the CMK-1/CaMK pathway could be tested to investigate whether increased GLR-1 activity is mediated by CMK-1/CaMK signaling.

Does CMK-1/CaMK itself signal from the synapse to the nucleus?

In Chapter 3, I present data that levels of CMK-1::GFP are increased in the VNC of *ckk-1* and *glr-1* mutants, and decreased in the VNC of *unc-11* mutants (Fig. 3-7). This suggests that CMK-1/CaMK itself may sense chronic changes in levels or activity of GLR-1 at the synapse and translocate to the nucleus in response to chronic changes in levels or activity of GLR-1. Future studies will investigate this question by using a photoconvertible Dendra-tagged version of CMK-1. Photoconversion of CMK-1/CaMK at synapses allows for measurement of the amount of CMK-1/CaMK translocating between the synapse and the nucleus in feedback pathway mutants. This can be tested, for example, in *unc-11* or GLR-1(A/T) mutants to investigate whether chronic increases in levels or activity of synaptic GLR-1 lead to increased translocation of CMK-1/CaMK from synapses to the nucleus.

CMK-1/CaMK targets CRH-1/CREB and CBP-1 to regulate glr-1 transcription

While CaMKIV has been implicated in synaptic scaling in mammals, it is not known which targets of CaMKIV are necessary to regulate GluRs. CaMKIV has several known targets in mammals including CREB, CBP, HDAC4, and HSP25 (Chow et al. 2005). One study has implicated CREB directly in synaptic scaling, showing that CREB activity is decreased after six hours of TTX treatment but increased after 48 hours (Kim and Ziff

2014). This suggests that, initially, long-term activity blockade reduces CREB activity. Since synaptic scaling up has been shown to occur within four hours (Ibata et al. 2008), decreased activated CREB may be correlated with decreased activated CaMKIV and increased AMPARs. This agrees with the finding in Chapter 3 that loss of CRH-1/CREB or CMK-1/CaMK triggers increased *glr-1* transcription (Figs. 3-2 and 3-3). Correspondingly, CRH-1/CREB mutants had increased synaptic GLR-1 protein (Fig. 3-7). While this data suggests CREB-mediated regulation of *glr-1* transcription, this regulation is more likely to be an indirect rather than a direct interaction of CRH-1/CBP-1 because the *glr-1* promoter does not contain canonical CREB binding sites. Furthermore, a recent study in *C. elegans* using gene expression microarrays in *crh-1* mutants did not identify *glr-1* as a target. Interestingly, only 37 of 722 differentially regulated genes have CRE sites, suggesting that CREB indirectly regulates more genes than it directly regulates (Lakhina et al. 2015). It is possible that the *glr-1* transcriptional reporter is more sensitive to changes in *glr-1* transcription than the microarray detection method. Thus the transcriptional reporter could detect a more subtle effect of *crh-1* mutation on *glr-1* transcription. Another explanation is that the microarray studies used mRNA from the whole animal, which could mask an effect specific to a subset of cells (such as the *glr-1* expressing interneurons), since CREB is expressed ubiquitously.

Similarly, there is strong evidence that mammalian AMPARs are not regulated by CREB. Specifically, functional assays suggest that CREB does not bind to potential CREB binding sites in AMPAR genes (Borges and Dingledine 2001). However, a CREB chromatin immunoprecipitation sequencing dataset does show weak binding of CREB at

the GluA1 promoter and weak expression upon forskolin activation, though this finding has not been validated (Zhang et al. 2005).

Calcineurin is necessary for the feedback mechanism

In addition to the CMK-1/CaMK signaling pathway, I also investigated whether calcineurin regulates *glr-1* transcription. Calcineurin, the only Ca^{2+}/calmodulin-activated phosphatase in the brain, canonically acts in opposition to the CaMK cascades, functioning to dephosphorylate downstream targets. Calcineurin also has a known role in transcription by regulating the transcription factor NFAT (Hogan et al. 2003, MacDonnell et al. 2009, Kim and Ziff 2014). In *C. elegans*, calcineurin is encoded by two genes, *cna-1* for the functional subunit, and *cnb-1* for the regulatory subunit. In agreement with a complementary role to CaMK signaling, I found that calcineurin mutants suppressed the increase in *glr-1* transcription in *glr-1* mutants (Fig. 3-11). Interestingly, while both *cna-1* and *cnb-1* appear to be necessary for increased *glr-1* transcription in the feedback mechanism, *cnb-1* mutants had decreased *glr-1* transcription basally, while *cna-1* mutants had no effect basally on transcription. This finding suggests that the regulatory subunit has a strong influence on maintaining basal *glr-1* transcription. It is also possible that in absence of the regulatory subunit in *cnb-1* mutants, the role of the functional subunit (*cna-1*) is altered, leading to repression of *glr-1* transcription. Regardless, these findings provide the basis for future experiments to determine the interaction of calcineurin with CaMK signaling in regulating *glr-1* transcription. Future studies include assessing double mutants of calcineurin and CaMK genes to determine if they function in the same pathway to regulate *glr-1* transcription.

There is well-studied functional overlap between CaMK and other kinase signaling pathways, such as the MAPK/RAS pathway (Wayman et al. 2008). In future studies it will be worthwhile to investigate the role of these pathways in *C. elegans* synaptic scaling and *glr-1* transcriptional regulation. This is especially interesting considering that, in mammals, members of the MAPK signaling pathway such as ERK have been implicated in activity-induced transcriptional regulation (Zhai et al. 2013). Importantly, many of these signaling pathways are conserved in *C. elegans*.

A Y1H screen to identify transcription factors regulating *glr-1*

In Chapter 4, I present the groundwork for a Y1H screen of the *glr-1* promoter and identify several potential positive hits from this screen. This screen has the potential for the discovery of novel transcription factors and elements that regulate *glr-1* under basal and activity-dependent conditions. Given the many conserved mechanisms for regulating GluRs between *C. elegans* and mammals ((Burbea et al. 2002, Stricker and Huganir 2003, Juo and Kaplan 2004, Zheng et al. 2004, Ng et al. 2009, Zhang et al. 2009, Schwarz et al. 2010, Wang et al. 2010, Kowalski et al. 2011, Lin et al. 2011, Lussier et al. 2011, Scudder et al. 2014, Huo et al. 2015), it is likely that transcriptional regulation also shares conserved mechanisms. After determining positive hits from the screen, the next step will be to acquire mutants for the given TF candidates. TF mutants can be assayed with the *glr-1* transcriptional reporter and then crossed into feedback mechanism mutants (e.g., *glr-1*, *eat-4*, *cmk-1, unc-11*, etc. . .). TFs necessary for the feedback response to decreased GLR-1 should block the increase in fluorescence of the *glr-1* transcriptional

reporter, while TFs necessary for the feedback response to increased GLR-1 should block the decrease in fluorescence.

Because both the *Pglr-1* (2.4 kb) and (0.7 kb) baits have relatively high levels of auto-activation, the Y1H screen may be subject to a high false negative rate. A complementary approach could be to use a TF RNAi screen. As an RNAi library of all the protein coding sequences in *C. elegans* has already been established, we could generate a mini-RNAi library of TFs and screen for changes in the *glr-1* transcriptional reporter *in vivo* after RNAi-knockdown of each TF. This approach could be used to validate hits from the Y1H (and vice versa) and also to identify *glr-1* TFs that do not interact strongly enough with *Pglr-1* to be detected in the Y1H.

Concluding remarks

This thesis establishes a novel connection between chronic activity, CMK-1/CaMK signaling, and AMPAR receptor transcription. In addition it establishes *C. elegans* as a model in which to study how chronic changes in activity regulate AMPAR transcription. While chronic changes in activity are known to be dependent on transcription and on CaMKIV, there has been no direct mechanistic link between activity, CaMKIV, and transcription of AMPARs. Here, I show that in response to changes in GLR-1 levels or GLR-1 activity, CMK-1/CaMK translocates between the nucleus and cytoplasm to regulate the *glr-1* promoter. Future studies, including the YIH currently underway, will be required to examine the regulation of *glr-1* transcription by factors within the nucleus. Already in mammals DNA methylation has been implicated in synaptic scaling,

providing one possible mechanism for AMPAR transcriptional regulation. It is unknown, however, if CaMKIV regulates this methylation response, or if these represent two separate pathways. Currently, regulation of GluR transcription in *C. elegans* remains incompletely understood and future studies will be able to use the tools established here, such as the Y1H, to study basal regulation of *glr-1* transcription as well as transcriptional regulation in response to changes in synaptic activity.

References

Abbott, L. F. and S. B. Nelson (2000). "Synaptic plasticity: taming the beast." Nat Neurosci **3 Suppl**: 1178-1183.

Anggono, V., R. L. Clem and R. L. Huganir (2011). "PICK1 loss of function occludes homeostatic synaptic scaling." J Neurosci **31**(6): 2188-2196.

Anggono, V. and R. L. Huganir (2012). "Regulation of AMPA receptor trafficking and synaptic plasticity." Curr Opin Neurobiol **22**(3): 461-469.

Aoto, J., C. I. Nam, M. M. Poon, P. Ting and L. Chen (2008). "Synaptic signaling by all-trans retinoic acid in homeostatic synaptic plasticity." Neuron **60**(2): 308-320.

Bading, H. (2013). "Nuclear calcium signalling in the regulation of brain function." Nat Rev Neurosci **14**(9): 593-608.

Bassani, S., A. Folci, J. Zapata and M. Passafaro (2013). "AMPAR trafficking in synapse maturation and plasticity." Cell Mol Life Sci **70**(23): 4411-4430.

Baumgartel, K. and I. M. Mansuy (2012). "Neural functions of calcineurin in synaptic plasticity and memory." Learn Mem **19**(9): 375-384.

Bear, M. F. (1995). "Mechanism for a sliding synaptic modification threshold." Neuron **15**(1): 1-4.

Bellocchio, E. E., H. Hu, A. Pohorille, J. Chan, V. M. Pickel and R. H. Edwards (1998). "The localization of the brain-specific inorganic phosphate transporter suggests a specific presynaptic role in glutamatergic transmission." J Neurosci **18**(21): 8648-8659.

Berger, A. J., A. C. Hart and J. M. Kaplan (1998). "G alphas-induced neurodegeneration in Caenorhabditis elegans." J Neurosci **18**(8): 2871-2880.

Bito, H., K. Deisseroth and R. W. Tsien (1996). "CREB phosphorylation and dephosphorylation: a Ca(2+)- and stimulus duration-dependent switch for hippocampal gene expression." Cell **87**(7): 1203-1214.

Bliss, T. V. and T. Lomo (1973). "Long-lasting potentiation of synaptic transmission in the dentate area of the anaesthetized rabbit following stimulation of the perforant path." J Physiol **232**(2): 331-356.

Borges, K. and R. Dingledine (2001). "Functional organization of the GluR1 glutamate receptor promoter." J Biol Chem **276**(28): 25929-25938.

Bredt, D. S. and R. A. Nicoll (2003). "AMPA receptor trafficking at excitatory synapses." Neuron **40**(2): 361-379.

Brenner, S. (1974). "The genetics of Caenorhabditis elegans." Genetics **77**(1): 71-94.

Brockie, P. J., D. M. Madsen, Y. Zheng, J. Mellem and A. V. Maricq (2001).

"Differential expression of glutamate receptor subunits in the nervous system of Caenorhabditis elegans and their regulation by the homeodomain protein UNC-42." J Neurosci **21**(5): 1510-1522.

Brockie, P. J. and A. V. Maricq (2006). "Ionotropic glutamate receptors: genetics, behavior and electrophysiology." WormBook: 1-16.

Brockie, P. J., J. E. Mellem, T. Hills, D. M. Madsen and A. V. Maricq (2001). "The C. elegans glutamate receptor subunit NMR-1 is required for slow NMDA-activated currents that regulate reversal frequency during locomotion." Neuron **31**(4): 617-630.

Burbea, M., L. Dreier, J. S. Dittman, M. E. Grunwald and J. M. Kaplan (2002). "Ubiquitin and AP180 regulate the abundance of GLR-1 glutamate receptors at postsynaptic elements in C. elegans." Neuron **35**(1): 107-120.

Burrone, J., M. O'Byrne and V. N. Murthy (2002). "Multiple forms of synaptic plasticity triggered by selective suppression of activity in individual neurons." Nature **420**(6914): 414-418.

Caldeira, M. V., C. V. Melo, D. B. Pereira, R. F. Carvalho, A. L. Carvalho and C. B. Duarte (2007). "BDNF regulates the expression and traffic of NMDA receptors in cultured hippocampal neurons." Mol Cell Neurosci **35**(2): 208-219.

Calderone, A., T. Jover, K. M. Noh, H. Tanaka, H. Yokota, Y. Lin, S. Y. Grooms, R. Regis, M. V. Bennett and R. S. Zukin (2003). "Ischemic insults derepress the gene silencer REST in neurons destined to die." J Neurosci **23**(6): 2112-2121.

Chang, H. C. and C. Rongo (2005). "Cytosolic tail sequences and subunit interactions are critical for synaptic localization of glutamate receptors." J Cell Sci **118**(Pt 9): 1945-1956.

Chow, F. A., K. A. Anderson, P. K. Noeldner and A. R. Means (2005). "The autonomous activity of calcium/calmodulin-dependent protein kinase IV is required for its role in transcription." J Biol Chem **280**(21): 20530-20538.

Cohen, S. M., B. Li, R. W. Tsien and H. Ma (2015). "Evolutionary and functional perspectives on signaling from neuronal surface to nucleus." Biochem Biophys Res Commun **460**(1): 88-99.

Colledge, M., E. M. Snyder, R. A. Crozier, J. A. Soderling, Y. Jin, L. K. Langeberg, H. Lu, M. F. Bear and J. D. Scott (2003). "Ubiquitination regulates PSD-95 degradation and AMPA receptor surface expression." Neuron **40**(3): 595-607.

Corish, P. and C. Tyler-Smith (1999). "Attenuation of green fluorescent protein half-life in mammalian cells." Protein Eng **12**(12): 1035-1040.

Correa, S. A., C. J. Hunter, O. Palygin, S. C. Wauters, K. J. Martin, C. McKenzie, K. McKelvey, R. G. Morris, Y. Pankratov, J. S. Arthur and B. G. Frenguelli (2012). "MSK1 regulates homeostatic and experience-dependent synaptic plasticity." J Neurosci **32**(38): 13039-13051.

Corsi, A. K., B. Wightman and M. Chalfie (2015). "A Transparent Window into Biology: A Primer on Caenorhabditis elegans." Genetics **200**(2): 387-407.

De Cesare, D., G. M. Fimia and P. Sassone-Corsi (1999). "Signaling routes to CREM and CREB: plasticity in transcriptional activation." Trends Biochem Sci **24**(7): 281-285.

Deisseroth, K., P. G. Mermelstein, H. Xia and R. W. Tsien (2003). "Signaling from synapse to nucleus: the logic behind the mechanisms." Curr Opin Neurobiol **13**(3): 354-365.

DePina, A. S., W. B. Iser, S. S. Park, S. Maudsley, M. A. Wilson and C. A. Wolkow (2011). "Regulation of Caenorhabditis elegans vitellogenesis by DAF-2/IIS through separable transcriptional and posttranscriptional mechanisms." BMC Physiol **11**: 11.

Deplancke, B., D. Dupuy, M. Vidal and A. J. Walhout (2004). "A gateway-compatible yeast one-hybrid system." Genome Res **14**(10B): 2093-2101.

Desai, N. S., R. H. Cudmore, S. B. Nelson and G. G. Turrigiano (2002). "Critical periods for experience-dependent synaptic scaling in visual cortex." Nat Neurosci **5**(8): 783-789.

Dhar, S. S., H. L. Liang and M. T. Wong-Riley (2009). "Nuclear respiratory factor 1 co-regulates AMPA glutamate receptor subunit 2 and cytochrome c oxidase: tight coupling of glutamatergic transmission and energy metabolism in neurons." J Neurochem **108**(6): 1595-1606.

Dupuy, D., Q. R. Li, B. Deplancke, M. Boxem, T. Hao, P. Lamesch, R. Sequerra, S. Bosak, L. Doucette-Stamm, I. A. Hope, D. E. Hill, A. J. Walhout and M. Vidal (2004). "A first version of the Caenorhabditis elegans Promoterome." Genome Res **14**(10B): 2169-2175.

Eastburn, D. J. and M. Han (2005). "A gain-of-function allele of cbp-1, the Caenorhabditis elegans ortholog of the mammalian CBP/p300 gene, causes an increase in histone acetyltransferase activity and antagonism of activated Ras." Mol Cell Biol **25**(21): 9427-9434.

Enslen, H., P. Sun, D. Brickey, S. H. Soderling, E. Klamo and T. R. Soderling (1994). "Characterization of Ca2+/calmodulin-dependent protein kinase IV. Role in transcriptional regulation." J Biol Chem **269**(22): 15520-15527.

Eto, K., N. Takahashi, Y. Kimura, Y. Masuho, K. Arai, M. A. Muramatsu and H. Tokumitsu (1999). "Ca(2+)/Calmodulin-dependent protein kinase cascade in Caenorhabditis elegans. Implication in transcriptional activation." J Biol Chem **274**(32): 22556-22562.

Evers, D. M., J. A. Matta, H. S. Hoe, D. Zarkowsky, S. H. Lee, J. T. Isaac and D. T. Pak (2010). "Plk2 attachment to NSF induces homeostatic removal of GluA2 during chronic overexcitation." Nat Neurosci **13**(10): 1199-1207.

Fiore, R., M. Rajman, C. Schwale, S. Bicker, A. Antoniou, C. Bruehl, A. Draguhn and G. Schratt (2014). "MiR-134-dependent regulation of Pumilio-2 is necessary for homeostatic synaptic depression." EMBO J **33**(19): 2231-2246.

Fire, A., S. W. Harrison and D. Dixon (1990). "A modular set of lacZ fusion vectors for studying gene expression in Caenorhabditis elegans." Gene **93**(2): 189-198.

Fu, A. K., K. W. Hung, W. Y. Fu, C. Shen, Y. Chen, J. Xia, K. O. Lai and N. Y. Ip (2011). "APC(Cdh1) mediates EphA4-dependent downregulation of AMPA receptors in homeostatic plasticity." Nat Neurosci **14**(2): 181-189.

Gainey, M. A., J. R. Hurvitz-Wolff, M. E. Lambo and G. G. Turrigiano (2009). "Synaptic scaling requires the GluR2 subunit of the AMPA receptor." J Neurosci **29**(20): 6479-6489.

Gainey, M. A., V. Tatavarty, M. Nahmani, H. Lin and G. G. Turrigiano (2015). "Activity-dependent synaptic GRIP1 accumulation drives synaptic scaling up in response to action potential blockade." Proc Natl Acad Sci U S A **112**(27): E3590-3599.

Glodowski, D. R., C. C. Chen, H. Schaefer, B. D. Grant and C. Rongo (2007). "RAB-10 regulates glutamate receptor recycling in a cholesterol-dependent endocytosis pathway." Mol Biol Cell **18**(11): 4387-4396.

Goel, A., B. Jiang, L. W. Xu, L. Song, A. Kirkwood and H. K. Lee (2006). "Cross-modal regulation of synaptic AMPA receptors in primary sensory cortices by visual experience." Nat Neurosci **9**(8): 1001-1003.

Goold, C. P. and R. A. Nicoll (2010). "Single-cell optogenetic excitation drives homeostatic synaptic depression." Neuron **68**(3): 512-528.

Gray, A. L., T. M. Hyde, A. Deep-Soboslay, J. E. Kleinman and M. S. Sodhi (2015). "Sex differences in glutamate receptor gene expression in major depression and suicide." Mol Psychiatry **20**(9): 1139.

Greer, E. L., M. A. Blanco, L. Gu, E. Sendinc, J. Liu, D. Aristizabal-Corrales, C. H. Hsu, L. Aravind, C. He and Y. Shi (2015). "DNA Methylation on N6-Adenine in C. elegans." Cell **161**(4): 868-878.

Grooms, S. Y., K. M. Noh, R. Regis, G. J. Bassell, M. K. Bryan, R. C. Carroll and R. S. Zukin (2006). "Activity bidirectionally regulates AMPA receptor mRNA abundance in dendrites of hippocampal neurons." J Neurosci **26**(32): 8339-8351.

Groth, R. D., M. Lindskog, T. C. Thiagarajan, L. Li and R. W. Tsien (2011). "Beta Ca2+/CaM-dependent kinase type II triggers upregulation of GluA1 to coordinate adaptation to synaptic inactivity in hippocampal neurons." Proc Natl Acad Sci U S A **108**(2): 828-833.

Grunwald, M. E., J. E. Mellem, N. Strutz, A. V. Maricq and J. M. Kaplan (2004). "Clathrin-mediated endocytosis is required for compensatory regulation of GLR-1 glutamate receptors after activity blockade." Proceedings of the National Academy of Sciences of the United States of America **101**(9): 3190-3195.

Hadziselimovic, N., V. Vukojevic, F. Peter, A. Milnik, M. Fastenrath, B. G. Fenyves, P. Hieber, P. Demougin, C. Vogler, D. J. de Quervain, A. Papassotiropoulos and A. Stetak

(2014). "Forgetting is regulated via Musashi-mediated translational control of the Arp2/3 complex." Cell **156**(6): 1153-1166.

Han, E. B. and C. F. Stevens (2009). "Development regulates a switch between post- and presynaptic strengthening in response to activity deprivation." Proc Natl Acad Sci U S A **106**(26): 10817-10822.

Hardingham, G. E., F. J. Arnold and H. Bading (2001). "Nuclear calcium signaling controls CREB-mediated gene expression triggered by synaptic activity." Nat Neurosci **4**(3): 261-267.

Hart, A. C., S. Sims and J. M. Kaplan (1995). "Synaptic code for sensory modalities revealed by C. elegans GLR-1 glutamate receptor." Nature **378**(6552): 82-85.

Hoerndli, F. J., D. A. Maxfield, P. J. Brockie, J. E. Mellem, E. Jensen, R. Wang, D. M. Madsen and A. V. Maricq (2013). "Kinesin-1 regulates synaptic strength by mediating the delivery, removal, and redistribution of AMPA receptors." Neuron **80**(6): 1421-1437.

Hoerndli, F. J., R. Wang, J. E. Mellem, A. Kallarackal, P. J. Brockie, C. Thacker, D. M. Madsen and A. V. Maricq (2015). "Neuronal Activity and CaMKII Regulate Kinesin-Mediated Transport of Synaptic AMPARs." Neuron **86**(2): 457-474.

Hogan, P. G., L. Chen, J. Nardone and A. Rao (2003). "Transcriptional regulation by calcium, calcineurin, and NFAT." Genes Dev **17**(18): 2205-2232.

Hou, Q., J. Gilbert and H. Y. Man (2011). "Homeostatic regulation of AMPA receptor trafficking and degradation by light-controlled single-synaptic activation." Neuron **72**(5): 806-818.

Hou, Q., D. Zhang, L. Jarzylo, R. L. Huganir and H. Y. Man (2008). "Homeostatic regulation of AMPA receptor expression at single hippocampal synapses." Proc Natl Acad Sci U S A **105**(2): 775-780.

Huang, Y., J. J. Doherty and R. Dingledine (2002). "Altered histone acetylation at glutamate receptor 2 and brain-derived neurotrophic factor genes is an early event triggered by status epilepticus." J Neurosci **22**(19): 8422-8428.

Huang, Y., S. J. Myers and R. Dingledine (1999). "Transcriptional repression by REST: recruitment of Sin3A and histone deacetylase to neuronal genes." Nat Neurosci **2**(10): 867-872.

Huganir, R. L. and R. A. Nicoll (2013). "AMPARs and synaptic plasticity: the last 25 years." Neuron **80**(3): 704-717.

Hunt, D. L. and P. E. Castillo (2012). "Synaptic plasticity of NMDA receptors: mechanisms and functional implications." Curr Opin Neurobiol **22**(3): 496-508.

Huo, Y., N. Khatri, Q. Hou, J. Gilbert, G. Wang and H. Y. Man (2015). "The deubiquitinating enzyme USP46 regulates AMPA receptor ubiquitination and trafficking." J Neurochem.

Ibata, K., Q. Sun and G. G. Turrigiano (2008). "Rapid synaptic scaling induced by changes in postsynaptic firing." Neuron **57**(6): 819-826.

Impey, S., A. L. Fong, Y. Wang, J. R. Cardinaux, D. M. Fass, K. Obrietan, G. A. Wayman, D. R. Storm, T. R. Soderling and R. H. Goodman (2002). "Phosphorylation of CBP mediates transcriptional activation by neural activity and CaM kinase IV." Neuron **34**(2): 235-244.

Ju, W., W. Morishita, J. Tsui, G. Gaietta, T. J. Deerinck, S. R. Adams, C. C. Garner, R. Y. Tsien, M. H. Ellisman and R. C. Malenka (2004). "Activity-dependent regulation of dendritic synthesis and trafficking of AMPA receptors." Nat Neurosci **7**(3): 244-253.

Juo, P., T. Harbaugh, G. Garriga and J. M. Kaplan (2007). "CDK-5 regulates the abundance of GLR-1 glutamate receptors in the ventral cord of Caenorhabditis elegans." Mol Biol Cell **18**(10): 3883-3893.

Juo, P. and J. M. Kaplan (2004). "The anaphase-promoting complex regulates the abundance of GLR-1 glutamate receptors in the ventral nerve cord of C. elegans." Curr Biol **14**(22): 2057-2062.

Kang, H., L. D. Sun, C. M. Atkins, T. R. Soderling, M. A. Wilson and S. Tonegawa (2001). "An important role of neural activity-dependent CaMKIV signaling in the consolidation of long-term memory." Cell **106**(6): 771-783.

Kauer, J. A., R. C. Malenka and R. A. Nicoll (1988). "NMDA application potentiates synaptic transmission in the hippocampus." Nature **334**(6179): 250-252.

Kim, S. and E. B. Ziff (2014). "Calcineurin mediates synaptic scaling via synaptic trafficking of Ca2+-permeable AMPA receptors." PLoS Biol **12**(7): e1001900.

Kimura, H., K. Sasaki, T. Meguro and J. H. Zhang (2002). "Phosphatidylinositol 3-kinase inhibitor failed to reduce cerebral vasospasm in dog model of experimental subarachnoid hemorrhage." Stroke **33**(2): 593-599.

Kowalski, J. R., C. L. Dahlberg and P. Juo (2011). "The deubiquitinating enzyme USP-46 negatively regulates the degradation of glutamate receptors to control their abundance in the ventral nerve cord of Caenorhabditis elegans." J Neurosci **31**(4): 1341-1354.

Lakhina, V., R. N. Arey, R. Kaletsky, A. Kauffman, G. Stein, W. Keyes, D. Xu and C. T. Murphy (2015). "Genome-wide functional analysis of CREB/long-term memory-dependent transcription reveals distinct basal and memory gene expression programs." Neuron **85**(2): 330-345.

Lakowski, B., S. Eimer, C. Gobel, A. Bottcher, B. Wagler and R. Baumeister (2003). "Two suppressors of sel-12 encode C2H2 zinc-finger proteins that regulate presenilin transcription in Caenorhabditis elegans." Development **130**(10): 2117-2128.

Lee, H. K. (2012). "Ca-permeable AMPA receptors in homeostatic synaptic plasticity." Front Mol Neurosci **5**: 17.

Lee, R. Y., E. R. Sawin, M. Chalfie, H. R. Horvitz and L. Avery (1999). "EAT-4, a homolog of a mammalian sodium-dependent inorganic phosphate cotransporter, is necessary for glutamatergic neurotransmission in caenorhabditis elegans." J Neurosci **19**(1): 159-167.

Letellier, M., S. Elramah, M. Mondin, A. Soula, A. Penn, D. Choquet, M. Landry, O. Thoumine and A. Favereaux (2014). "miR-92a regulates expression of synaptic GluA1-containing AMPA receptors during homeostatic scaling." Nat Neurosci **17**(8): 1040-1042.

Li, X., X. Zhao, Y. Fang, X. Jiang, T. Duong, C. Fan, C. C. Huang and S. R. Kain (1998). "Generation of destabilized green fluorescent protein as a transcription reporter." J Biol Chem **273**(52): 34970-34975.

Lin, A., Q. Hou, L. Jarzylo, S. Amato, J. Gilbert, F. Shang and H. Y. Man (2011). "Nedd4-mediated AMPA receptor ubiquitination regulates receptor turnover and trafficking." J Neurochem **119**(1): 27-39.

Lisman, J. E. (2009). "The pre/post LTP debate." Neuron **63**(3): 281-284.

Lissin, D. V., S. N. Gomperts, R. C. Carroll, C. W. Christine, D. Kalman, M. Kitamura, S. Hardy, R. A. Nicoll, R. C. Malenka and M. von Zastrow (1998). "Activity differentially regulates the surface expression of synaptic AMPA and NMDA glutamate receptors." Proc Natl Acad Sci U S A **95**(12): 7097-7102.

Lu, W. and K. W. Roche (2012). "Posttranslational regulation of AMPA receptor trafficking and function." Curr Opin Neurobiol **22**(3): 470-479.

Lussier, M. P., Y. Nasu-Nishimura and K. W. Roche (2011). "Activity-dependent ubiquitination of the AMPA receptor subunit GluA2." J Neurosci **31**(8): 3077-3081.

Ma, H., R. D. Groth, S. M. Cohen, J. F. Emery, B. Li, E. Hoedt, G. Zhang, T. A. Neubert and R. W. Tsien (2014). "gammaCaMKII shuttles Ca(2)(+)/CaM to the nucleus to trigger CREB phosphorylation and gene expression." Cell **159**(2): 281-294.

Mabb, A. M. and M. D. Ehlers (2010). "Ubiquitination in postsynaptic function and plasticity." Annu Rev Cell Dev Biol **26**: 179-210.

MacDonnell, S. M., J. Weisser-Thomas, H. Kubo, M. Hanscome, Q. Liu, N. Jaleel, R. Berretta, X. Chen, J. H. Brown, A. K. Sabri, J. D. Molkentin and S. R. Houser (2009).

"CaMKII negatively regulates calcineurin-NFAT signaling in cardiac myocytes." Circ Res **105**(4): 316-325.

Maghsoodi, B., M. M. Poon, C. I. Nam, J. Aoto, P. Ting and L. Chen (2008). "Retinoic acid regulates RARalpha-mediated control of translation in dendritic RNA granules during homeostatic synaptic plasticity." Proc Natl Acad Sci U S A **105**(41): 16015-16020.

Mahanty, N. K. and P. Sah (1998). "Calcium-permeable AMPA receptors mediate long-term potentiation in interneurons in the amygdala." Nature **394**(6694): 683-687.

Mair, W., I. Morantte, A. P. Rodrigues, G. Manning, M. Montminy, R. J. Shaw and A. Dillin (2011). "Lifespan extension induced by AMPK and calcineurin is mediated by CRTC-1 and CREB." Nature **470**(7334): 404-408.

Malenka, R. C. and M. F. Bear (2004). "LTP and LTD: an embarrassment of riches." Neuron **44**(1): 5-21.

Mangone, M., A. P. Manoharan, D. Thierry-Mieg, J. Thierry-Mieg, T. Han, S. D. Mackowiak, E. Mis, C. Zegar, M. R. Gutwein, V. Khivansara, O. Attie, K. Chen, K. Salehi-Ashtiani, M. Vidal, T. T. Harkins, P. Bouffard, Y. Suzuki, S. Sugano, Y. Kohara, N. Rajewsky, F. Piano, K. C. Gunsalus and J. K. Kim (2010). "The landscape of C. elegans 3'UTRs." Science **329**(5990): 432-435.

Maricq, A. V., E. Peckol, M. Driscoll and C. I. Bargmann (1995). "Mechanosensory signalling in C. elegans mediated by the GLR-1 glutamate receptor."

Matsuzaki, M., N. Honkura, G. C. Ellis-Davies and H. Kasai (2004). "Structural basis of long-term potentiation in single dendritic spines." Nature **429**(6993): 761-766.

Matthews, R. P., C. R. Guthrie, L. M. Wailes, X. Zhao, A. R. Means and G. S. McKnight (1994). "Calcium/calmodulin-dependent protein kinase types II and IV differentially regulate CREB-dependent gene expression." Mol Cell Biol **14**(9): 6107-6116.

Meadows, J. P., M. C. Guzman-Karlsson, S. Phillips, C. Holleman, J. L. Posey, J. J. Day, J. J. Hablitz and J. D. Sweatt (2015). "DNA methylation regulates neuronal glutamatergic synaptic scaling." Sci Signal **8**(382): ra61.

Mellem, J. E., P. J. Brockie, Y. Zheng, D. M. Madsen and A. V. Maricq (2002). "Decoding of polymodal sensory stimuli by postsynaptic glutamate receptors in C. elegans." Neuron **36**(5): 933-944.

Miller, K. D. (1996). "Synaptic economics: competition and cooperation in synaptic plasticity." Neuron **17**(3): 371-374.

Molnar, E. (2011). "Long-term potentiation in cultured hippocampal neurons." Semin Cell Dev Biol **22**(5): 506-513.

Monteiro, M. I., S. Ahlawat, J. R. Kowalski, E. Malkin, S. P. Koushika and P. Juo (2012). "The kinesin-3 family motor KLP-4 regulates anterograde trafficking of GLR-1 glutamate receptors in the ventral nerve cord of Caenorhabditis elegans." Mol Biol Cell **23**(18): 3647-3662.

Muller, D., M. Joly and G. Lynch (1988). "Contributions of quisqualate and NMDA receptors to the induction and expression of LTP." Science **242**(4886): 1694-1697.

Myers, S. J., J. Peters, Y. Huang, M. B. Comer, F. Barthel and R. Dingledine (1998). "Transcriptional regulation of the GluR2 gene: neural-specific expression, multiple promoters, and regulatory elements." J Neurosci **18**(17): 6723-6739.

Ng, D., G. M. Pitcher, R. K. Szilard, A. Sertie, M. Kanisek, S. J. Clapcote, T. Lipina, L. V. Kalia, D. Joo, C. McKerlie, M. Cortez, J. C. Roder, M. W. Salter and R. R. McInnes (2009). "Neto1 is a novel CUB-domain NMDA receptor-interacting protein required for synaptic plasticity and learning." PLoS Biol **7**(2): e41.

Nicoll, R. A. (2003). "Expression mechanisms underlying long-term potentiation: a postsynaptic view." Philos Trans R Soc Lond B Biol Sci **358**(1432): 721-726.

O'Brien, R. J., S. Kamboj, M. D. Ehlers, K. R. Rosen, G. D. Fischbach and R. L. Huganir (1998). "Activity-dependent modulation of synaptic AMPA receptor accumulation." Neuron **21**(5): 1067-1078.

Okuda, T., L. M. Yu, L. A. Cingolani, R. Kemler and Y. Goda (2007). "beta-Catenin regulates excitatory postsynaptic strength at hippocampal synapses." Proc Natl Acad Sci U S A **104**(33): 13479-13484.

Orlandi, C., L. La Via, D. Bonini, C. Mora, I. Russo, A. Barbon and S. Barlati (2011). "AMPA receptor regulation at the mRNA and protein level in rat primary cortical cultures." PLoS One **6**(9): e25350.

Patrick, G. N., B. Bingol, H. A. Weld and E. M. Schuman (2003). "Ubiquitin-mediated proteasome activity is required for agonist-induced endocytosis of GluRs." Curr Biol **13**(23): 2073-2081.

Pfaffl, M. W. (2001). "A new mathematical model for relative quantification in real-time RT-PCR." Nucleic Acids Res **29**(9): e45.

Pokala, N., Q. Liu, A. Gordus and C. I. Bargmann (2014). "Inducible and titratable silencing of Caenorhabditis elegans neurons in vivo with histamine-gated chloride channels." Proc Natl Acad Sci U S A **111**(7): 2770-2775.

Pozo, K. and Y. Goda (2010). "Unraveling mechanisms of homeostatic synaptic plasticity." Neuron **66**(3): 337-351.

Pratt, K. G., E. C. Zimmerman, D. G. Cook and J. M. Sullivan (2011). "Presenilin 1 regulates homeostatic synaptic scaling through Akt signaling." Nat Neurosci **14**(9): 1112-1114.

Qiu, Z., E. L. Sylwestrak, D. N. Lieberman, Y. Zhang, X. Y. Liu and A. Ghosh (2012). "The Rett syndrome protein MeCP2 regulates synaptic scaling." J Neurosci **32**(3): 989-994.

Rebola, N., B. N. Srikumar and C. Mulle (2010). "Activity-dependent synaptic plasticity of NMDA receptors." J Physiol **588**(Pt 1): 93-99.

Reece-Hoyes, J. S., B. Deplancke, M. I. Barrasa, J. Hatzold, R. B. Smit, H. E. Arda, P. A. Pope, J. Gaudet, B. Conradt and A. J. Walhout (2009). "The C. elegans Snail homolog CES-1 can activate gene expression in vivo and share targets with bHLH transcription factors." Nucleic Acids Res **37**(11): 3689-3698.

Reece-Hoyes, J. S. and A. J. Marian Walhout (2012). "Yeast one-hybrid assays: a historical and technical perspective." Methods **57**(4): 441-447.

Reece-Hoyes, J. S. and A. J. Walhout (2012). "Gene-centered yeast one-hybrid assays." Methods Mol Biol **812**: 189-208.

Reimers, J. M., J. A. Loweth and M. E. Wolf (2014). "BDNF contributes to both rapid and homeostatic alterations in AMPA receptor surface expression in nucleus accumbens medium spiny neurons." Eur J Neurosci **39**(7): 1159-1169.

Richmond, J. E., R. M. Weimer and E. M. Jorgensen (2001). "An open form of syntaxin bypasses the requirement for UNC-13 in vesicle priming." Nature **412**(6844): 338-341.

Rongo, C. and J. M. Kaplan (1999). "CaMKII regulates the density of central glutamatergic synapses in vivo." Nature **402**(6758): 195-199.

Rongo, C., C. W. Whitfield, A. Rodal, S. K. Kim and J. M. Kaplan (1998). "LIN-10 is a shared component of the polarized protein localization pathways in neurons and epithelia." Cell **94**(6): 751-759.

Rutherford, L. C., S. B. Nelson and G. G. Turrigiano (1998). "BDNF has opposite effects on the quantal amplitude of pyramidal neuron and interneuron excitatory synapses." Neuron **21**(3): 521-530.

Satterlee, J. S., W. S. Ryu and P. Sengupta (2004). "The CMK-1 CaMKI and the TAX-4 Cyclic nucleotide-gated channel regulate thermosensory neuron gene expression and function in C. elegans." Curr Biol **14**(1): 62-68.

Schild, L. C., L. Zbinden, H. W. Bell, Y. V. Yu, P. Sengupta, M. B. Goodman and D. A. Glauser (2014). "The balance between cytoplasmic and nuclear CaM kinase-1 signaling controls the operating range of noxious heat avoidance." Neuron **84**(5): 983-996.

Schratt, G. M., E. A. Nigh, W. G. Chen, L. Hu and M. E. Greenberg (2004). "BDNF regulates the translation of a select group of mRNAs by a mammalian target of rapamycin-phosphatidylinositol 3-kinase-dependent pathway during neuronal development." J Neurosci **24**(33): 7366-7377.

Schwarz, L. A., B. J. Hall and G. N. Patrick (2010). "Activity-dependent ubiquitination of GluA1 mediates a distinct AMPA receptor endocytosis and sorting pathway." J Neurosci **30**(49): 16718-16729.

Scudder, S. L., M. S. Goo, A. E. Cartier, A. Molteni, L. A. Schwarz, R. Wright and G. N. Patrick (2014). "Synaptic strength is bidirectionally controlled by opposing activity-dependent regulation of Nedd4-1 and USP8." J Neurosci **34**(50): 16637-16649.

Seeburg, D. P., M. Feliu-Mojer, J. Gaiottino, D. T. Pak and M. Sheng (2008). "Critical role of CDK5 and Polo-like kinase 2 in homeostatic synaptic plasticity during elevated activity." Neuron **58**(4): 571-583.

Segal, M. (2005). "Dendritic spines and long-term plasticity." Nat Rev Neurosci **6**(4): 277-284.

Sheng, M., M. A. Thompson and M. E. Greenberg (1991). "CREB: a Ca(2+)-regulated transcription factor phosphorylated by calmodulin-dependent kinases." Science **252**(5011): 1427-1430.

Shepherd, J. D., G. Rumbaugh, J. Wu, S. Chowdhury, N. Plath, D. Kuhl, R. L. Huganir and P. F. Worley (2006). "Arc/Arg3.1 mediates homeostatic synaptic scaling of AMPA receptors." Neuron **52**(3): 475-484.

Soares, C., K. F. Lee, W. Nassrallah and J. C. Beique (2013). "Differential subcellular targeting of glutamate receptor subtypes during homeostatic synaptic plasticity." J Neurosci **33**(33): 13547-13559.

Stellwagen, D. and R. C. Malenka (2006). "Synaptic scaling mediated by glial TNF-alpha." Nature **440**(7087): 1054-1059.

Stetak, A., F. Horndli, A. V. Maricq, S. van den Heuvel and A. Hajnal (2009). "Neuron-specific regulation of associative learning and memory by MAGI-1 in C. elegans." PLoS One **4**(6): e6019.

Stricker, N. L. and R. L. Huganir (2003). "The PDZ domains of mLin-10 regulate its trans-Golgi network targeting and the surface expression of AMPA receptors." Neuropharmacology **45**(6): 837-848.

Strutz-Seebohm, N., M. Werner, D. M. Madsen, G. Seebohm, Y. Zheng, C. S. Walker, A. V. Maricq and M. Hollmann (2003). "Functional analysis of Caenorhabditis elegans glutamate receptor subunits by domain transplantation." J Biol Chem **278**(45): 44691-44701.

Sun, P., H. Enslen, P. S. Myung and R. A. Maurer (1994). "Differential activation of CREB by Ca2+/calmodulin-dependent protein kinases type II and type IV involves phosphorylation of a site that negatively regulates activity." Genes Dev **8**(21): 2527-2539.

Sutton, M. A., N. R. Wall, G. N. Aakalu and E. M. Schuman (2004). "Regulation of dendritic protein synthesis by miniature synaptic events." Science **304**(5679): 1979-1983.

Sutton, Y., K. McBride and S. Pye (2006). "An ultrasound mini-balance for measurement of therapy level ultrasound." Phys Med Biol **51**(14): 3397-3404.

Szostak, E. and F. Gebauer (2013). "Translational control by 3'-UTR-binding proteins." Brief Funct Genomics **12**(1): 58-65.

Thiagarajan, T. C., M. Lindskog and R. W. Tsien (2005). "Adaptation to synaptic inactivity in hippocampal neurons." Neuron **47**(5): 725-737.

Tononi, G. and C. Cirelli (2006). "Sleep function and synaptic homeostasis." Sleep Med Rev **10**(1): 49-62.

Trasande, C. A. and J. M. Ramirez (2007). "Activity deprivation leads to seizures in hippocampal slice cultures: is epilepsy the consequence of homeostatic plasticity?" J Clin Neurophysiol **24**(2): 154-164.

Traynelis, S. F., L. P. Wollmuth, C. J. McBain, F. S. Menniti, K. M. Vance, K. K. Ogden, K. B. Hansen, H. Yuan, S. J. Myers and R. Dingledine (2010). "Glutamate receptor ion channels: structure, regulation, and function." Pharmacol Rev **62**(3): 405-496.

Turrigiano, G. (2008). Homeostatic synaptic plasticity. Structural And Functional Organization Of The Synapse, Springer**:** 535-552.

Turrigiano, G. G., K. R. Leslie, N. S. Desai, L. C. Rutherford and S. B. Nelson (1998). "Activity-dependent scaling of quantal amplitude in neocortical neurons." Nature **391**(6670): 892-896.

Vermeirssen, V., B. Deplancke, M. I. Barrasa, J. S. Reece-Hoyes, H. E. Arda, C. A. Grove, N. J. Martinez, R. Sequerra, L. Doucette-Stamm, M. R. Brent and A. J. Walhout (2007). "Matrix and Steiner-triple-system smart pooling assays for high-performance transcription regulatory network mapping." Nat Methods **4**(8): 659-664.

Vitureira, N., M. Letellier and Y. Goda (2012). "Homeostatic synaptic plasticity: from single synapses to neural circuits." Curr Opin Neurobiol **22**(3): 516-521.

Walker, C. S., M. M. Francis, P. J. Brockie, D. M. Madsen, Y. Zheng and A. V. Maricq (2006). "Conserved SOL-1 proteins regulate ionotropic glutamate receptor desensitization." Proc Natl Acad Sci U S A **103**(28): 10787-10792.

Wang, G. J., L. Kang, J. E. Kim, G. S. Maro, X. Z. Xu and K. Shen (2010). "GRLD-1 regulates cell-wide abundance of glutamate receptor through post-transcriptional regulation." Nat Neurosci **13**(12): 1489-1495.

Wang, R., J. E. Mellem, M. Jensen, P. J. Brockie, C. S. Walker, F. J. Hoerndli, L. Hauth, D. M. Madsen and A. V. Maricq (2012). "The SOL-2/Neto auxiliary protein modulates the function of AMPA-subtype ionotropic glutamate receptors." Neuron **75**(5): 838-850.

Wayman, G. A., Y. S. Lee, H. Tokumitsu, A. J. Silva and T. R. Soderling (2008). "Calmodulin-kinases: modulators of neuronal development and plasticity." Neuron **59**(6): 914-931.

White, J. G., E. Southgate, J. N. Thomson and S. Brenner (1986). "The structure of the nervous system of the nematode Caenorhabditis elegans." Philos Trans R Soc Lond B Biol Sci **314**(1165): 1-340.

Wierenga, C. J., K. Ibata and G. G. Turrigiano (2005). "Postsynaptic expression of homeostatic plasticity at neocortical synapses." J Neurosci **25**(11): 2895-2905.

Wong-Riley, M. T. and P. Jacobs (2002). "AMPA glutamate receptor subunit 2 in normal and visually deprived macaque visual cortex." Vis Neurosci **19**(5): 563-573.

Yan, D., Z. Wu, A. D. Chisholm and Y. Jin (2009). "The DLK-1 kinase promotes mRNA stability and local translation in C. elegans synapses and axon regeneration." Cell **138**(5): 1005-1018.

Yi, J. J. and M. D. Ehlers (2007). "Emerging roles for ubiquitin and protein degradation in neuronal function." Pharmacol Rev **59**(1): 14-39.

Yu, H., Y. Su, J. Shin, C. Zhong, J. U. Guo, Y. L. Weng, F. Gao, D. H. Geschwind, G. Coppola, G. L. Ming and H. Song (2015). "Tet3 regulates synaptic transmission and homeostatic plasticity via DNA oxidation and repair." Nat Neurosci **18**(6): 836-843.

Yu, Y. V., H. W. Bell, D. A. Glauser, S. D. Van Hooser, M. B. Goodman and P. Sengupta (2014). "CaMKI-dependent regulation of sensory gene expression mediates experience-dependent plasticity in the operating range of a thermosensory neuron." Neuron **84**(5): 919-926.

Zhai, S., E. D. Ark, P. Parra-Bueno and R. Yasuda (2013). "Long-distance integration of nuclear ERK signaling triggered by activation of a few dendritic spines." Science **342**(6162): 1107-1111.

Zhang, W., F. St-Gelais, C. P. Grabner, J. C. Trinidad, A. Sumioka, M. Morimoto-Tomita, K. S. Kim, C. Straub, A. L. Burlingame, J. R. Howe and S. Tomita (2009). "A transmembrane accessory subunit that modulates kainate-type glutamate receptors." Neuron **61**(3): 385-396.

Zhang, X., D. T. Odom, S. H. Koo, M. D. Conkright, G. Canettieri, J. Best, H. Chen, R. Jenner, E. Herbolsheimer, E. Jacobsen, S. Kadam, J. R. Ecker, B. Emerson, J. B. Hogenesch, T. Unterman, R. A. Young and M. Montminy (2005). "Genome-wide analysis of cAMP-response element binding protein occupancy, phosphorylation, and target gene activation in human tissues." Proc Natl Acad Sci U S A **102**(12): 4459-4464.

Zheng, Y., P. J. Brockie, J. E. Mellem, D. M. Madsen and A. V. Maricq (1999). "Neuronal control of locomotion in C. elegans is modified by a dominant mutation in the GLR-1 ionotropic glutamate receptor." Neuron **24**(2): 347-361.

Zheng, Y., P. J. Brockie, J. E. Mellem, D. M. Madsen, C. S. Walker, M. M. Francis and A. V. Maricq (2006). "SOL-1 is an auxiliary subunit that modulates the gating of GLR-1 glutamate receptors in Caenorhabditis elegans." Proc Natl Acad Sci U S A **103**(4): 1100-1105.

Zheng, Y., J. E. Mellem, P. J. Brockie, D. M. Madsen and A. V. Maricq (2004). "SOL-1 is a CUB-domain protein required for GLR-1 glutamate receptor function in C. elegans." Nature **427**(6973): 451-457.